ABSTRACT

Title of Document:	GENERIC DYNAMIC MODEL FOR A RANGE OF THERMAL SYSTEM COMPONENTS.
	Shenglan Xuan Doctor of Philosophy, 2010
Directed By:	Professor, Reinhard Radermacher, Department of Mechanical Engineering

The simulation of a thermal system consists of a simulation of its components and their interactions. The advantages of thermal system simulations have been widely recognized. They can be used to explore the performance of a newly designed system, to identify whether the design meets the design criteria, to develop and test controls, and to optimize the system by minimizing the cost or power consumption, and maximizing the energy efficiency and/or capacity. Thermal system simulations can also be applied to existing systems to explore prospective modifications and improvements.

Much research has been conducted on aspects of thermal system and component simulation, especially for steady-state simulation. Recently, transient simulations for systems and components have gained attention, since dynamic modeling assists the understanding of the operation of thermal systems and their controls.

This research presents the development of a generic component model that allows users to easily create and customize any thermal component with a choice of working fluids and levels of complexity for either transient or steady-state simulation. The underlying challenge here is to design the code such that a single set of governing equations can be used to accurately describe the behavior of any component of interest. The inherent benefits to this approach are that maintenance of the code is greatly facilitated as compared to competing approaches, and that the software is internally consistent. This generic model features a user-friendly description of component geometry and operating conditions, interactive data input and output, and a robust component solver.

The open literature pertaining to thermal component models, especially the components of vapor compression systems, is reviewed and commented on in this research. A theoretical evaluation of the problem formulation and solution methodology is conducted and discussed. A generic structure is proposed and developed to simulate thermal components by enabling and disabling a portion of the set of governing equations. In addition, a system solver is developed to solve a system composed of these components. The component/system model is validated with experimental data, and future work is outlined.

GENERIC DYNAMIC MODEL FOR A RANGE OF THERMAL SYSTEM COMPONENTS

By

Shenglan Xuan

Dissertation submitted to the Faculty of the Graduate School of the
University of Maryland, College Park, in partial fulfillment
of the requirements for the degree of
Doctor of Philosophy
2010

Advisory Committee:
Professor Reinhard Radermacher, Chair
Professor Linda Schmidt
Professor Byeng Youn
Professor Peter Wolfe
Professor Bao Yang

Dedication

This work is dedicated to my parents and my wife Bo Zhao.

Acknowledgements

First, I would like to thank my advisor Dr. Reinhard Radermacher for providing me the opportunity and support to study at University of Maryland, College Park. His guidance and patience make me possible to pass through this process. I also thank Dr. Schmidt, Dr. Wolfe, Dr. Yang and Dr. Youn, who can serve on my thesis committee.

I also want to express my deepest gratitude and love to my parents, my wife and my sister, who always believe in me and support me.

Lastly, I want to thank my colleagues, Virkrant Aute, Jothana Winkler, Omar and many other CEEE colleagues, to discuss with me and provide me experimental data to finish this work.

Table of Contents

List of Tables

List of Figures

Nomenclature

Latin	Refers to	Unit
A	Area	m^2
C	Heat capacity	
D	Hydraulic diameter	m
h	Enthalpy, heat transfer coefficient	kJ/kg $kW/m^2.K$
HTC	Heat transfer coefficient	$kW/m^2.k$
k	Conductivity, k factor	kW/m.K
l	Liquid	
Le	Lewis number	
m	Mass	kg
$\dot{m}$	Mass flow rate	kg/s
P	Pressure	Pa
Pr	Prandtl number	
Q	Heat	kJ
$\dot{Q}$	Heat flow rate	kW
r	Residual	
Re	Reynolds number	
T	Temperature	Kelvin
t	Time, coordinate	Second
U	Velocity, internal energy	m/s kJ
u	Specific internal energy	kJ/kg
V	Volume, vapor	m^3
W	Power	kW
x	Quality	
Z	Length, coordinate	m

Greek	Refers to	Unit
α	Void fraction	
ρ	Density	kg/m^3
η	Efficiency	
ω	Humidity	kg/kg

Chapter 1: Introduction

1.1 Dynamic Simulation Motivation

With continually increasing energy costs, the need to improve thermal system efficiency, reduce thermal system cost, and optimize thermal system design is often the primary objective for system designers and manufacturers. In past decades, many mathematical models, simulation tools, and techniques have been developed to simulate or predict the performance of thermal systems. At present, with the development of computer hardware and computing technologies, traditionally complicated thermal models can be solved easily and quickly. Compared with physical prototypes, simulation models – virtual prototypes – are attracting more and more attention from manufacturers and designers because of their potential for reducing design cost and time. This thesis focuses on vapor compression cooling systems, which are a subset of thermal systems.

Most of the available models and their corresponding solution methodologies are restricted to a particular system or component application, such as a water chiller, a heat pump, a heat exchanger, or a compressor. Due to the characteristics of particular applications, their uses are limited to a certain range of similar products and applications. In addition, most of the models only focus on the simulation of steady-state conditions at several operating conditions, ignoring that transient states occurs most of the time during realistic operating conditions, which affects performance and energy consumption considerably.

A dynamic model which simulates a transient component or system helps to accurately predict system performance and energy consumption during all operating conditions. It also aids in the development of optimized system controls and improves system reliability by simulating and evaluating its transient phenomena. Once energy costs become a big portion of the total bill, operating costs become an important consideration. Accordingly, dynamic models become more and more important when developing systems.

1.2 Introduction of Transient Vapor Compression System

The operation of a vapor compression system can be categorized in two time regimes: transient state or steady state. In the latter, the system parameters including input and output change cyclically within limits over time. In the former, the system parameters are not steady and do change with time, especially in the start-up or shut-down period or while moving between one steady state to another due to disturbances. These disturbances could be load or ambient temperature changes, or feedback from the system control. In all of these cases, system inputs and outputs are not constant, and transient modeling can be used as a predictive tool to analyze system performance during these conditions.

In practice, a third time regime exists, called quasi-steady state, in which the system responses are much faster than the transients of inputs. This means the system changes quickly throughout a sequence of steady states subjected to varying time conditions. For such cases, steady-state modeling can be used to study transient behavior.

1.3 Literature Review

1.3.1 Steady State Vapor Compression System Simulation

There is no doubt that simulation of vapor compression systems increases productivity of researchers and engineers. Since the 1970s, many effective vapor compression system simulation tools have been created.

Hiller and Glicksman (1976) as well as Davis and Scott (1976) offered the first modern looks at simulation, which were limited to air-to-air heat pump simulations. Ellison and Creswick in 1978 then used the Hiller and Glicksman model to examine the change in system performance due to changes in components. Around the same time, a simulation for optimizing the heating function of heat pumps was conducted by Carrington (1978). In 1979, Ellison and Rice gave a report on the Oak Ridge heat pump model, a model that continued to evolve over the years, and indeed still exists and continues to evolve today.

After the 1980s, due to the development of computer and computing technology, more and more vapor compression system simulations were conducted. In 1983, Domanski and Didion created a model (HPSIM) for the United States National Bureau of Standards (NBS, now known as the National Institute for Testing and Standards, NIST). The HPSIM model is still in existence today, and over the years has undergone many enhancements that allow it to be very flexible.

Parise (1986) offered a simulation model based upon the governing equations for its component models, rather than performance maps and empirical equations. Parise claimed that empirical performance maps were responsible for the deviations of simulations from actual equipment behavior.

A “toolkit” for chiller simulation was presented by Bourdouxh et al. (1994); this toolkit represented an ASHRAE initiative for simple simulation of HVAC components for building simulation. Levins et al. (1996) used simulation to explore the effects of over-sizing residential air conditioning units.

In the 2000s, simulation research moved in the direction of component-based modeling. Grossman et al. (2001) presented ABSIM, a simulation of absorption systems, presenting a modular format to simulations. Here Grossman discusses the advantages of using modular simulation components for the sharing of work as well as for the development of the tool.

Richardson (2003) developed a component-based vapor compression system model by constructing a system framework: a component standard along with a junction solver. The component standard defines the standard dependent and independent properties of different components and allows the system to easily recognize and replace components during the simulation, which greatly enhances the system’s flexibility and extension capability.

1.3.2 Dynamic Vapor Compression System Simulation

Meanwhile, dynamic performance of the vapor compression system has also been of interest during the past two decades. Dhar and Soedel (1979) were some of the earliest researchers to simulate a complete dynamic vapor compression system to study the dynamic behavior of compressors at start-up. In this model of a window air conditioner, the heat exchangers were constructed in a moving boundary manner. The

pressure in the heat exchanger was neglected to avoid solving the momentum equation.

Chi and Didion (1982) developed a complete air-to-air heat pump system. In this model, the transient momentum balance was considered. The heat exchangers were modeled in a single node. All of the component's dynamics, including the heat exchanger fans and motor shafts, were included. The start-up of a system's cooling operation was analyzed, and the comparison between simulation and experimental measurement showed good agreement.

MacArthur (1984) presented the one of the earliest models to move from the lump-parameters approach to the distributed-parameters approach in the simulation of a complete vapor compression system. In this model, the heat exchanger discretization was fully implicit, which allows a stable solution for the time step of up to 10 seconds, but the homogenous mass flow rate and uniform velocity assumption caused an inaccurate prediction on the mass distribution (MacArthur and Grald, 1987).

Murphy and Goldschmidt (1984, 1985) developed a specifically simplified residential air conditioner system model to study its start-up and shut-down transients. For both scenarios, not all of the components in the system were modeled. In the start-up study, the condenser was treated as a three-zone model and its exit condition was calculated. In the shut-down study, both heat exchangers were treated as tanks which contained two-phase refrigerant at different pressures.

Sami et al. (1987) developed a dynamic model to simulate the transient behavior of a heat pump. The proposed model was a lumped-parameter model. A

control volume formulation was employed for heat pump components. This model was built to allow both cooling and heating operations in the system. Validation of this model was provided for the start-up performance of a water chiller. Sami and Comeau (1992), Sami and Dahmani (1996) expanded on the model of Sami et al. (1987). The finite difference formulation was used to re-write the conservation equations.

Ploug-Sørensen et al. (1997) developed a domestic refrigerator model in SINDA/FLUENT to demonstrate the capability of the software package. The system components model was constructed by a set of general purpose elements, based on the fundamental energy/mass/momentum conservation equations. The solution technique details of SINDA/FLUENT were not fully addressed.

Rossi and Braun (1999) developed a fast, real-time transient model for a rooftop unit with compressor on/off control. In this model, a smart time step-sizing algorithm was implemented to capture the performance of the start-up and shut-down period.

Winkler (2009) developed a component based transient system model. The heat exchanger model in his work was based on the "Tube and Tank" concept, which calculates the pressure drop and heat transfer separately in a tube model and a tank model. This approach improved the simulation efficiency and robustness.

1.3.3 Existing Simulation Package

Many current software packages can be used for energy system steady-state and dynamic simulation. Refrigeration system simulation is included in the tasks of

those simulation packages. Generally, those simulation packages come in two groups or a hybridization of the groups. One group is the general equation solver, which simulates the system by solving a set of governing equations. The second group represents advanced energy system simulations.

General equation solvers are valid for any energy system and thus for vapor compression systems. However, their ability to solve a system heavily depends upon the model's formulation and the user's specification, as the solver itself has no intelligence regarding a specific problem. Examples of this type of software package include Energy Equation Solver (F-Chart) and Matlab (Mathworks).

Advanced energy system software usually specifies the task of the energy system, such as a refrigeration system, a power plant, or a gas turbine. Often modification and generalization of the specific task is difficult or impossible. Examples of advanced energy system software include Gate Cycle (Stork) and GT Pro (Thermoflow).

Among the advanced energy system software, two categories exist: "application-specific" and "fully-flexible." An application-specific program is a special-purpose tool, focusing exclusively on one type of energy system cycle. The program includes a general model from which the user selects a subset via a guided, structured procedure. A fully-flexible program is a general purpose tool, which allows its user to construct any model by connecting appropriate build-in components, in a flexible and unfettered fashion. Application-specific programs place modeling features and details in a logically ordered manner, but the features and details are limited within the pre-defined scope of the general models. Examples of

application-specific programs are VapCyc (CEEE) and Cycle_D (NIST). Fully-flexible programs are more general, and in principle can model any system that its user wishes to define. The program provides a library of component models, which can be graphically connected by users to construct any configuration. This allows a greater variety of models to be included in an application-specific program. However, since the program cannot always "know" what its user is trying to do, the possibility of inconsistencies and crashes is increased relative to a robust, well-organized, application-specific program. This type of software includes Thermoflex (Thermoflow) and Dymola (Dynasim).

Hybridizations of general equation solvers and advanced energy system simulations offer a fixed-system model, but users can create and define the component model. An example of hybridization software is SINDA/FLUENT (C&R). Each of the three types of software has advantages and disadvantages, often leading users to create their own custom software to specifically suit their individual needs.

1.3.4 Summary

There are many software packages and simulations that can facilitate custom system models. It is clear from the literature that most often, simulations are created to fill a specific need, rather than to serve as a general purpose tool. For the simulation of a vapor compression refrigeration system, the outputs of concern are the performance, charge inventory, and optimization of the specific system. Additional

outputs include transient performance and system response time from one state to another one for a dynamic system simulation.

Many existing simulations offer generality through a wide range of component independent variables. For most of them, the system cycle is pre-defined; component models themselves are integrated into the simulation, and therefore are not subject to any changes once the simulation is created.

Recently, the trend of the system simulation is moving toward the component-based modeling methodology, which improves the code sharing, maintenance, and extendibility as well as enhancing the flexibility of a specific system simulation by separating the component model and system solver. However, two main challenges are inherent in current modeling in regard to creating generalized component-based vapor compression system modeling tools: (1) allowing for flexible system configurations that can be assembled at run time and (2) creating components easily with a minimum of maintenance effort.

1.4 System and Components

A system is a group of interacting, interrelated, or interdependent elements forming a complex whole. In the context of this thesis, a system consists of multiple components. Building a system model means building a series of individual component models and integrating them into a system model. For the system model to truly represent realistic system behaviors, each component model must accurately represent the respective component behavior. Developing a system model requires a thorough understanding of the physical phenomena occurring in the individual

components and the interaction among components. Furthermore, the capability of mathematically describing these phenomena with sufficient accuracy must be developed.

1.5 Component Based Simulation

To reduce development time and cost, most new system designs and developments usually adopt components from existing systems. Similarly, a component-based system simulation tool allows users to configure a new system model by adopting an existing system model and replacing some of the existing components instead of rebuilding a new system model completely. This kind of component-based simulation tool provides flexibility to the users and improves modeling efficiency and speed. However, due to varying software infrastructure, creating various component models is still time consuming. If a generic component model that could readily be modified to represent specific components were available, the speed of creating a specific component or system would be significantly improved.

1.6 The Challenges in Thermal System Dynamic Simulation

The findings from the literature demonstrate that although energy system simulation is mature (specifically the air conditioning and refrigeration system simulation), there are still dynamic system simulation research opportunities. In previous studies, researchers have focused either on specific components or on the

improvement of a specific system. There is no research that gives much attention to the generality of those different thermal systems and components.

As mentioned above, a significant engineering challenge is the creation of a general-purpose simulation tool for dynamic thermal systems capable of serving many different cycles and applications. Ideally, this tool should be smart enough to know how to adopt component models in order to construct or reconstruct a system, but should not need to know the details of the component itself.

Besides the challenges faced in the development of dynamic system simulation tools, another significant related engineering challenge is the creation of a generic dynamic component model. Since different component models usually have different functions and methodologies, different thermal components are not typically interchangeable due to either different component structures or different input and output parameters. Even the same type of component is sometimes not interchangeable due to different modeling methodologies or different application environments. This challenge could be easily solved if there were a generic dynamic component model available and if this generic component model could represent many individual and specific components.

1.7 An Unique Tool for Both Steady State and Transient Simulation

Generally, the vapor compression system transient simulation and steady state simulation have different purposes. Steady state simulation is usually used for system design and off-design condition prediction, determination of energy efficiency, and

the evaluation of first cost. These models include a high level of detail and have considerable execution time, but they have great accuracy. Transient simulation is traditionally used either for the study and design of control algorithms or for the overall system performance evaluation under transient conditions. Because transient models are executed many times during a relatively short time interval, they are highly simplified in order to minimize execution time, at the expense of the representation of details. However, the system steady state performance also can be obtained by running the transient simulation to a steady state, but this is an expensive approach due to the long execution time and is rarely utilized for steady state simulation.

Since both simulations have different purposes, the vapor compression system manufacturers usually develop two sets of tools for steady state and transient simulation which have different component models and solution methodologies, and the steady state results of the two models are not consistent.

Ideally, if there is a single tool which can meet both unique purposes and be used for both simulations, it will greatly benefit the manufacturers. There are many benefits if a single tool can be used for both simulations. First, even though both simulations require new model development, there is no need to develop two sets of models for a single component or system, thus it will be cost and time effective. Second, if both simulations are required for new product development, using a single tool can improve the consistency of simulation results due to the consistent inputs and level of detail, and can reduce potential mistakes which may be caused by re-

inputting all parameters or correction factors, and by accounting for or omitting important details.

As mentioned above, the steady state performance can be obtained by running a transient simulation to a steady state. If this process can be shortened or ignored all together, the transient simulation tool may also be used as a steady state simulation tool.

1.8 Research Objectives and Expected Benefits

In order to solve the engineering challenges faced in thermal system dynamic simulation, based on previous research, a generic thermal component model is proposed in this dissertation. The idea is to create a generic thermal component model by creating a component that can easily represent all kinds of thermal components, such as a heat exchanger, a compressor, a valve, or a connecting pipe that exhibits pressure drop and heat loss. More specifically, a generic thermal component is a structure that accommodates all relevant governing equations in a given order and format; these equations represent the component's physical and chemical phenomena. By changing parameters to those equations inside the structure, different thermal components can be created easily. Furthermore, since those created components are in the same structure, it should be easy to connect those components to build a system, and at the same time, improve the system robustness.

The first primary research objective of this dissertation is to develop a generic component model which can simulate any thermal system component of interest here. This research focuses exclusively on the air conditioning and refrigeration system

components, and all the examples studied here are vapor compression systems. Eventually, the model can be expanded to all kinds of energy conversation systems.

In order to represent a realistic component accurately, this generic component model must be able to:

- Accommodate both steady-state and transient-state simulation
- Work with any working fluid
- Calculate local heat transfer and mass transfer coefficient
- Track flow regime change
- Account for moisture, water condensation, and frost accumulation in the working fluid
- Account for pressure drop or rise
- Account for all energy transfers such as heat transfer and input or output of work

Another primary research objective of this dissertation is the development a system solver, to accommodate component models and create systems in an object-oriented manner. As a flexible application simulation tool, the system solver must be robust and flexible. In addition, the developed model should be validated by laboratory experimental data or other mature and validated simulation tools.

It is expected that this research will result in savings in time and cost of the development of dynamic thermal system and component models that predict system or component performance. It is also expected that the research will aid in conducting system or component control studies to develop better control algorithms.

1.9 Reference

Bourdouxh, J.H., Grodent, M, Lebrun, J.J, Saavedra, C, Silva, K, 1994, "A Toolkit for Primary HVAC System Energy Calculation-Part 2: Reciprocating Chiller Models". ASHRAE Transactions 100 (2): pp. 774-786

Chi, J. and Didion, D., 1982, "A Simulation Model of a Heat Pump's Transient Performance", International Journal of Refrigeration, Vol. 5 No. 3, pp. 176-184

Carrington, C.G., 1978, "Optimizing a heat pump for heating purposes", International Journal of Energy Research, Vol. 2, pp. 153-170

Davis, G.L., Scott, T.C., 1976, "Component Modeling Requirements for Refrigeration Systems Simulation", Proceedings of the 1976 Purdue Compressor Technology Conference, West Lafayette, USAA, July 1976, pp. 401-408

Dhar, M. and Soedel, W., 1979, "Transient Analysis of a Vapor Compression Refrigeration System, Part I: The Mathematical Model & Part II: Computer Simulation and Results", Proc. 15th International Congress of Refrigeration (Venezia)

Domanski, P., Didion, D, 1983. "Computer Modeling of the Vapor Compression Cycle with Constant Flow Area Expansion Device", NBS Building Science Series 155, May 1983

Ellison, R.D. and Creswick, F.A. 1978. "A Computer Simulation of Steady-State Performance of Air-To-Air Heat Pumps", Report ORNL/CON-16, Department of Energy, Oak Ridge National Laboratory, Tennessee, USA

Ellison, R.D. and Rice, C.K. 1979. "ORNL Heat Pump Model Update – May 1979", Department of Energy, Oak Ridge National Laboratory, Tennessee, USA

Grossman, G., Zaltash, A., 2001, "ABSIM – Modular Simulation of Advanced Absorption Systems", International Journal of Refrigeration, 2001, Vol. 24, pp 531-543

Hiller, C.C., Glicksman, L.R., 1976, "Improving Heat–Pump Performance via Compressor Capacity Control – Analysis and Test". Volumes I and II, Energy Laboratory Reports MIT-EL 76-0001 and MIT-EL 76-0002, Department of Mechanical Engineering, Massachusetts Institute of Technology, Massachusetts, USA (January 1976)

Levins, W., Rice, C.K., Baxter, V.D. 1996, "Modeled And Measured Effects Of Compressor Downsizing In An Existing Air Conditioner/Heat Pump In The Cooling Mode", ASHRAE Transactions, V 102, Pt 2

Murphy, W., Goldschmidt, V., 1984, "Transient response of air-conditioners – a qualitative interpretation through a sample case", ASHRAE Transactions, Vol. 90, Part 1

Murphy, W., Goldschmidt, V., 1985, "Cyclic characteristics of a typical residential air-conditioner – modeling of start-up transients", ASHRAE Transactions, Vol. 91, Part 2

Parise, J, 1986. "Simulation of Vapour-Compression Heat Pumps" Simulation 46(2): pp. 71-76

Ploug-Sørensen L., Fredsted J.P., Williatzen M, 1997, "Improvements in the modeling and simulation of refrigeration: aerospace tools applied to a domestic refrigerator", International Journal of HVAC&R Research, October 1997, pp. 387-403.

Richardson, D., 2006, "An Object Oriented Simulation Framework for Steady-State Analysis of Vapor Compression Refrigeration System and Components", Ph.D. thesis, University of Maryland

Rossi T.M and Braun J.E., 1999, "A real-time transient model for air conditioners", Proc. 20th International Congress of Refrigeration, Sydney, Paper No. 743

Sami, S.M, Duong, T.N., Mercadier, N. and Galanis, N., 1987 "Prediction of the Transient Response of Heat Pumps", ASHRAE Transactions Vol. 93, Part 2, pp. 471-490

Sami S.M., Comeau M.A., 1992, "Development of a simulation model for predicting dynamic behavior of heat pumps with non-azeotropic refrigerant mixtures", International Journal of Energy Research, Vol. 16, pp. 431-444.

Sami, S.M., Dahmani, A., 1996, Numerical Prediction of Dynamic Performance of Vapor Compression Heat Pump Using New HFC Alternatives to HCFC-22", Journal of Applied Thermal Engineering, Vol. 16, Issue 8/9, pp. 691-705

Ploug-Sorensen L., Fredsted J.P., Williatzen M, 1997, "Improvements in the modeling and simulation of refrigeration: aerospace tools applied to a domestic refrigerator", International Journal of HVAC&R Research, October 1997, pp. 387-403.

"Sinda/Fluint" Introduction Document, July 23, 2008.
http://www.crtech.com/docs/tutorials/sinda_intro.pdf
http://www.crtech.com/docs/tutorials/fluint_intro.pdf

Chapter 2: Generic Component Model Structure

An air conditioning or refrigeration system is usually composed of a compressor, a condenser, an evaporator and an expansion device. The different thermal components have different functions and working mechanisms. However, when any component is represented by mathematical equations describing physical principles, regardless of the mechanism applied to the component, the rules of momentum, energy and mass conservation are always followed. This is the basis for using a general model to represent the any thermal component.

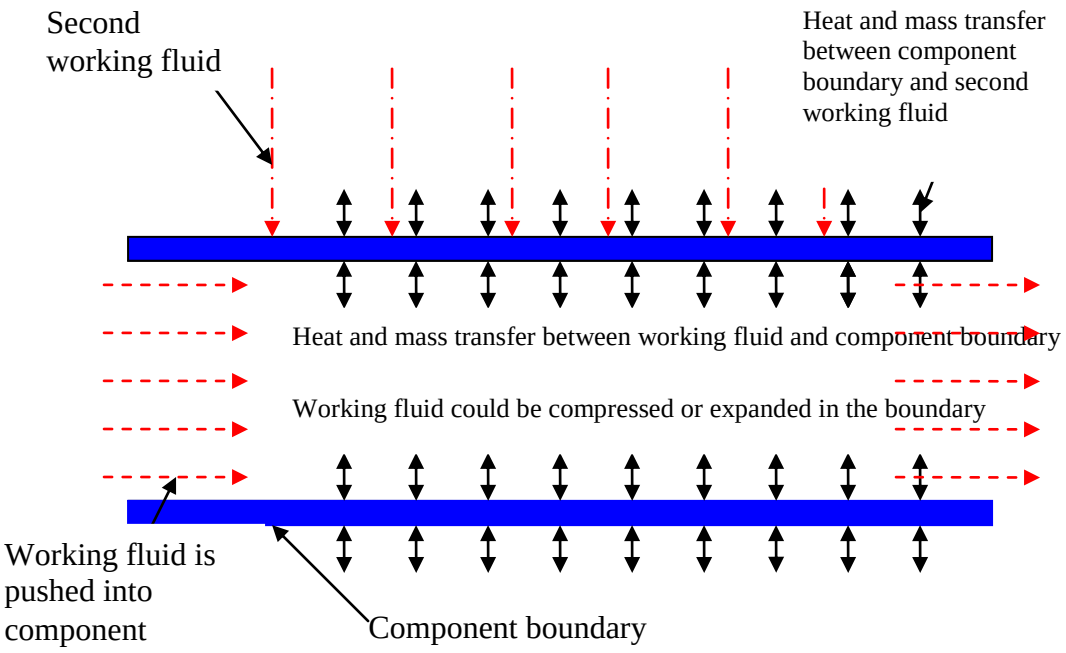

Figure 2.1: Schematic of a generic thermal component

Figure 2.1 is a schematic of a generic thermal component model. The solid bold lines represent the physical boundaries of a component, whether it is the surface of a heat exchanger tube, the housing of a compressor or the chamber of a combustor.

In this physical boundary, several key processes occur individually or together, including:

1. Working fluids enter and/or exit and/or store in the boundary.
2. Heat and/or mass transfers between the working fluids and boundary, and/or between the boundary and environment/a second working fluid.
3. Physical and/or chemical reactions may occur within the boundary. More specifically, refrigerant phase change or change of phase regimes may occur in a heat exchanger, compression may occur in a compressor, or metering or expansion may occur in the expansion device.

2.1 Problem Formulation

For a non-isothermal system, there are three conservation equations that describe the relationship between the inlet and outlet conditions of the stream(s):

1. The mass balance equation (given in equation 2.1) obtained by integrating the equation of continuity over the flow system.
2. The momentum equation (given in equation 2.2) obtained by integrating the equation of motion over the flow system.
3. The energy balance equation (given in equation 2.3) obtained by integrating the energy equation over the flow system.

Mass balance equation:

$$\frac{\partial(\rho)}{\partial t} + \frac{\partial(\rho U)}{\partial z} = 0 \qquad (2.1)$$

Energy balance equation:

$$A_{cs}\frac{\partial(\rho u)}{\partial t}+\frac{\partial(\dot{m}h)}{\partial z}=\dot{Q}+W \tag{2.2}$$

Momentum balance equation:

$$\frac{\partial(\rho U)}{\partial t}+U\frac{\partial(\rho U)}{\partial z}+\frac{\partial P}{\partial z}=0 \tag{2.3}$$

where ρ is the density of the working fluid, U is the velocity of the working fluid, h and u represent the specific enthalpy and internal energy, A_{cs} is the cross section area of the flow, $\dot{Q}$ is the heat flux, W is the work added into the system, P is the pressure, and t and z represent the time and distance along the flow direction.

In this model, in order to simplify the equations, the following assumptions will be made:

- One-dimensional flow, ignoring flow diffusion
- In the radial direction, the flow has a uniform temperature, and there is no heat conduction in the flow along this direction.

The transferred heat can be calculated based on the local heat transfer coefficient and temperature difference between the working fluid and the component physical boundary, which is:

$$\dot{Q}=HTC*A*\Delta T \tag{2.4}$$

where HTC represents the heat transfer coefficient between the working fluids and the physical boundary, A is the heat transfer area between the physical boundary and the working fluid, and ΔT is the temperature difference between both substances.

If the component physical boundary is not thin enough, we assume both sides of the boundary have working fluids present, and the energy conservation equation for the boundary itself can be written as:

$$m\ c\ \frac{dT}{dt} = \Delta \dot{Q} \tag{2.5}$$

where m is the total mass of the component physical boundary material, and c is the specific heat of the material.

2.2 Component Simulation Data Structure

The component model in this thesis is a generic model. More specifically, it is a generalized component simulation framework - a generic thermal element. The individual application of this component model is created by enabling or disabling some features of this thermal element or a set of connected thermal elements.

The simulation of the component was enabled through use of a programming language construct generally classified as a data structure. Once a component model contains more than one thermal element, the data structure facilitates communication of information between different thermal elements of the component.

2.2.1 Selection of Dependent and Independent Properties

The framework created in this thesis is based upon the premise that components satisfy their own mass, momentum and energy balance equations.

As mentioned previously, typical dynamic simulation approaches often simulate each component differently from the others. For example, heat exchangers and pipes are often provided as independent variables of mass flow rate, the thermodynamic state of the inlet fluid and the initial state of fluid in the component. In these cases, the component dependent variables are the thermodynamic state of the outlet fluid and the new fluid states in the component. Compressors and valves are often provided as independent variables of the thermodynamic state of the inlet fluid and the outlet pressure, while the component dependent variables are the mass flow rate through the component and the thermodynamic state of the exit flows, if the mass and energy storage are ignored. When components possess different independent and dependent variables such as these, it places a burden on an algorithm attempting to solve a system comprised of these components. Often the algorithm requires additional information about variables that are specific to a given component. Additionally, often the evaluation order of the components has an effect on the solution algorithm.

In this thesis, the generality of the framework requires that all components have the same set of independent variables and that the same set of dependent variables is calculated. Prior to simulating a system, *a priori* knowledge is usually required, which in this case includes system geometry, flow direction and inlet conditionings of the system. Therefore, for the framework developed in this thesis, the working fluid pressure, fluid enthalpy and fluid mass flow rate at the component inlet points are used as component independent variables. The working fluid pressure, enthalpy and mass flow rate at outlet conditions are the calculated dependent values.

For a vapor compression system component, these properties are adequate for defining the fluid thermodynamic state.

2.2.2 Component Segmentation

One general thermal element can represent a thermal component if the processes are the same everywhere in the component. However, one component may have different processes; for example, the inlet and outlet part of a compressor can be regarded as pipes, whereas the core of the compressor is a compression chamber, which has different thermodynamic processes than pipes. A single thermal element is not sufficient to represent such a component, and hence more thermal elements are required to simulate this type of component accurately enough to describe the physical phenomena precisely. In other words, in this situation, segmentation is necessary to represent this type of component more accurately.

In addition, some users may not solely consider the overall performance and boundary conditions of a thermal component; rather, the thermal properties and performances at different locations along the component may also be of interest. It may not be adequate to provide users with a uniform property along the entire component, and segmentation in these cases is necessary to help users explore the local performance in the component through the simulation.

In this generalized framework, the component can be divided into segments based on the user's requirements or the features of the component following the flow direction of the working fluid.

2.3 Component Specification

There are some properties and methods that the generalized simulation framework must possess independent of the processes specific to a component, and these are listed in table 2.1 below. Given knowledge of these properties, the performance of a thermal component can be described.

Properties	**Description**
Enthalpy	The enthalpy of working fluid at the inlet and outlet
Mass flow rate	The mass flow rate of working fluid at the inlet and outlet
Pressure	The inlet and outlet pressure
Temperature or quality	The inlet and outlet temperature (or quality) of the working fluid at the inlet and outlet
Property states in the component	The average pressure, enthalpy, internal energy, mass, temperature and/or quality within the component

Table 2.1 Properties in the simulation framework

2.4 Numerical Algorithm

2.4.1 Discretized Equations

Once a thermal component is divided into a number of control volumes or segments, the energy and mass conservation equations in each segment are rewritten

as:

$$\dot{m}_i - \dot{m}_{i+1} = \frac{A_{cr}\Delta z}{dt}(\bar{\rho} - \bar{\rho}^0) \tag{2.6}$$

$$\dot{m}_i h_i - \dot{m}_{i+1} h_{i+1} = \frac{(U - U^0)}{dt} + \dot{Q} + \dot{W} \tag{2.7}$$

where $\bar{\rho}$ is the working fluid average density in the segment, and $\overline{\rho^0}$ is the working fluid average density during the previous time step. U is the current internal energy in the segment, and U^0 is the internal energy of the previous time step.

In order to simplify the problem, in the transient analysis of this thesis, the momentum equation is simplified; hence the outlet pressure of the segment is calculated from the pressure drop by:

$$P_{i+1} = P_i - \Delta p \tag{2.8}$$

2.4. 2 Residual Equations

As mentioned above, the components are solved by solving a set of equations, and more specifically here, a set of discretized energy and mass balance equations. In numerical simulation, this is done by solving a set of residual equations, which can be written as:

$$r_{1,i} = \dot{m}_i - \dot{m}_{i+1} - \frac{A_{cr}\Delta z}{dt}(\bar{\rho}_i - \bar{\rho}_i^0) \tag{2.9}$$

$$r_{2,i} = \dot{m}_i h_i - \dot{m}_{i+1} h_{i+1} - \frac{(U_i - U_i^{\,0})}{dt} + \dot{Q}_i + W \tag{2.10}$$

Obviously, solving these residual equations requires information about the internal energy of the control volume, which can be expressed as a function of enthalpy. Hence, the average enthalpy in the control volume needs be obtained. Since, in engineering applications, the Peclet number (a dimensionless number relating the rate of advection of a flow to its rate of diffusion, often thermal diffusion. It is equivalent to the product of the Reynolds number with the Prandtl number in the case of thermal diffusion, and the product of the Reynolds number with the Schmidt number in the case of mass diffusion.) is usually very large in a thermal component and the flow of the component can be considered as "one-way" flow, by applying the modified upwind scheme (MacArther, 1984), the average enthalpy can be described as:

$$\overline{h_i} = h_{i+1} \qquad \text{if } \dot{m}_{i+1} > 0 \tag{2.11}$$

Once the average enthalpy in the control volume is obtained, the average density can be calculated either by the thermal property equations if no void fraction model is considered, or by applying a void fraction model if the working fluid is two-phase flow and accurate charge calculation is considered. The void fraction correlations could be selected from the Anasova model (Anosova et al., 1990), the Budrick model (Budrick et al., 1990), the Hughmark model (Hughmark, 1962) or the Zivi model (Zivi, 1964). In this research, the Zivi model is implemented in the simulation because it gives the best results for the transient simulation (Judge, 1996). The density calculation is described in equation 2.12

$$\overline{\rho} = \alpha\rho_v + (1-\alpha)\rho_l \tag{2.12}$$

Calculating the average density of the control volume builds a relationship between both residual equations and reduces the unknown variables in this set of equations. Consequently, the first residual equation can be eliminated and the problem solution is simplified.

2.4.3 Solution of Model Structure

The generic component framework code structure is described in figure 2.2. The generic component framework is a set of code which is written in Microsoft. NET platform. The framework includes several modules and procedures used for data input, output and math calculation etc. Depending on the type of component that framework needs to represent, those modules and procedures will be executed in a certain order. In the framework, a numerical algorithm and many functions are already predefined in the modules and procedures. Different pressure drop and heat transfer correlations which are used in the calculations will be called in the solving procedures. By making a minor change to the code in the structure, such as enabling or disabling mass storage terms in the block, and/or changing the pressure drop term to be a pressure rising term, this generic component framework can easily simulate various vapor compression system components with very little effort.

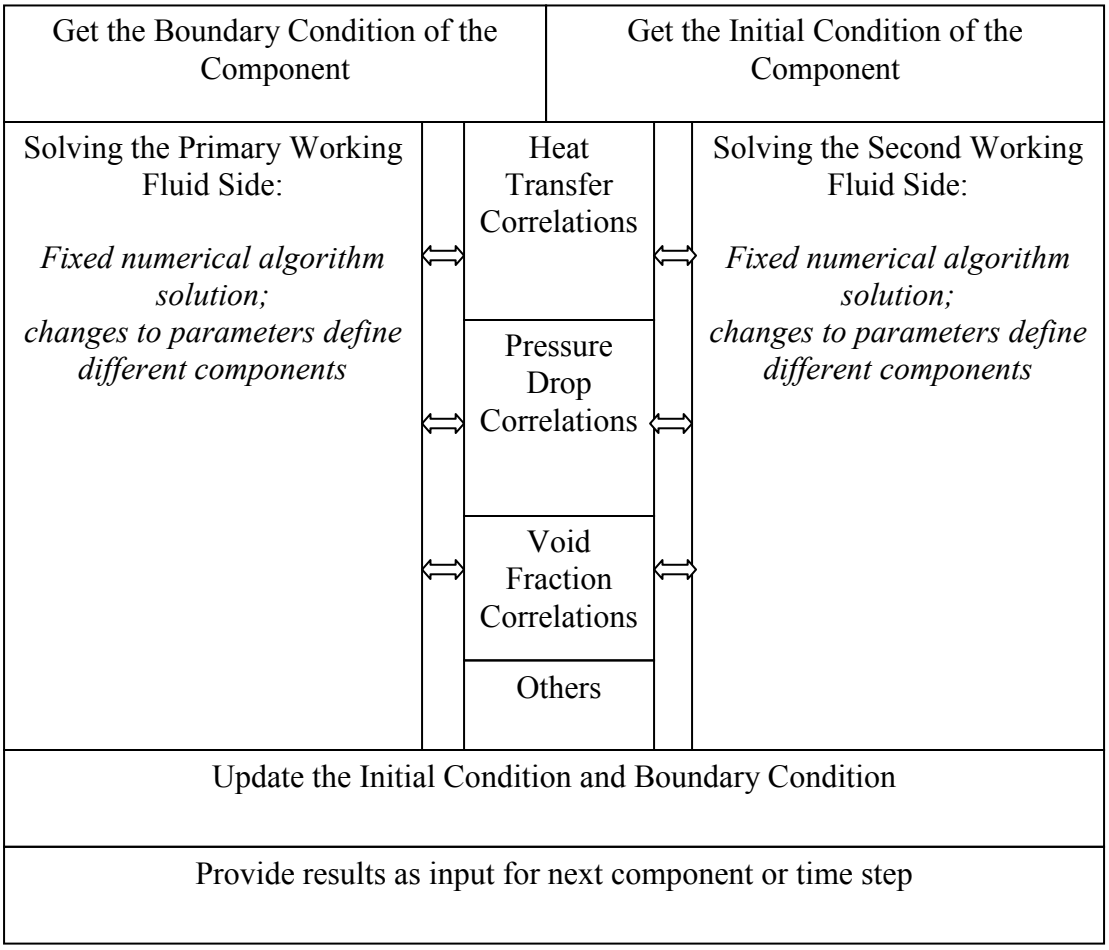

Figure 2.2 Code structure of the generic component framework

The complete numerical algorithm to solve for a thermal component constructed with this framework is described in the following flow chart (Figure 2.3). The component is divided into one or more control volumes, called segments. The number of segments is based on the user's requirements and the physical phenomena occurring within the component. The number of segments usually determines the accuracy level of the simulation results. If a large number of segments are implemented, solving all equations in all segments is time-consuming. In order to

solve the component efficiently, a marching algorithm is used, which means a former segment is solved prior to a latter segment, and the necessary conditions are passed to the next segment. This technique partly adopts the concept of successive substitution and reduces the memory requirement. Since the inlet condition of the component is known during the simulation, the known inlet condition, usually the inlet pressure, mass flow rate and enthalpy, can be supplied to the first segment to obtain the outlet condition. By repeating this step, all the segments of the component can be solved to obtain the entire component outlet condition. Meanwhile, both sides of the heat load for each segment are calculated, which are then used to update the component thermal boundary temperature. Finally, the solver moves to the next time step and repeats the process until steady state is reached or total simulation time ends.

The convergence can be approached by employing any non-linear equation solver, such as the Newton-Raphson or Broyden methods. In this thesis, a Broyden method is used because of its better computational efficiency (Broyden, 1965, Selim 1994).

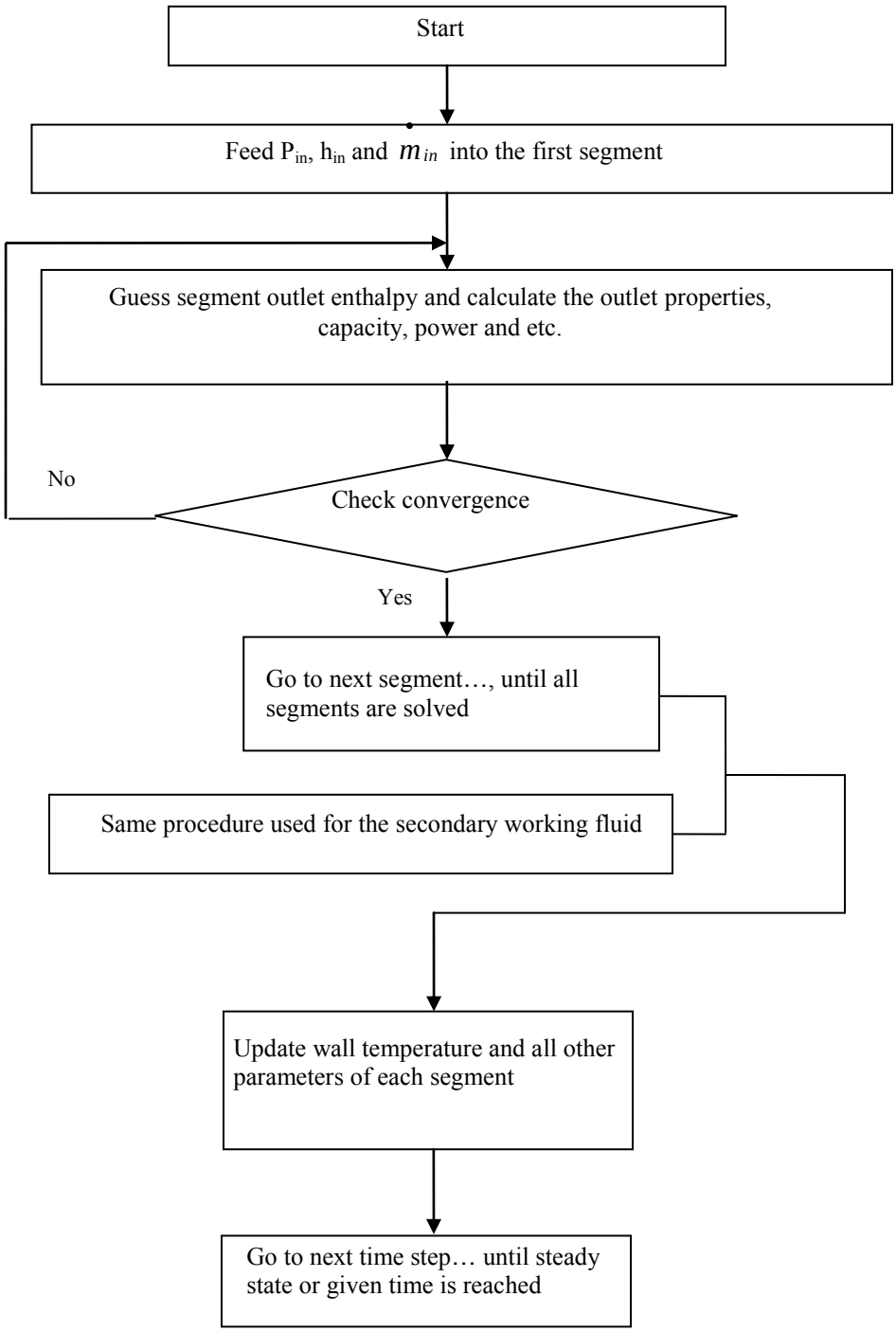

Figure 2.3 Flow Chart of the component structure solution numerical algorithm

2.4.4 Time Step

The dynamic numerical simulation method is very much dependent on the time step, which affects the simulation stability, numerical accuracy and computational efficiency. In the component model structure, the time step may be a fixed or variable value depending on the time evolution of boundary conditions. In a system level simulation, since the component model is typically a part of a system model, the time step can be inherited from the system solver or system solution domain. Alternatively, the component can also pass time step information to the system solver and let the system solver determine the time step for the entire system.

The time step size has a significant impact on the accuracy for transient simulations, especially at the start up or shut down period. In order to accurately capture the transient performance, a smaller time step size is always preferred. However, using a small time step size always means a longer computational time. Especially when the system approaches steady state and its thermal properties do not change dramatically, still using a small time step will not improve its accuracy much but it will greatly increase its computational time. Hence, it will be greatly helpful if an effective variable time step algorithm can be developed to balance the computational speed and results' accuracy.

In most cases, for a simple implementation, a fixed time step is used in the generic component framework. However, an adaptive time step algorithm which explores the possibility of balancing the level of accuracy and computational speed is studied in this thesis.

2.4.5 Adaptive Time Step Algorithm

A variable time step procedure for the vapor compression system transient simulation has been discussed by various authors (Anand, 1999; Rossi and Braun, 1999). However, the procedure used in Anand's model is not generic and was specifically designed for his refrigerator simulation. In Rossi's method, several reasonable time constants for the system have to be predefined, which usually are unknowns for most users.

In the book "*Numerical Recipes: The Art of Scientific Computing, Third Edition*" (Cambridge University Press, 2007), a general adaptive time step algorithm is discussed by the author. This method is called "Step doubling" which is used in ODE equation solving. In this method, a new time step size can be doubled or decreased to half based on the current time step size. However, it requires solving the ODE equations several times before the new time step size is determined.

Fu et al (2003) proposed a variable time step algorithm used in his vapor compression system dynamic simulation. This algorithm refers the "step doubling" method, and the new time step size will be determined based on the key parameters of the vapor compression system, such as saturated temperature, mass flow rate etc. However, this method still needs to calculate system performance at least twice in each time step in order to determine the new time step size.

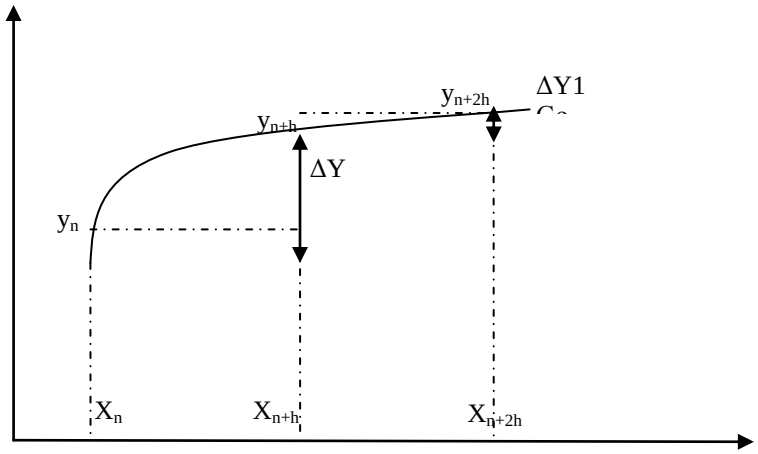

Figure 2.4 A typical ODE equation curve

In this thesis, a new adaptive time algorithm is proposed and integrated into the generic framework. This method refers above methods but needs fewer calculations compared to Fu's method. The concept of the method is demonstrated in figure 2.4. Here, y is a system performance curve which is a function of x (time), and h is the time step size, ΔY is the error between y_{n+h} and $y_{n,}$ ΔY1 is the error between y_{n+2h} and $y_{n+h.}$

If ΔY1 = ΔY, it means the function derivatives in both time step size is the same, and the function trend to approach a steady state neither becomes better nor worse.

If ΔY1 < ΔY, it means that the trend of the function is to approach a steady state, then a larger time step size can be allowed.

If ΔY1 > ΔY, it means the time step size should be reduced.

If ΔY is not a fixed value but a range of the error, the time step size could be kept if the error is located in that range. Otherwise, the time step size could be increased or decreased.

For the dynamic component model constructed by the generic framework, this new adaptive time step algorithm can be described as following:

1. Start from a very small time step and solve the system performance at the first and second time step. The small time step size can ensure it is a reasonable value.
2. When the thermal element outlet conditions are solved, the error (that is the deviation in results between the two time steps) can be calculated as

$$e_i = \frac{|y_{i+1} - y_i|}{|y_{i+1}| + 1} \tag{2.13}$$

   here, i represents different key parameters (enthalpy, pressure, mass flow rate) which can represent the status of the component, y_{i+1} is the parameter values in current time step, and y_i is the values of previous time step, e_i is a relative error of those two values. If y_{i+1} and y_i are small values, this error equation can ensure that the relative error will not become a huge number.
3. For each parameter, we set the maximum and minimum error value $error_{max}$ and $error_{min}$, if $error_{min} < e_i < error_{max}$, we keep current time step size. If $e_i > error_{max}$, we reduce the time step to half. Otherwise, we double the time step size.

4. Select the smallest time step size from all new time step sizes which are determined by different parameters. Use it as the new time step size for the simulation of next time step.

2.4.6 Boundary and Initial Conditions

The boundary and initial conditions are required to solve a time-dependent numerical problem. In this generic thermal component model, the initial conditions are the initial states of the working fluids in or surrounding the component thermal boundary, including the working fluid's pressure, enthalpy, charge in the segment, and the initial component physical boundary temperature. The boundary conditions are the inlet conditions of the working fluids, specifically, the inlet pressure, enthalpy and mass flow rates, which are defined as independent properties in chapter 2.2.

2.5 Applying the Generic Framework for the Steady State Simulation

In chapter 2.4.1, Equation 2.6 to 2.8 are the discretized energy and mass balance equations. If the steady state is being approached, there will not be the mass and energy storage in the component. Hence these items can be ignored in equations for the steady state simulation, they become:

$$\dot{m}_i - \dot{m}_{i+1} = \frac{A_{cr}\Delta z}{dt}(\bar{\rho} - \bar{\rho}^0) \qquad \dot{m}_i - \dot{m}_{i+1} = 0 \tag{2.14}$$

$$\dot{m}_i h_i - \dot{m}_{i+1} h_{i+1} = \frac{(U - U^0)}{dt} + \dot{Q} + W \qquad \dot{m}_i h_i - \dot{m}_{i+1} h_{i+1} = Q + \dot{W} \tag{2.15}$$

$$P_{i+1} = P_i - \Delta p \qquad P_{i+1} = P_i - \Delta p \qquad (2.16)$$

Since the equations used for steady state simulation are coming from the equations used for transient simulation, but just by ignoring the time derivative terms, obviously, the generic dynamic model also can be used to do steady state simulation if the time dependent items are ignored in the model.

The algorithm how the generic dynamic component model do both steady state and transient simulation is described in the below flow chart (Figure 2.5). The procedure of solving the primary and second working fluid thermal elements are almost the same for both simulations except the time derivative items will equal zero in the steady state simulation. Another difference is that the thermal element wall temperature is provided as an initial condition in the transient simulation, but it is an unknown in the steady state simulation. Hence this temperature should be solved for by solving the energy balance of the thermal elements.

2.5.1 Limitation for the Steady State Simulation

Even though both steady state and transient simulation can be solved in the updated generic component framework, there are still limitations once a counter-flow type component needs to be simulated. If the flow pattern is parallel flow, all thermal elements can be solved one by one. This is because both stream inlets are located in the same segment. However, if the flow pattern is the counter-flow, all thermal element wall temperatures cannot be solved one by one and they have to be solved

simultaneously. If there are many thermal elements in the component, the execution time and complexity will be significantly increased.

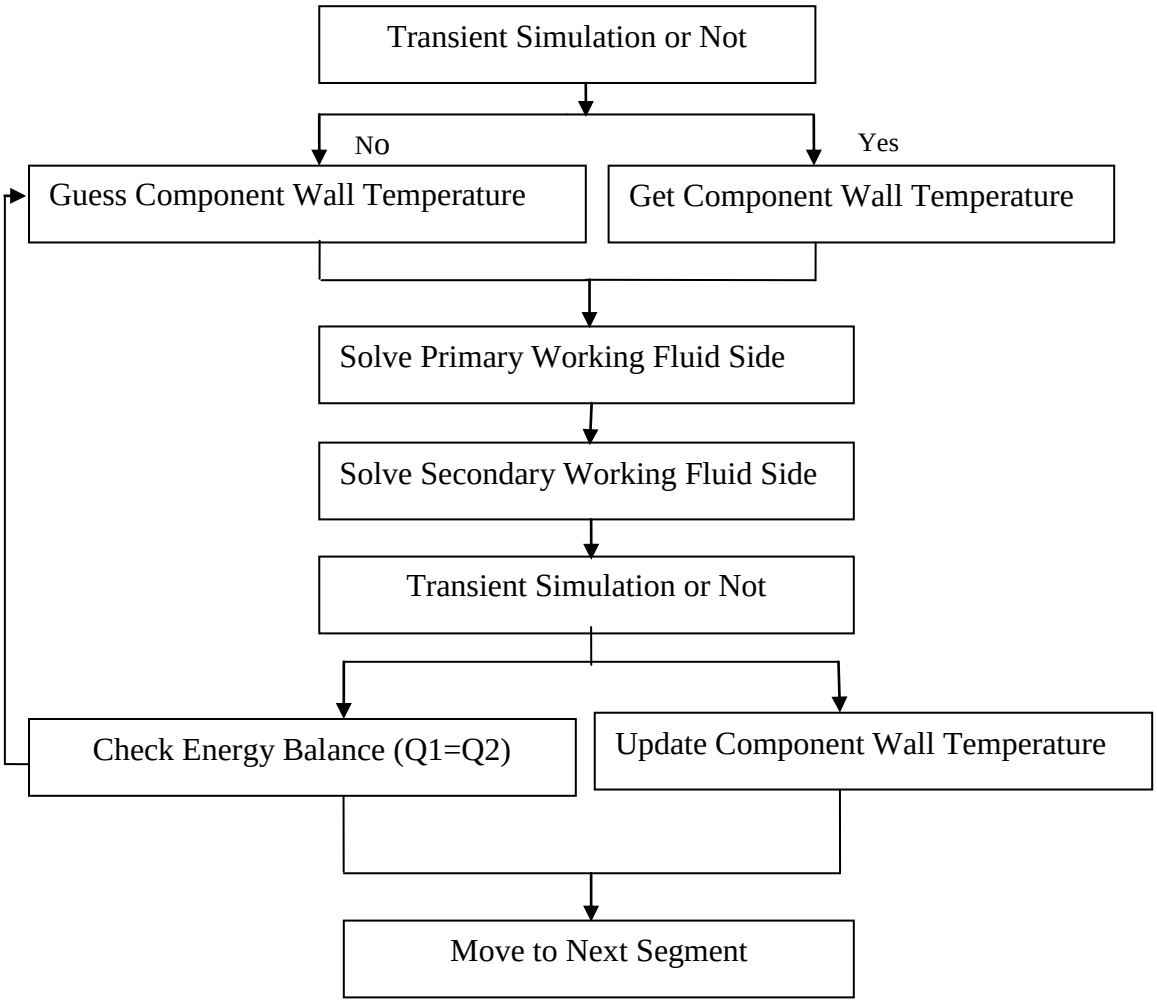

Figure 2.5 Algorithm for integrated transient and steady state simulation

2.6 Summary

In this chapter, a general thermal component framework with its code structure is described. This framework can simulate different thermal components, specifically the components of vapor compression systems, by enabling or disabling some equations in the framework. This results in a considerable advantage in time saving when the user needs to construct a new component.

A numerical simulation solver for components is introduced in this chapter, and the detailed numerical algorithm is presented. In addition, a set of independent and dependent properties of the model is introduced. In order to solve the model accurately, model segmentation and equation discretization can be implemented. By implementing the upwind scheme method, the residual equation number is reduced.

A fixed time step size is usually used in this framework for the dynamic simulation. However, an adaptive time step algorithm is discussed in this chapter which will be used to explore whether it could benefits the computational efficiency of the dynamic simulation. The further study will be discussed in Chapter 3.

Even though the generic component framework is originally designed for the dynamic simulation, it also can be used for the steady state simulation by minor changes in the code structure. Hence, both solvers are essentially integrated together in this framework to do both simulations.

2.7 Reference

Numerical Receipts: The Art of Scientific Computing, William H. Press

MacArthur, J.W., 1984a, "Analytical Representation of the Transient Energy Interactions in Vapor Compression Heat Pumps." ASHRAE Paper, HT-84-19, Vol. 90, Part 1

ZIVI, S.M., 1964, "Estimation a Steady-State Steam of Void Fraction by Means of the Principle of Minimum Entropy Production." Transactions ASME, Journal of Heat Transfer, Series C, Vol. 86, May, pp. 247-252.

Broyden, C.G., 1965, "A Class of Methods for Solving Nonlinear Simultaneous Equations." Mathematics of Computation (American mathematical Society) 1992, pp. 577-593.

Selim, A., 1994, "An Investigation of the Use of Broyden's Method in Load Flow Analysis", Master Thesis, Ohio University

Rossi T.M and Braun J.E., 1999, "A real-time transient model for air conditioners", Proc. 20th International Congress of Refrigeration, Sydney, Paper No. 743

Fu, L. et al., 2003, Dynamic Simulation of Air to Water Dual-Mode Heat Pump with Screw Compressor, Applied Thermal Engineering 23 (2003), 1629-1645

Chapter 3: Simulation of Vapor Compression System Components

Although a general framework for thermal components has been established, some specifications still need to be configured to represent the characters and features of individual components, such as heat and mass transfer coefficients and pressure drop, in order to simulate different thermal components.

There are three major components in a vapor compression system: heat exchangers, compressors and expansion devices. In this chapter, these components will be modeled by implementing a generic framework, which represents the specifics of each component and is universal in simulating other types of vapor compression system components.

3.1 Simulation of a Heat exchanger

3.1.1 Introduction

Heat exchangers play an important role in the vapor compression system. A number of transient heat exchanger models, with a wide range of complexity, have been developed since the 1970's. Several categories of the exchanger models are reviewed as follows.

One sub-classification of modeling techniques used for heat exchanger simulation includes two methods, 1) the phase-dependent moving boundary method, and 2) the phase-independent finite volume method. In the first approach, the heat exchanger is divided into different sections according to the flow regimes of the

refrigerant—i.e. sub-cooled, two-phase or superheated. During transient operation, these sections cannot be constant due to phase regime changes; therefore, it is necessary to track boundaries between the adjacent phases that move within the heat exchanger. The second approach typically divides the heat exchangers into a number of elements with a constant volume. Each element is defined by its own state properties. All transient conservation equations are discretized into elements and will be solved sequentially or simultaneously.

Another sub-category of modeling technique includes the lumped parameter method and distributed parameter method. The lumped parameter method is fast and computationally simple, since it solves only the first-order ordinary differential equations. However, it loses spatial details by averaging the state parameters over the entire control volume. The distributed parameter method conserves the spatial details; nonetheless, it has the disadvantages of excessive computational time compared with the lumped parameter method.

Wedekind et al. (1978) were among the earliest to study the transient behavior in their modeling of a two-phase flow heat exchanger. Their model was built from a moving boundary formulation using a variable volume form of the volumetric mean void fraction over the two-phase region. This simplifies the representation of the two-phase flow region. A significant achievement of this method is that a complete two-phase region can be treated in adequate detail while avoiding the necessity of handling the transient form of the momentum equation.

Dhar and Soedel (1979) presented one of the earliest transient models of a complete vapor compression refrigeration system, wherein the two-phase heat

exchanger was treated as a few lumps using a moving boundary approach. The development focused on the refrigerant side and left secondary refrigerant open for the user to choose. All major transients were well captured.

MacArthur (1984) presented one of the earliest models to move from the lumped parameter approach to a distributed formulation. This, along with the studies of MacArthur and Grald (1987) and Rasmussen et al (1987), constituted a body of work using similar formulations for the system components. The time-dependent conservation equations were simplified by assuming one-dimensional flow in both heat exchangers. The two-phase region in the condenser was treated as homogenous, whereas in the evaporator the liquid and vapor phases were modeled separately. One disadvantage of the MacArthur (1984) work was that the pressure response of the heat exchangers was de-coupled from the thermal response by the imposition of uniform flow velocities along the heat exchanger length. This yielded inaccurate mass distribution predictions. This issue was addressed in McArthur and Grald (1987), where the mass balance was coupled to the energy balance and allowed to dictate the pressure response. In all of these studies, the heat-exchanger's discretizations were fully implicit, thereby allowing stable solutions for time steps up to 10s.

Murphy and Goldschmidt (1984, 1985) developed simplified system models of transient behaviors of an air-to-air system. In their work, both the heat exchangers were modeled during the shut-down period as tanks which contain two-phase refrigerant at different pressures. The air crossing the coil was considered as the secondary fluid cooling or heating the coils by natural convection.

Nyers and Stoyan (1994) modeled an evaporator using the moving boundary

formulation but with the finite volume method adopted within each phase. This model had been used to predict the evaporator's behavior under step jump, exponential saturation, and periodic oscillation of the temperature and flow rate of the secondary fluid, compressor speed, condenser pressure, and throttle.

Williatzen et al. (1998) presented a model for simulating the transient flow dynamics in a heat exchanger, in the form of a set of lumped parameter moving boundary formulations. The structure of the model allowed for any physically possible combination of phases within the heat exchanger to be handled by an algorithm that switched between the appropriate sets of equations. Pettit et al. (1998) applied this formulation to the case of an evaporator and studied the phenomena of the appearance and disappearance of flow regimes within the evaporator.

Rossi and Braun (1999) developed a fast-yet-large model of a roof-top air conditioning unit. The heat exchanger model was formulated by the finite volume method. The importance of real time simulation was emphasized, and a smart, automatic-integration, step-sizing algorithm was presented that robustly simulated start-up and on-off cycling.

Jakobsen et al. (1999) analyzed the relative accuracy of assuming homogenous flow and slip-flow patterns in a heat exchanger. They concluded that the homogenous flow model was an inadequate representation that over-predicted the sensitivity of the evaporator. They recommended the use of the slip-flow model when the dynamics of the refrigerant are of interest.

Bendapudi et al. (2004) implemented both finite volume and moving boundary approaches to develop a shell-tube heat exchanger model, and they

conducted a comprehensive study on heat exchangers. Within each approach, two methods were used. In the finite volume approach, these were the direct method and the sequential method. In the moving boundary approach, the direct and state-space solution methods were studied. Implicit integration was incorporated in the sequential solution method of the finite volume approach.

In Bendapudi's thesis (2004), he compared the accuracy and execution speed of both models based on the experimental data. He found that both approaches closely capture the correct pressure and chilled/cooled water leaving temperature in the evaporator/condenser at steady state and transient state. The accuracy rate of both approaches is nearly identical. The comparison also showed that the moving boundary approach had a 55-70% reduction in computation time compared to the finite volume approach for a comparable accuracy.

Based on these previous studies, it is clear that one disadvantage of the moving boundary approach is the prediction of refrigerant charge inventory. Because the refrigerant average density is estimated based on flow regime boundary conditions, it is relatively not as accurate as the finite volume approach. Another issue of the moving boundary approach is the difficulty of system transient modeling. For the condenser in a vapor compression system model, if its heat exchanger is simulated by using the moving boundary approach it is expected that the inlet state is superheated vapor coming from compressor discharge. For the evaporator, it is expected that the inlet state is a two-phase flow coming from the expansion device. Since the inlet flows come from the compressor and expansion device of the system, the model imposes the compressor and expansion device to provide appropriate inlet

conditions—superheat and two-phase flow, respectively—during the entire simulation period. However, during the start-up transient period, it is numerically possible to have two-phase flow at the compressor inlet and outlet, as well as superheated vapor at the inlet of the expansion device. These abnormal boundary conditions of the moving boundary heat exchanger model could result in the moving boundary approach not properly solving the component. This problem can be solved by implementing a better method, which is described in the following section.

3.1.2 A Combined Moving Boundary and Finite Volume Heat Exchanger Model

As discussed above, the finite volume and moving boundary methods are the most popular methods used on heat exchanger simulations. Both methods have advantages and drawbacks. The moving boundary method divides the entire heat exchanger into a few control volumes (usually two control volumes for evaporators and three control volumes for condensers) by seeking the boundary of different flow regimes. It reduces the control volume number and produces relatively accurate results, since different phases mean distinct heat transfer coefficients and pressure drop relationships. However, the spatial detail in the heat exchanger cannot be explored, and the model's accuracy is not as good as that of the finite volume model. In addition, the moving boundary method may not properly predict results once it is integrated into a system transient model.

The finite volume method divides the entire heat exchanger into many control volumes, and the accuracy is high once the local heat transfer coefficient and pressure drop are fed into the model to explore the spatial detail of the heat exchanger.

Consequently, the computational time or computational cost is higher than the moving boundary model and lumped model.

Furthermore, different users and different applications may have different requirements for the heat exchanger model. As a part of a system simulation, the user may not want to spend too much time on the component simulation—for example, if this component is not his or her object of particular interest, or if the model demands excessive computational time. A user who wants to explore both performance and spatial detail of the heat exchanger may want a model that is only adequately accurate. Hence, it is necessary to develop a model with flexibility that allows users to choose between accuracy and execution speed, thus meeting the users' various requirements.

In this dissertation, a combined moving boundary and finite volume method is proposed. The methods are summarized as follows. First, a finite volume method is adopted. Users can divide the heat exchanger into a number of control volumes – segments. Since the upper-level model implements the finite volume method, the abnormal boundary condition described in chapter 3.1.1 can be accommodated. In addition, because the moving boundary approach is still implemented in each control volume, the accuracy level is still high even if a small control volume number is specified. If the phase change occurs in the control volume, or a phase boundary exists in the control volume, the segment is divided into sub-segments based on the flow regimes of the refrigerant. The transition point is sought by the golden section search method.

The flow chart describing this method is shown in figure 3.1. The detailed steps are listed as follows. Once the simulation starts,

1) The inlet pressure, enthalpy and mass flow rate of the component are fed into the first segment of this component.

2) By solving segment heat and mass balance equations, the segment outlet thermal properties can be solved.

3) Based on the segment outlet thermal properties, the model determines if a phase regime change occurs in this segment. If so, the segment will be divided into two sub-segments. The length of sub-segments and transition point are found by using the golden section search method. Then the entire process is repeated in the second sub-segment until all phase transitions are accommodated.

If the phase change does not occur in the first segment, the first segment outlet properties are fed into the second segment to solve its outlet properties.

4) Step 3 is repeated for each of segments until the last segment is solved.

5) The same procedure is used to solve the second fluid out properties and heat transfer in all of the segments.

6) Each segment wall temperature is updated based on the transferred heat on both sides.

7) Calculations move on to the next time step until a steady state or given time limit is reached.

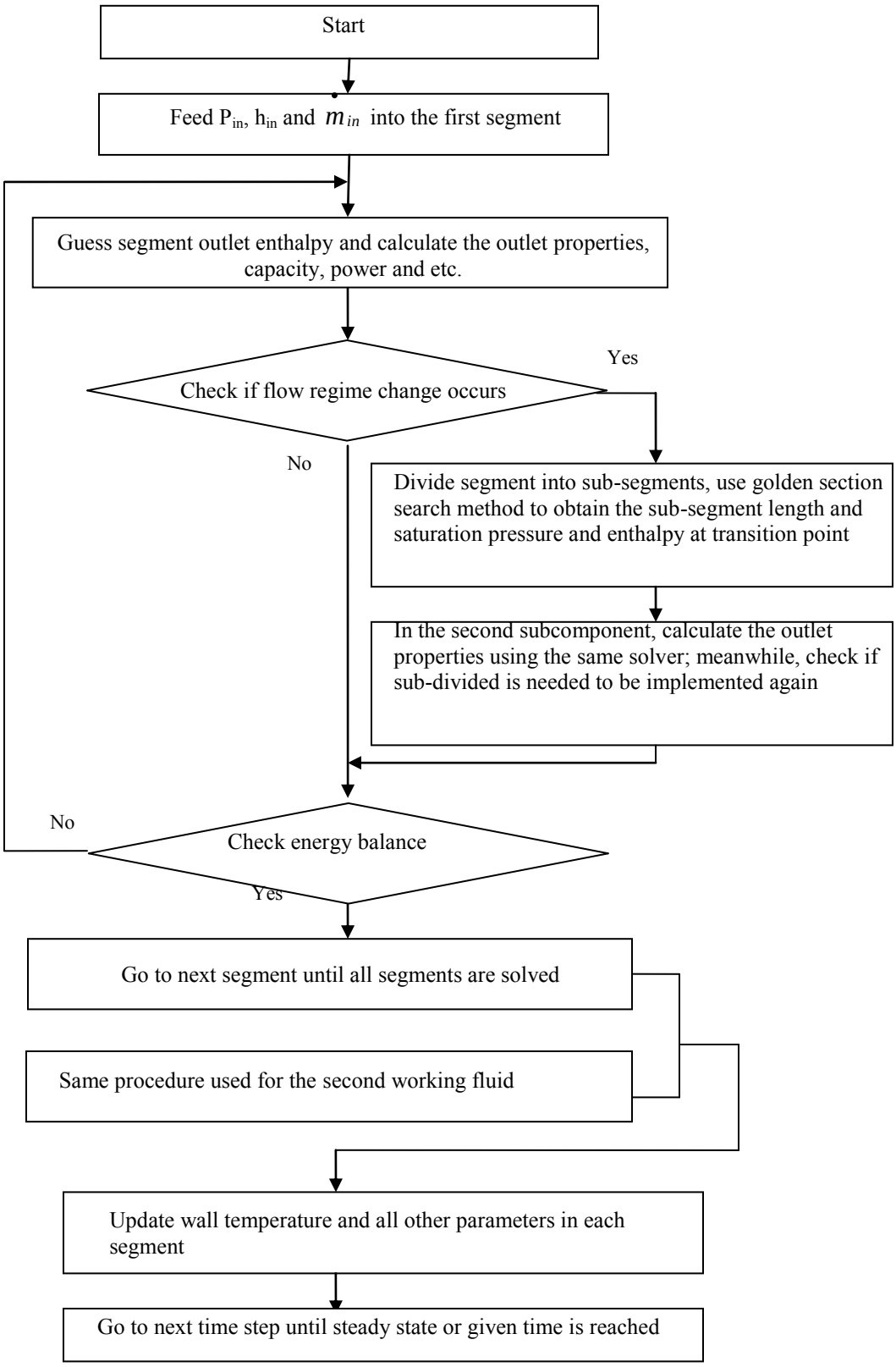

Figure 3.1 Modified flow chart for heat exchanger model

3.1.3 Pressure Drop Calculation

The outlet pressure of a segment should be determined by the momentum equation. In order to simplify the calculation, the outlet pressure can be expressed by the following hydraulic equation:

$$P_{out} = P_{in} - \Delta P \tag{3.1}$$

$$\Delta P = \Delta P_a + \Delta P_g + \Delta P_f \tag{3.2}$$

Where ΔP_f is the friction term, which can be calculated by the equation,

$$\Delta P_f = c \frac{2l}{\pi \rho D^3} \dot{m}^2 \tag{3.3}$$

ΔP_a is the accelerational term,

$$\Delta P_a = \frac{16 \dot{m}^2}{\pi^2 D^4} \left(\frac{1}{\rho i_n} - \frac{1}{\rho_{out}} \right) \tag{3.4}$$

and ΔP_g is the gravitational term, which is calculated by

$$\Delta P_g = 0.5(\rho_{in} + \rho_{out}) g l \sin\theta \tag{3.5}$$

Among the friction, accelerational, and gravitational pressure drop components, the friction term is dominant; hence the other two components can be ignored in practice.

Various correlations and empirical equations are used to obtain the frictional pressure drop in the heat exchanger for both single-phase and two-phase flow, depending on the flow pattern, type of working fluids, tube geometry and operating conditions. The default correlations used in this simulation are the Churchill

correlation and Jung-Radermacher correlation for single-phase and two-phase flow, respectively.

3.1.4 Refrigerant Side Heat Transfer Coefficients

In the single-phase region, the convective heat transfer coefficient is calculated using the Churchill (1976) and Gnieliski (Kakac, 2002) equations for laminar and turbulent flow, respectively, which are

$$Nu_d = \frac{0.6774 \mathrm{Pr}^{1/3} \mathrm{Re}_L^{1/2}}{[1+(0.0468/\mathrm{Pr})^{2/3}]^{1/4}} \tag{3.6}$$

$$f = (1.58 \ln(\mathrm{Re}) - 3.28)^{-2} \tag{3.7}$$

$$Nu_d = \frac{(f/2)(\mathrm{Re}-1000)\mathrm{Pr}}{1+12.7(f/2)^{1/2}(\mathrm{Pr}^{2/3}-1)} \tag{3.8}$$

$$h = Nu_d k / d \tag{3.9}$$

In condensing flow, the convective heat transfer coefficient is calculated using the correlation methods from Dobson and Chato (1998), Shah (1989), Soliman (1968), and Traviss (1973).

In evaporating flow, the convective heat transfer coefficient comes from the correlations developed by Gunger (1986), Jung (1989b, 1991, 1993), Kandilikar (1990, 1991, 1997), Klimenko (1988), Lee (2001), and Shah (1982).

3.1.5 Air Side Pressure Drop and Heat Transfer Coefficients Calculation

Air-side pressure drop and heat transfer coefficient are also calculated by empirical or semi-empirical correlations which depend on the tube geometry, fin type

and surface condition. There are several correlations available based on the literature. (Chang [1997, 2000], Kim [2002], Kim [1997,1999], Sahnoun [1992], Wang [1997]). The default correlation for a tube-fin heat exchanger is from Wang, Chi and Chang (2000), and the basic equations are written as

$$i = C_1 \, \mathrm{Re}_{Dc}^{C_2} \tag{3.10}$$

$$j = C_3 \, \mathrm{Re}_{Dc}^{C_4} \tag{3.11}$$

The C_1, C_2, C_3 and C_4 are dimensionless parameters which depend on the physical dimensions of the heat exchanger, and the Re_{Dc} is the Reynolds number based on the tube collar diameter.

3.1.6 Void Fraction

The void fraction is defined as the fraction of the volume that is not occupied by liquids. Several void fraction models have been developed to account for the charge distribution for a two-phase flow. Among them, the Zivi model developed by Xu and Clodic (1996) gave the best results for transient simulation (Judge 1996), which is

$$\alpha = \frac{1}{\left[1 + \left(\frac{1-x}{x}\right)\left(\frac{\rho_l}{\rho_v}\right)^{2/3}\right]} \tag{3.12}$$

$$\rho = \rho_l (1-\alpha) + \rho_v \alpha \tag{3.13}$$

where x is the quality of two-phase refrigerant and α is the void fraction.

Besides using the Zivi model, users also have the option to choose other void fraction models, such as Lockheed-Martin's model, based on their experience or

different applications. If the mass inventory is not the concern in the simulation, a simple homogeneous model can be used instead of the more complicated void fraction model.

3.1.7 Wet Surface Condition on Air Side

Real air contains moisture. When the heat exchanger surface temperature is below the dew point, the water vapor in the air condenses on the surface of the heat exchanger. Hence the moisture transfer and related latent heat transfer have to be accounted for in this model. Then the overall transferred heat of a heat exchanger becomes

$$q = h_{air}(T_\infty - T_s) + h_d h_{fg}(\omega_\infty - \omega_s) \tag{3.14}$$

where Ts and ω_s are the temperature and humidity ratio of saturated air at the surface.

In the analysis of the dehumidification process, the mass transfer coefficient is determined by applying the Colburn analogy approach – a heat and mass transfer analogy:

$$h_d = \frac{Le^{(m-1)} h_{air}}{\rho_{air} Cp_{air}} \tag{3.15}$$

where Le is the Lewis number with a range of 0.81 - 0.86 over the temperature range of 10°C - 60°C and is valid from completely dry air to saturated air (McQuiston, 1994). The number m equals 1/3 for most applications (Incropera and Dewitt, 2002). Since the driving potential of water condensation is the difference of the bulk flow humidity ratio and saturated humidity ratio at heat exchanger surface temperature, assuming the ideal gas law applies, the condensate flow rate is calculated from

$$\dot{m}_w = h_d \rho A(\omega_\infty - \omega_s) \quad (3.16)$$

with ρ as the bulk flow density. The model allows outlet humidity below 100% and water condensation at the same time.

3.1.8 Suction Line Liquid Line Heat Exchanger

The use of suction line liquid line heat exchanger is very common in the commercial refrigeration applications. This component is often employed to ensure only single phase liquid is entering into the expansion device and single phase vapor is entering into the compressor.

The simulation of suction line liquid line heat exchanger is same as the normal air to refrigerant heat exchanger, except the second working fluid is a refrigerant but not the air. In order to adopt the model in the generic component framework, the heat leakage from heat exchanger to the environment will be ignored. This assumption is reasonable because this heat load is a small portion compare to the total heat load of the heat exchanger.

3.1.9 Heat Exchangers in Parallel and Series

Many air conditioning and refrigeration systems have more than one condenser and evaporator. For example, a refrigeration system may have multiple evaporators which cool multiple display cabinets; a de-superheater could be placed prior to a condenser to improve the system efficiency. In addition, a multiple row heat exchanger also can be treated as several heat exchangers in series to assemble a complex heat exchanger by using several simple ones.

Once those heat exchangers are placed in parallel or series, they can be considered as a large component or a sub-system which consists of several small components. This type of subsystem or components can be constructed and modeled by connecting several generic dynamic component models.

If the heat exchangers in series are modeled, there is no additional work needing to be done. However, if the heat exchangers in parallel should be modeled, the inlet mass flow rate of each heat exchangers has to be solved because usually only total mass flow rate of those heat exchangers will be given or passed from formal components. Since those heat exchangers are in parallel, during the operation, all of the heat exchangers will have the same pressure at their inlets and outlets. Hence, the additional residual equations used to solve individual mass flow rate of each heat exchanger can be described with the following equation:

$$\vec{r} = \begin{bmatrix} P_{HX\,2\_out} - P_{HX\,1\_out} \\ P_{HX\,3\_out} - P_{HX\,1\_out} \\ \ldots\ldots \\ P_{HXN\_out} - P_{HX\,1\_out} \end{bmatrix} \tag{3.17}$$

3.2 Heat Exchanger Simulation Numerical Results

Although there are several different types of heat exchangers, the main concerns for vapor compression system applications are with the recuperative type of heat exchanger, in which working fluids exchange heat on either side of a dividing wall. This type of heat exchanger can be divided into parallel flow, counter flow and

cross flow heat exchangers according to the working fluid flowing directions.

Shown on the left of Figure 3.2 is a schematic drawing of a counter flow heat exchanger where one fluid flows through a pipe and exchanges heat with the second fluid flowing through an annulus surrounding the pipe; on the right are associated temperature distributions along the pipe axis. In this heat exchanger, the two working fluids flow in opposite directions. Figure 3.3 shows a schematic of a parallel flow heat exchanger with its temperature distribution. The structure of the parallel flow heat exchanger is the same as that of the counter flow exchanger except that the two fluids have the same flow direction. Figure 3.4 shows the schematics and temperature distribution of a cross flow exchanger, where the directions of fluids are perpendicular to each other.

Each of these three types of heat exchangers has advantages and disadvantages. Among them, the counter flow heat exchanger design is the most efficient design when comparing their heat transfer rates per unit surface area. This is because the average temperature difference between the two fluids over the heat exchanger is maximized. Cross flow heat exchangers are usually applied in the design, in which one fluid has a much larger heat capacity than the other one.

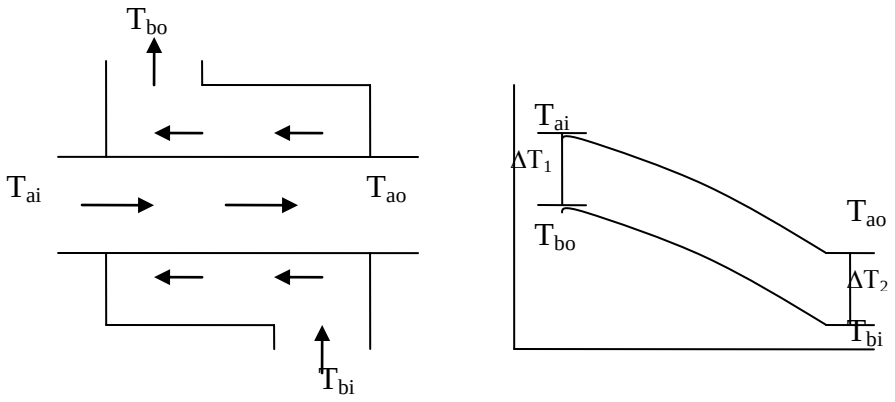

Figure 3.2 Counter flow heat exchanger schematic with its temperature distribution

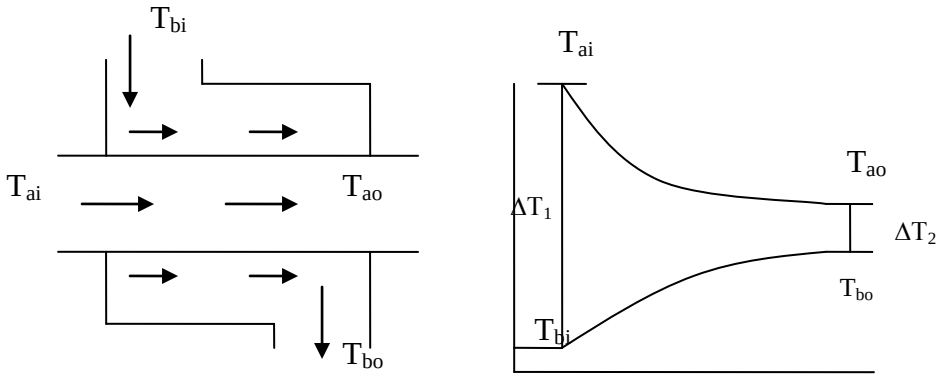

Figure 3.3 Parallel flow heat exchanger schematic with its temperature distribution

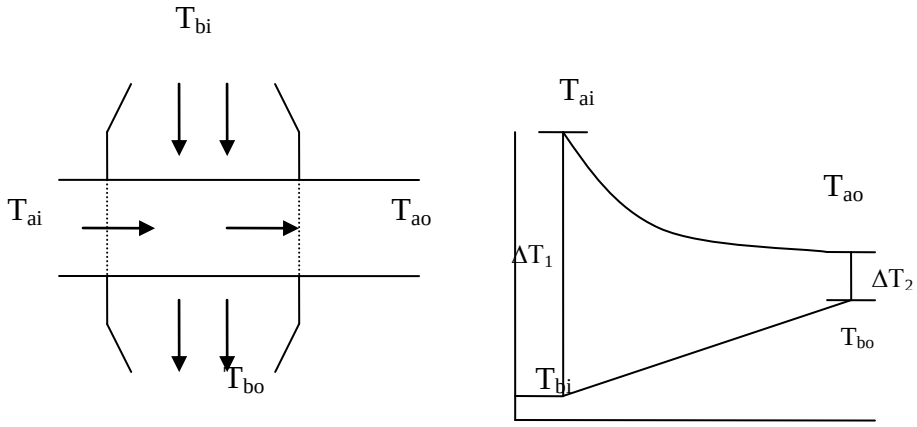

Figure3.4 Cross flow heat exchanger schematic with its temperature distribution

In the model presented in this thesis, the counter flow and cross flow heat exchanger, the two most applicable heat exchangers in a vapor compression system are simulated as examples to show the capability of this model in handling different types of heat exchangers. The results should demonstrate the temperature distribution characteristics as shown above. Both single-phase flow and two-phase flow will be used in this simulation in order to highlight the difference on the temperature, pressure, and heat transfer coefficient for different flow types in heat exchangers.

The mathematical model and numerical procedure discussed above are the theoretical foundation of the present simulation program. The code is written in the .NET platform, which can conveniently call functions written in various languages.

The numerical results are obtained by feeding the required independent properties, described in Chapter 2, into the heat exchanger model. The boundary conditions are predefined before the simulation starts. All heat exchangers are divided

into one hundred segments of equal length. This is determined based on the studies shown in Chapter 3.2.5, which demonstrate that the simulation results do not change with a smaller segment length in our setting. If refrigerants are chosen as a working fluid, the inlet conditions will be set up as two-phase flow states to represent the process of phase change. Because each component simulation is run individually and does not get a time step from a system solver, an empirical time step of 0.01 second is chosen for each simulation case to show that the working fluid states change gradually.

3.2.1 Single Phase Flow Heat Exchanger

In this section we will discuss the heat exchange in a single-phase counter flow heat exchanger.

Figure 3.5 shows the temperature distribution of a counter flow air-to-air heat exchanger at steady state. The temperature (y-axis) is plotted as a function of the length of the heat exchanger (x-axis). Warm air flows through the heat exchanger from the left side to the right side, and the cold air flows in the opposite direction. The initial value for the warm air inlet temperature is 310K, and that for the cold air inlet temperature is 278K, and that for the heat exchanger wall temperature is 298K. At steady state, the warm air temperature decreases along the flow direction due to heat losses and increases for the cold air due to heat gain. The heat exchanger wall temperature is between the temperatures of the warm and cold air to maintain a steady heat transfer between both fluids.

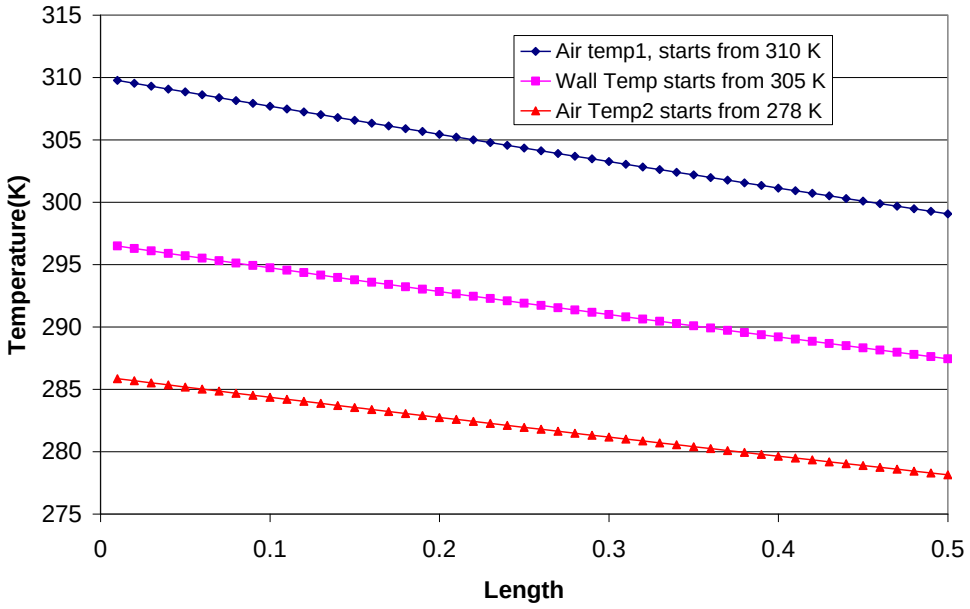

Figure 3.5 Temperature distribution of a counter flow air-to-air heat exchanger

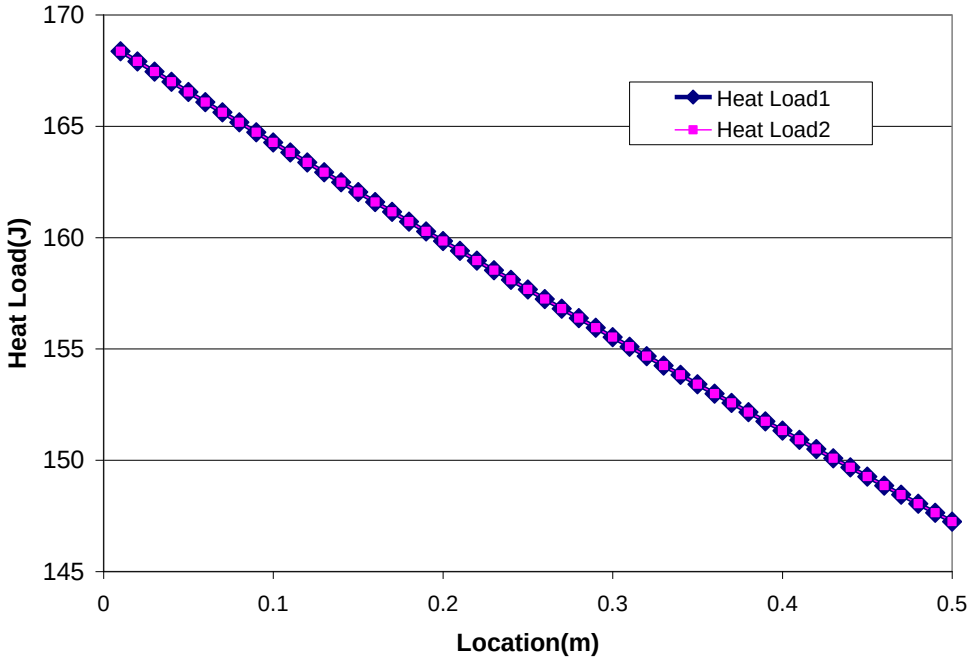

Figure 3.6 Heat load profile of a counter flow air-to-air heat exchanger

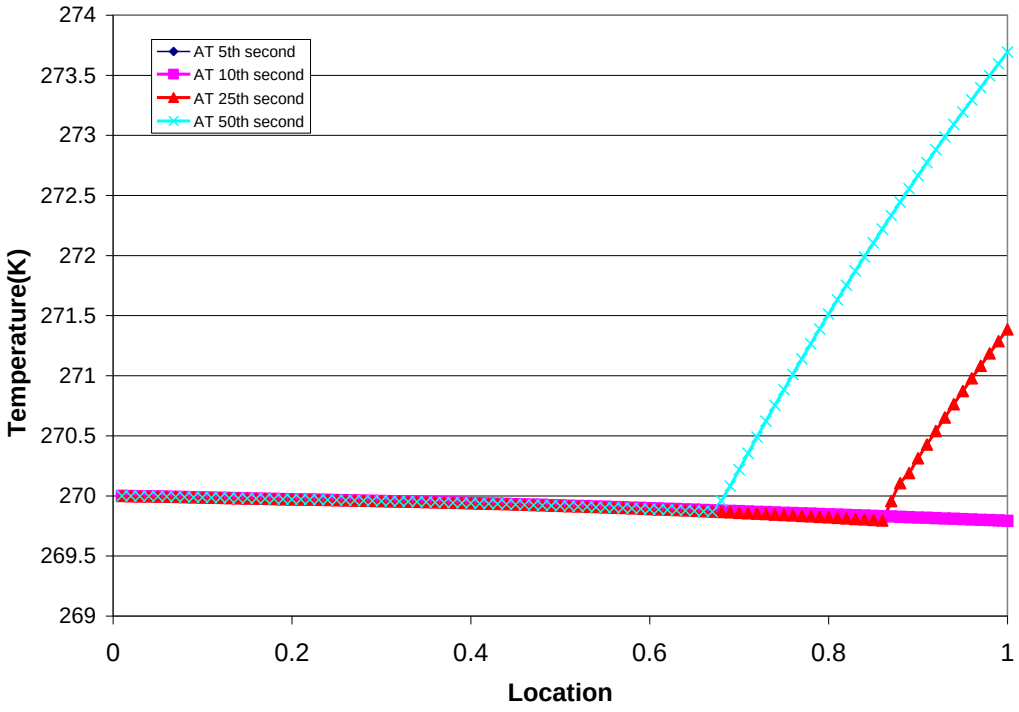

Figure 3.7 Temperature profile of an air-to-refrigerant heat exchanger

Figure 3.6 shows the heat load of this heat exchanger at steady state. It is clear that at steady state, both sides have the same heat load since the conditions no longer change. The heat lost on high temperature side equals the heat gained on low temperature side.

3.2.2 Two Phase Flow Heat Exchanger

Figure 3.7 represents the temperature profile in a cross flow air-to-refrigerant heat exchanger. Refrigerant absorbs or releases heat by phase change depending on heat loss or heat gain. In this case, the refrigerant is heated and evaporated. We set up the refrigerant inlet temperature as 298 K and inlet quality as 0.1. Initially, the temperature in the heat exchanger does not change because the refrigerant is at two-phase state and the temperature is the saturation temperature. The refrigerant which

is close to outlet becomes superheated vapor with time and its temperature increases. The superheated region enlarges gradually, and the refrigerant temperature in this region keeps increasing until a steady state is reached.

Figure 3.8 shows the heat load profile of this heat exchanger. At the beginning, we set up the heat exchanger wall temperature equivalent to the refrigerant temperature. Once the heat exchanger is heated and the heat transfer starts, the temperature difference between air and heat exchanger wall decreases, and that between heat exchanger wall and refrigerant increases. Hence, the heat load of the refrigerant side keeps increasing as time elapses, and the heat load of the air side keeps decreasing at the same time. Later, once superheat region occurs in the refrigerant side, there is no boiling heat transfer any more and only convective heat transfer in this region, which causes a small overall heat transfer coefficient between air and refrigerant decrease. This is why the heat load on both sides decreases after a certain time period.

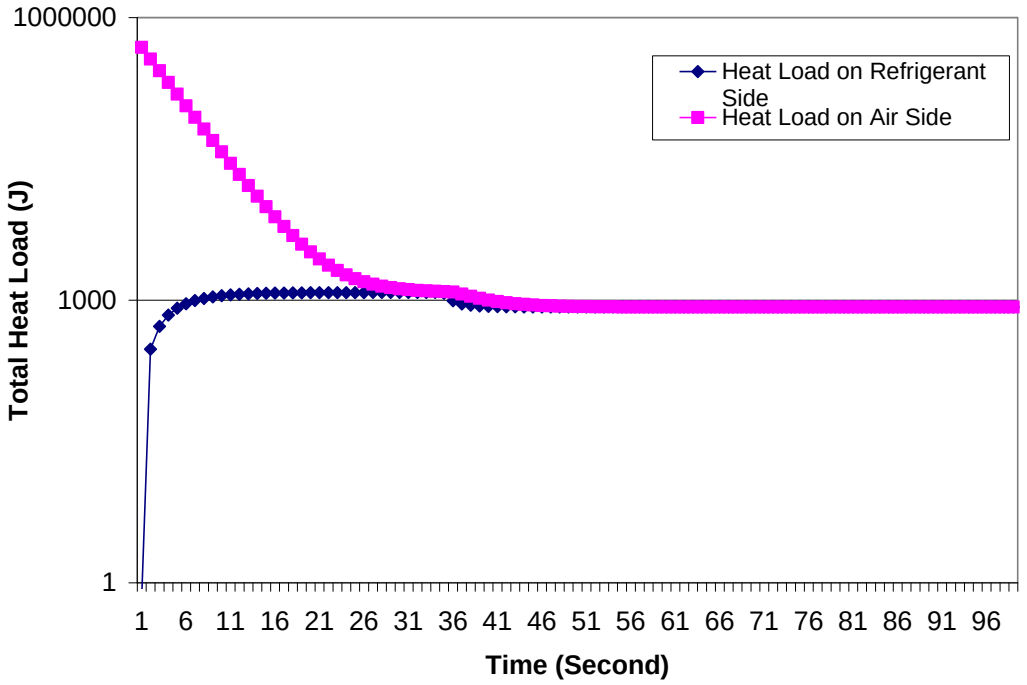

Figure 3.8 Heat load profile of an air-to-refrigerant heat exchanger

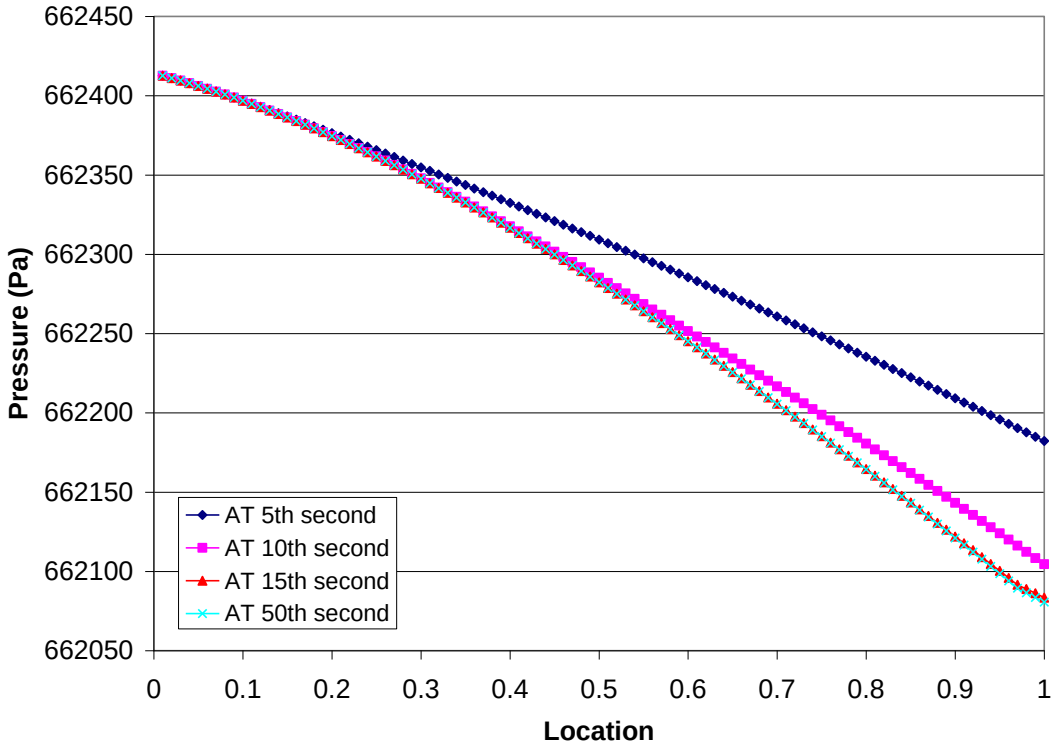

Figure 3.9 Pressure distribution of an air-to-refrigerant heat exchanger

Figure 3.9 shows the pressure distribution in an air-to-refrigerant heat exchanger with increasing time. The pressure (y-axis) is plotted as a function of the scaled location of the heat exchanger (x-axis). As the figure shows, from inlet to outlet, the heat exchanger pressure keeps decreasing due to the friction force, since refrigerant quality keeps increasing along the flow direction and with increasing time. This means more and more vapor is produced along the direction and refrigerant velocity also increases with time, and thus pressure drop becomes even larger.

Figure 3.10 shows the mass flow rate profile in an air-to-refrigerant heat exchanger. The x-axis is the scaled location of the heat exchanger. At the beginning of the simulation, we can see the mass flow rate continues to increase along the flow direction because the refrigerant is evaporated in the heat exchanger. With more and more refrigerant pushed out, the refrigerant inventory continues to decrease. Hence, in the heat exchanger, the total amount of refrigerant that could be evaporated becomes less and less until the heat exchanger inlet and outlet have the same mass flow rate and refrigerant inventory does not decrease any further.

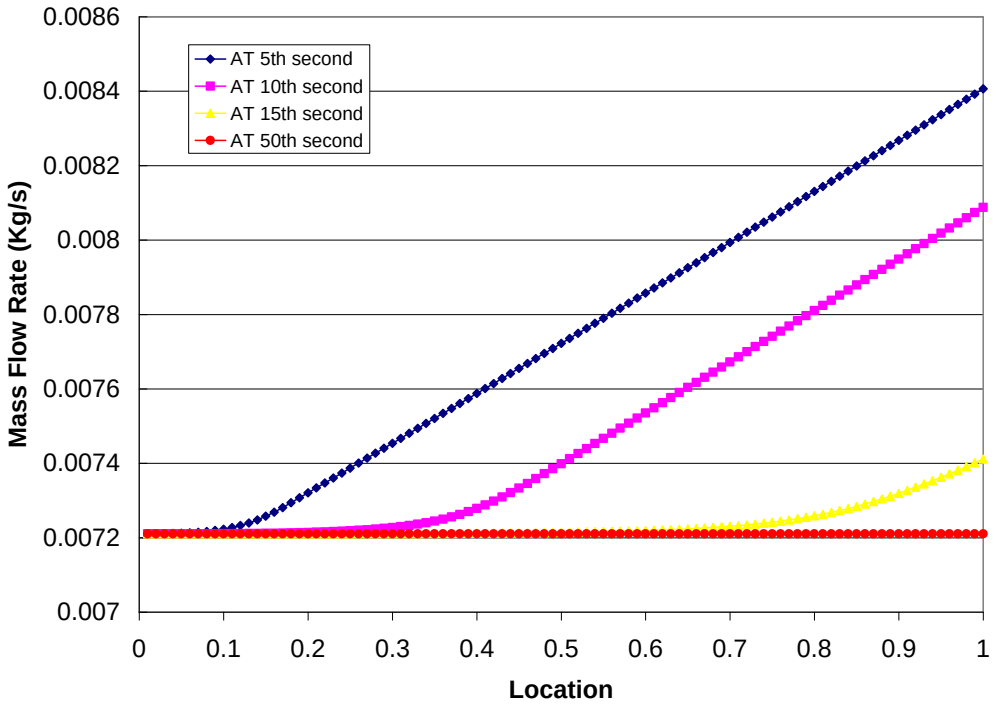

Figure 3.10 Mass flow rate profile in an air-to-refrigerant heat exchanger

3.2.3 Heat Exchanger on Wet Surface Conditions

Figure 3.11 to 3.16 shows the simulation results of a cross flow evaporator, which condenses the water vapor in the air and wets the surface of the evaporator. The initial conditions for this simulation are as follows: the air inlet temperature starts at 280 Kelvin with a relative humidity of 73%, and the refrigerant inlet temperature starts at 260 Kelvin with a refrigerant quality of 0.2. The length of the entire heat exchanger is 1 meter and is divided into 10 segments. The initial heat exchanger tube temperature and refrigerant temperature in the tube are both set at 260 Kelvin.

Figure 3.11 shows how the air outlet temperature changes with time at the exit of the heat exchanger. From the plot, we can observe how the air outlet temperature changes with time. At the beginning, the outlet air is at its lowest temperature in the

entire simulation period because the heat exchanger walls have the coldest temperature. Once the heat exchanger is gradually heated by warm air, the outlet air temperature also increases gradually because of the lower temperature difference and lower heat transfer between the air and heat exchanger.

Figures 3.12 and 3.13 show the heat exchanger capacity profile (y-axis) with time (x-axis). The figure clearly shows that the air-side capacity, including the sensible portion and latent portion, decreases gradually with time due to increasingly smaller temperature differences. In contrast, the refrigerant-side capacity gradually increases with time due to the increase in temperature difference.

Figure 3.14 shows the profile of the air relative humidity and its humidity ratio (y-axis) with time (x-axis) at the exit of heat exchanger. Since the cold tube surface temperature is below the dew point temperature of inlet air, the moisture in the air is condensed and removed by the heat exchanger. Once the heat exchanger tube becomes warmer with time passing, the dew-point temperature on the tube surface also becomes higher. Hence less moisture is removed, and both humidity ratio and relative humidity of outlet air increase at the air outlet.

Figures 3.15 and 3.16 show the air relative humidity and humidity ratio (y-axis) at different locations (x-axis) along with the heat exchanger. If the refrigerant regime in the heat exchanger is two-phase, the refrigerant temperature at the exit of the tube is lower than that at the inlet of the tube due to a pressure drop along the flow direction in the tube. Also, the tube temperature at the heat exchanger exit is colder than that at the heat exchanger inlet. Hence, a lower humidity ratio occurs at the location of the heat exchanger exit.

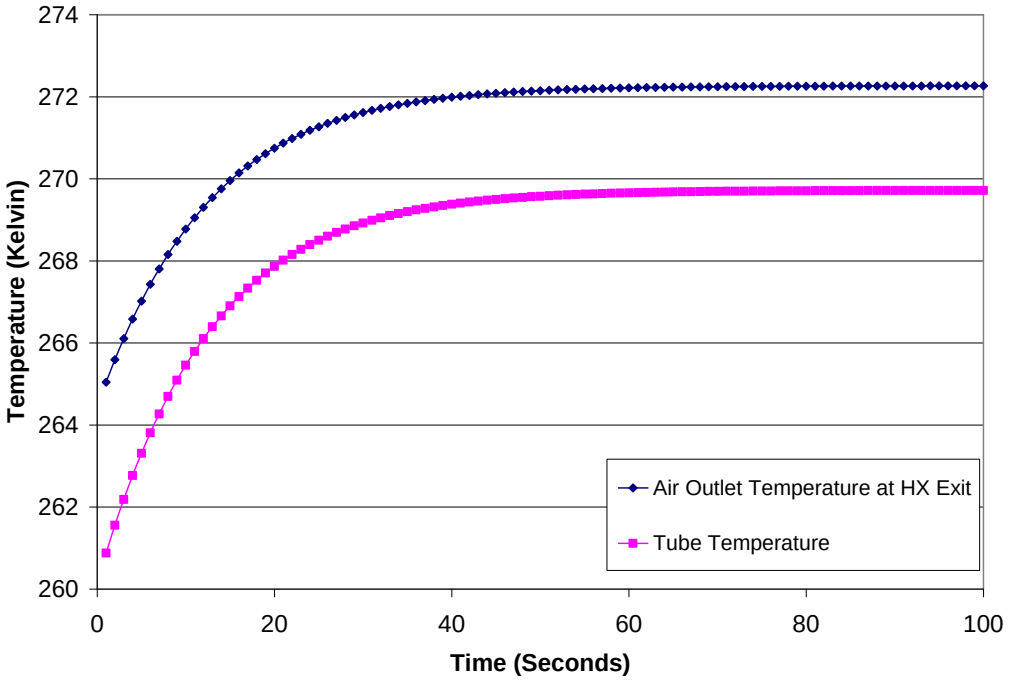

Figure 3.11 Air outlet and tube temperature profile

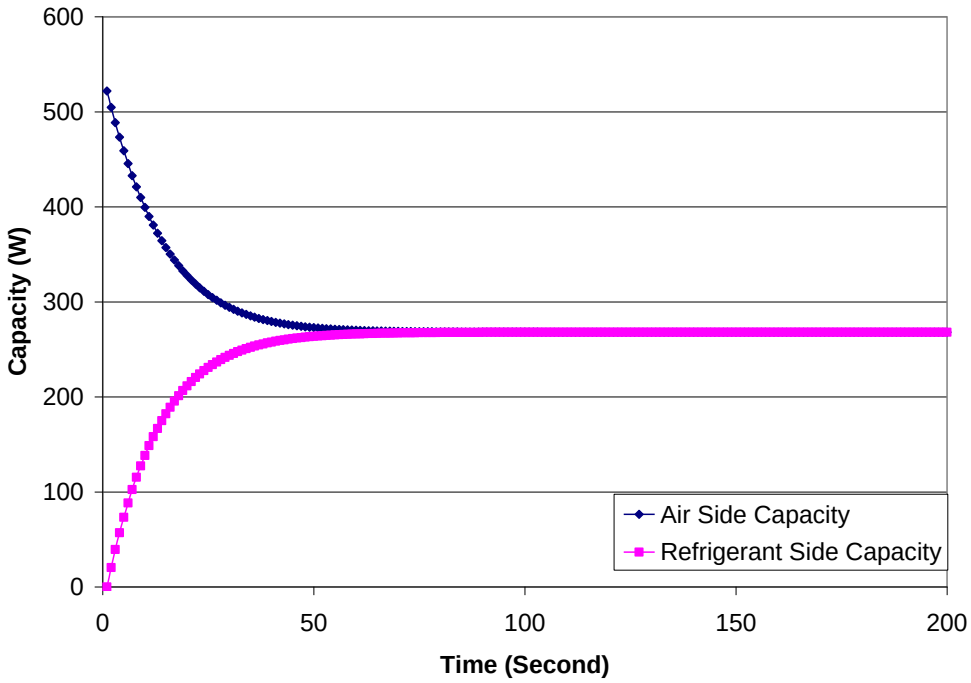

Figure 3.12 Air and refrigerant side capacity profile

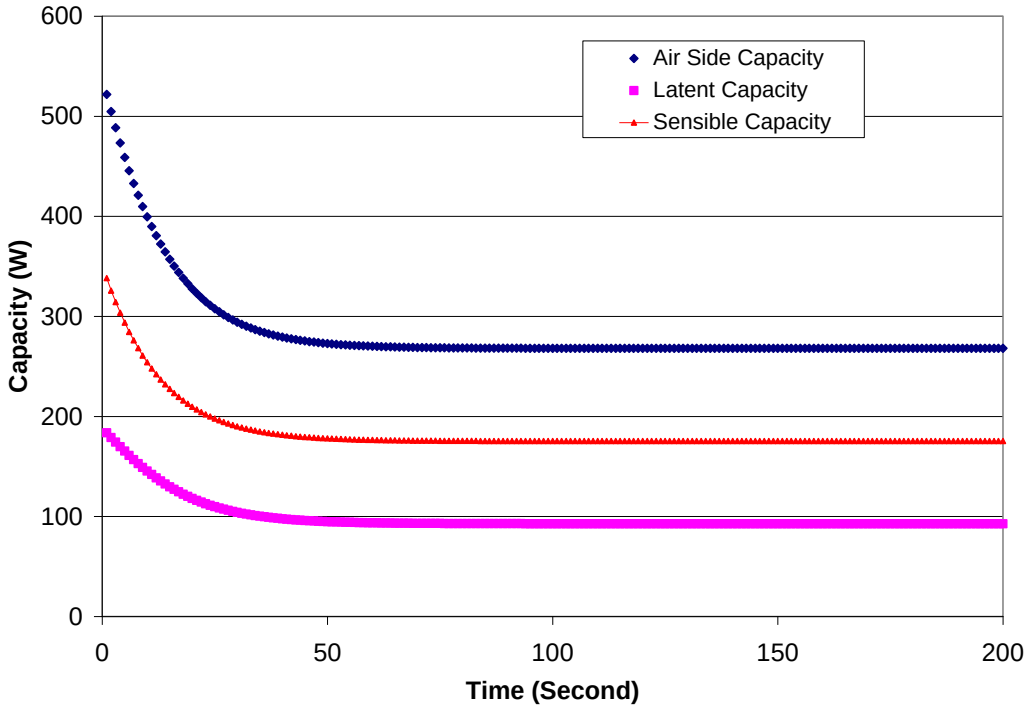

Figure 3.13 Heat exchanger sensible and latent capacity profile

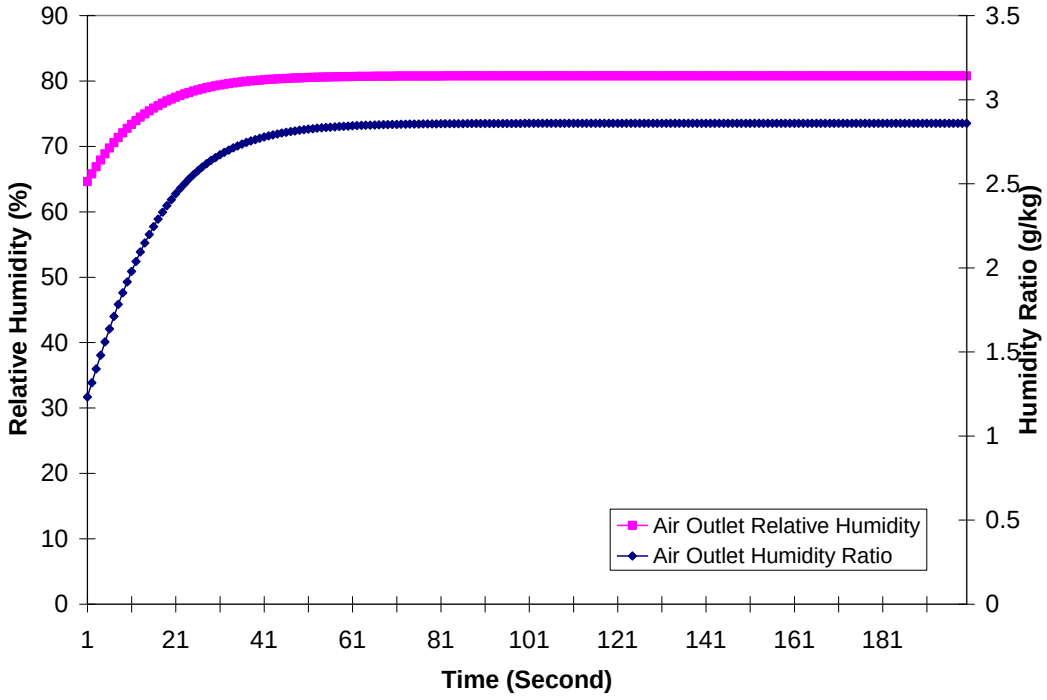

Figure 3.14 Air outlet humidity ratio and relative humidity profile

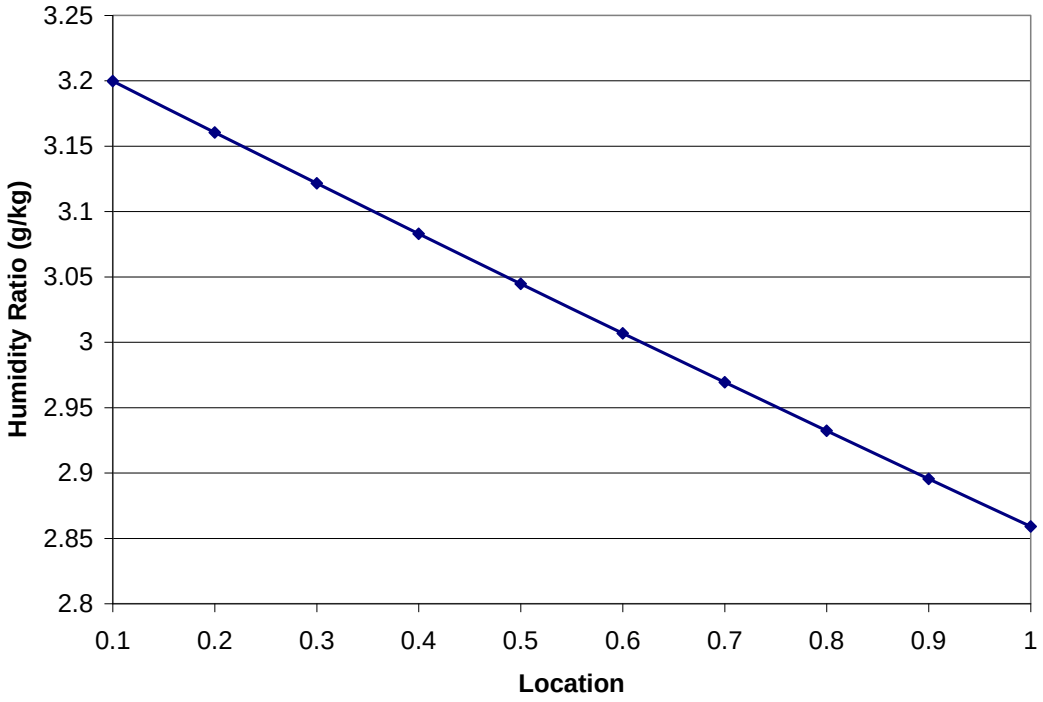

Figure 3.15 Relative humidity at different locations

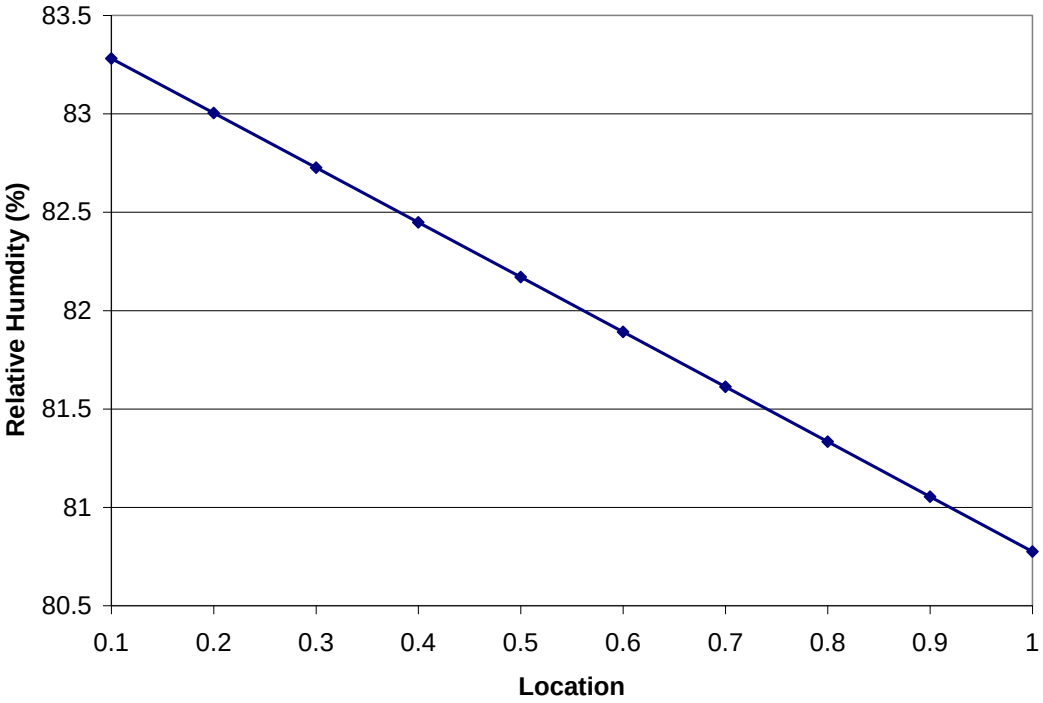

Figure 3.16 Relative humidity distribution at different locations

Figures 3.17 to 3.20 show the simulation results for the heat exchanger discussed above with the same inlet and boundary conditions except that the initial tube wall temperature starts at 280 Kelvin, which is same as the air inlet temperature.

In Figure 3.19, it is observed that there is no latent load at the beginning, which means that there is no water condensing due to a warm tube temperature. As the tube becomes colder and its temperature starts to be lower than the air's dew-point temperature, water condensing starts.

Correspondingly, in Figure 3.20, it is observed that the humidity ratio does not change at the beginning of the process, and the relative humidity is raised due to the temperature decreasing and reaching a peak value once the tube temperature is cooled to dew point.

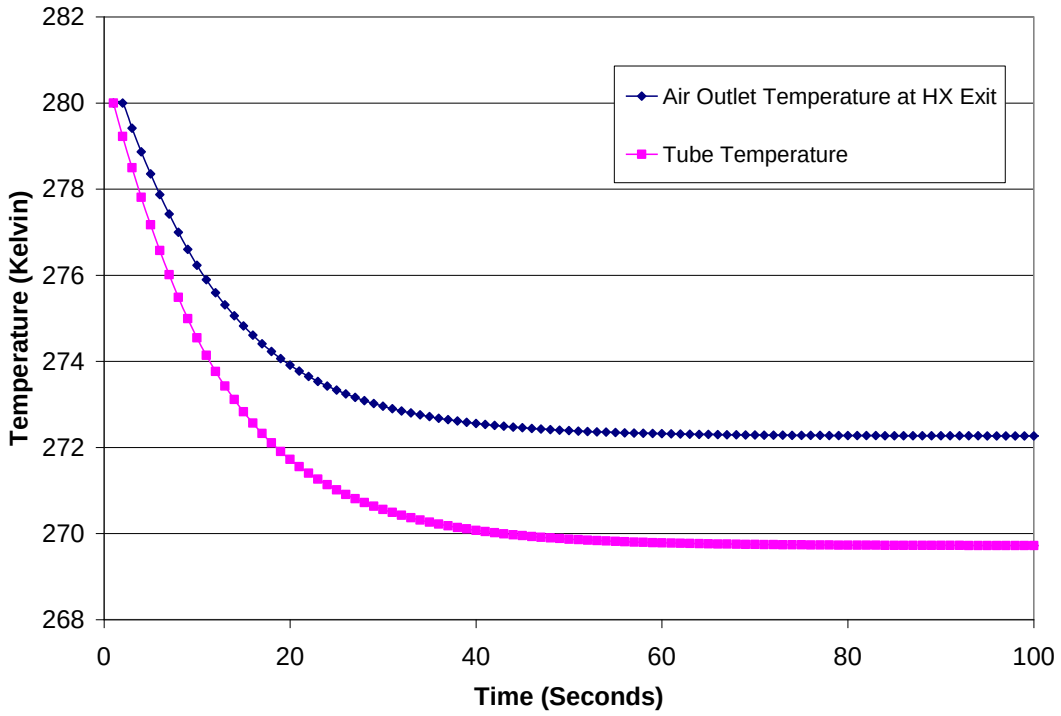

Figure 3.17 Air outlet and heat exchanger tube temperature profile

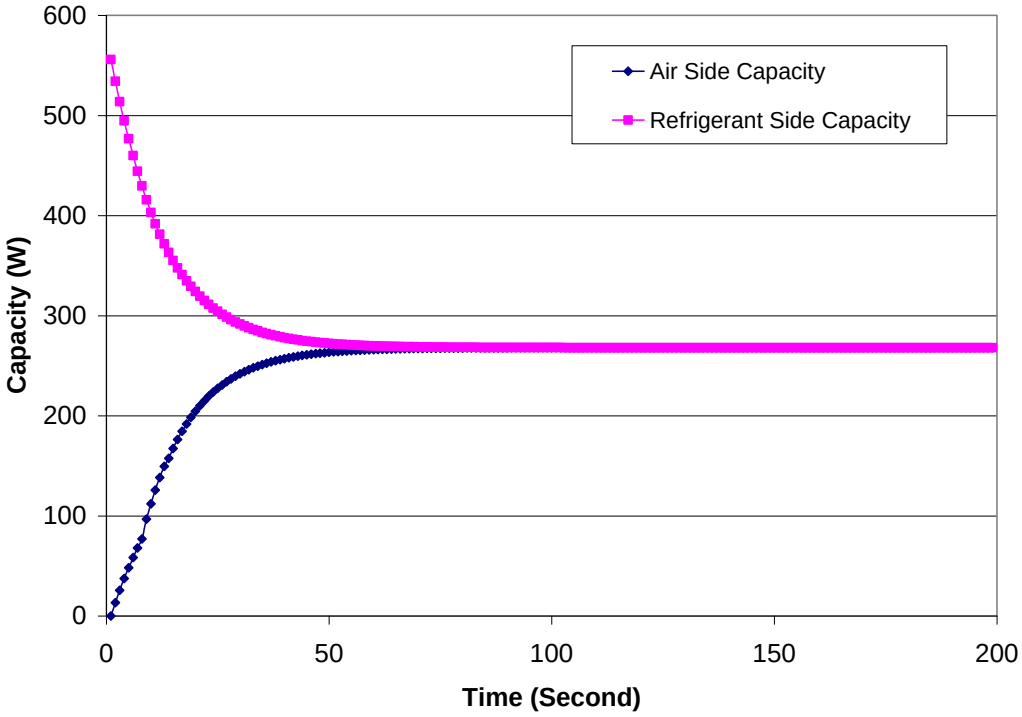

Figure 3.18 Air and refrigerant side capacity profile

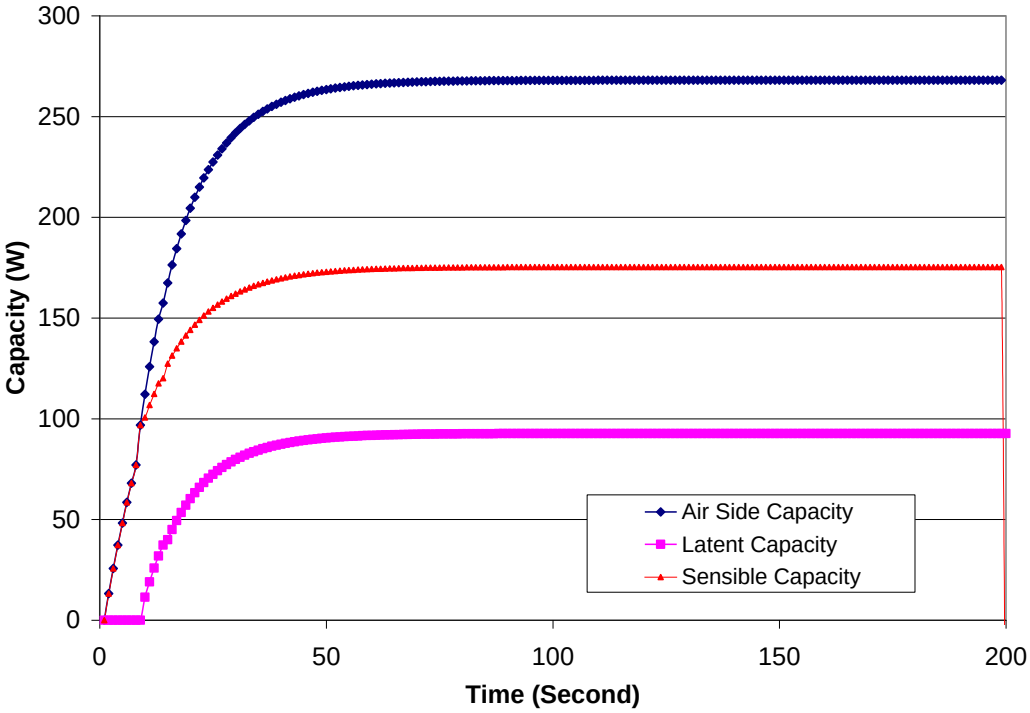

Figure 3.19 Heat exchanger sensible and latent capacity profile

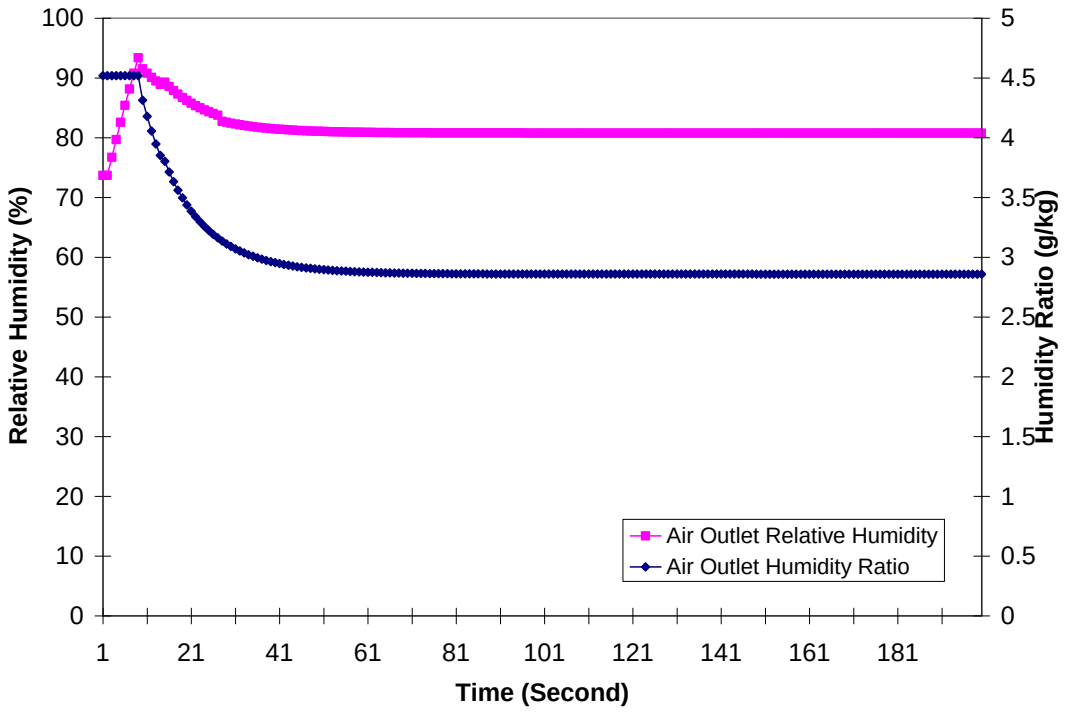

Figure 3.20 Air outlet relative humidity and humidity ratio profile

3.2.4 Suction Line Liquid Line Heat Exchanger

In order to simplify the problem, it is assumed that the heat exchanger is an adiabatic component. Hence there is no heat exchange between the heat exchanger and the environment. The inlet condition of liquid stream is subcooled liquid (entering temperature 303K, 7K subcooling), and the inlet condition of vapor stream is superheated vapor (entering temperature 265K, 5K superheating). Before the simulation starts, all liquid and vapor have the same properties as the liquid and vapor stream inlet conditions. The initial tube temperature is 280K.

Figure 3.21 shows how the vapor and liquid stream outlet temperatures change with time. Overall, the outlet temperature of the liquid stream decreases due to the temperature difference of two streams. However, it only decreases rapidly at

the start period but rises a little bit with time because the temperature difference only occurs at the start up period. The vapor stream outlet temperature keeps rising because the temperature difference between vapor stream and heat exchanger wall keeps rising as well.

Figure 3.22 shows the temperature distribution of this heat exchanger at steady state. The temperature (y-axis) is plotted as a function of the length of the heat exchanger (x-axis). The liquid temperature drops from its inlet to outlet and the vapor temperature increases from its inlet to outlet. The heat exchanger wall temperature is between the temperatures of the warm and cold streams to maintain a steady heat transfer between both fluids.

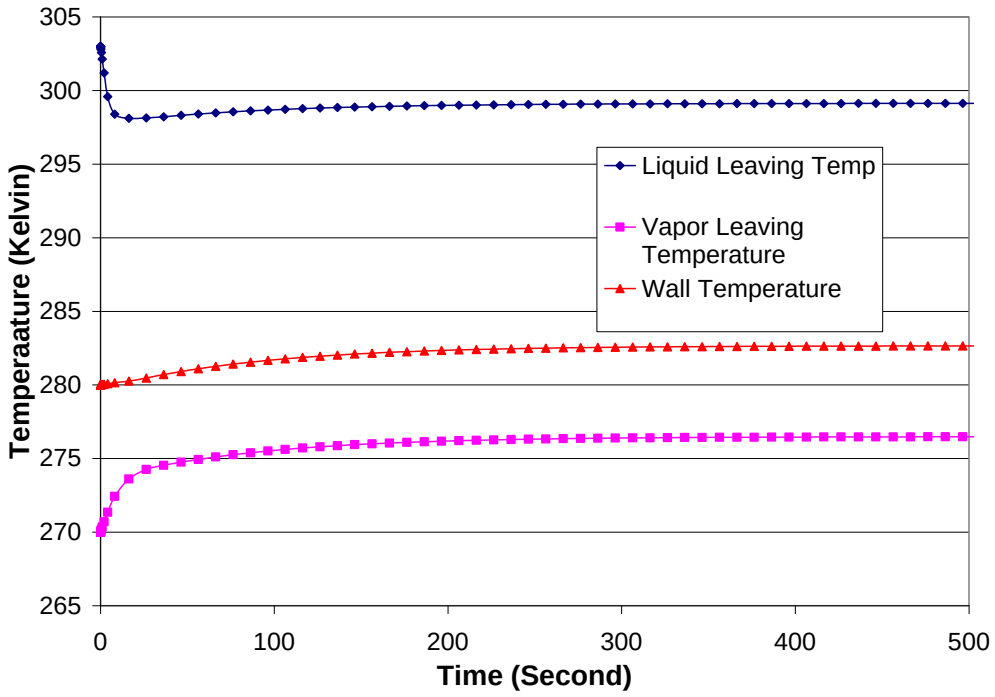

Figure 3.21 Temperature profile in the heat exchanger

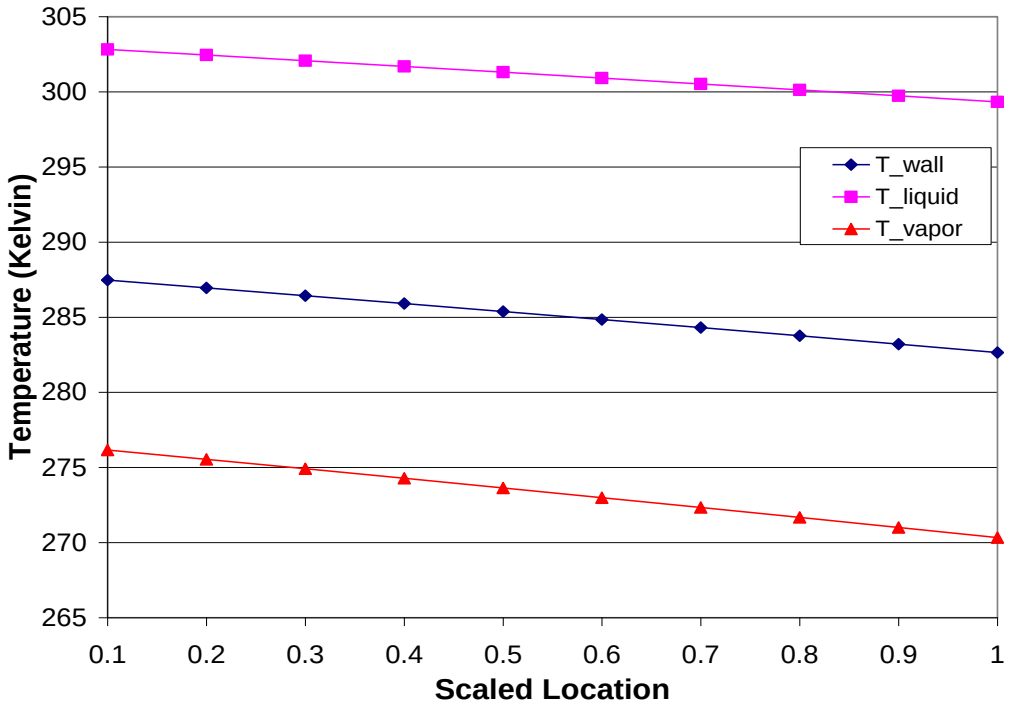

Figure 3.22 Temperature profile distributions at different Locations

3.2.5 Heat Exchangers in Parallel

Figure 3.23 shows the simulation results when two heat exchangers are located in parallel. Those two heat exchangers have the same initial conditions and boundary conditions in the simulation, but the length of the second heat exchanger is 10% longer and its entering air temperature is 2 degree higher compared to the first heat exchanger.

In this simulation, only the total mass flow rate is given and the mass flow rate of individual heat exchangers is obtained by using the residual equation described in Chapter 3.1.10. In this plot, it can be found that the inlet mass flow rate is not constant in each heat exchanger. The calculated inlet mass flow rates will slightly change at different times to ensure both heat exchangers having the same outlet

pressure. Since more refrigerant is evaporated in the second heat exchanger due to the longer length and higher air temperature, and if both mass flow rates don't change, the pressure drop in the second heat exchanger will become larger. Thus the inlet mass flow rate of the first heat exchanger slightly increases with time to keep both outlet pressures balanced. In addition, no matter how the inlet mass flow rate changes in individual heat exchangers, the total mass flow rate is always constant, which equals the given total inlet mass flow rate. The outlet pressure of the second heat exchanger looks slightly higher than the first heat exchanger at the steady state. This is due to the numerical tolerance which is used to determine the pressure balance. In this simulation, 1 pa is used as the tolerance, and the gap between both outlet pressures is always less than the tolerance.

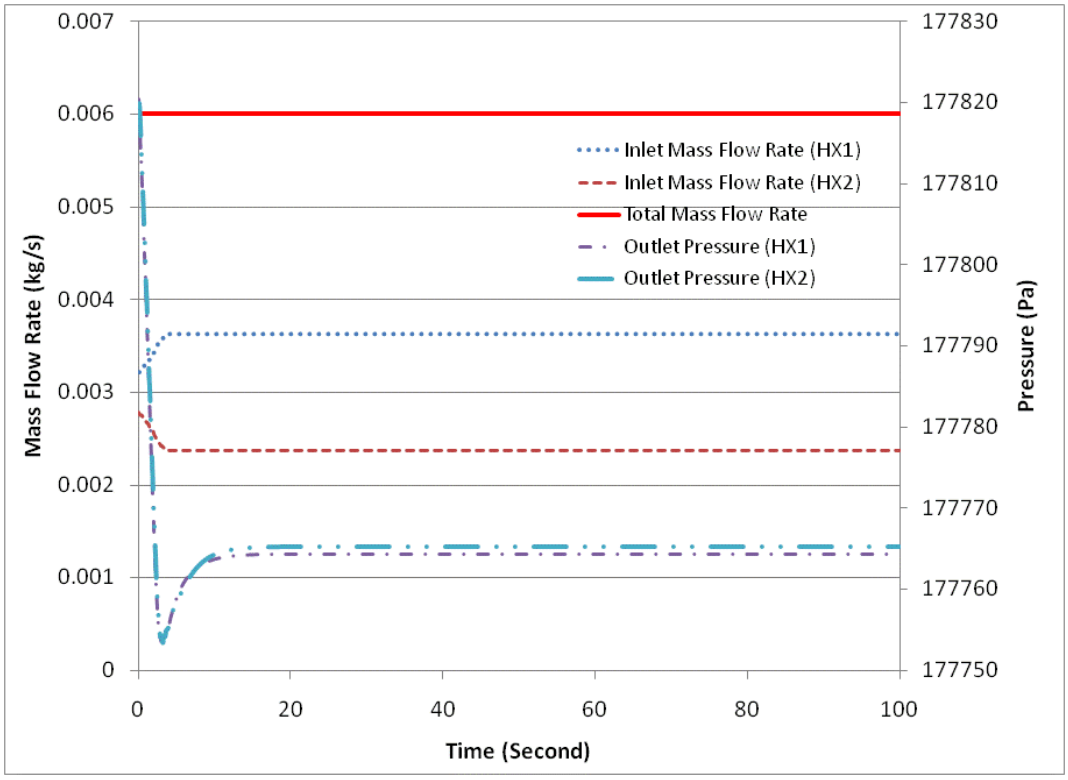

Figure 3.23 HX mass flow rate distribution and outlet pressure Profile

3.2.6 Heat Exchangers in Series

Figure 3.24-3.26 shows the simulation results for two heat exchangers in series. These two heat exchangers are exactly the same and are connected. Their initial and boundary conditions are exactly the same, except the air entering temperature of second heat exchanger is 2 degrees lower than the first heat exchanger.

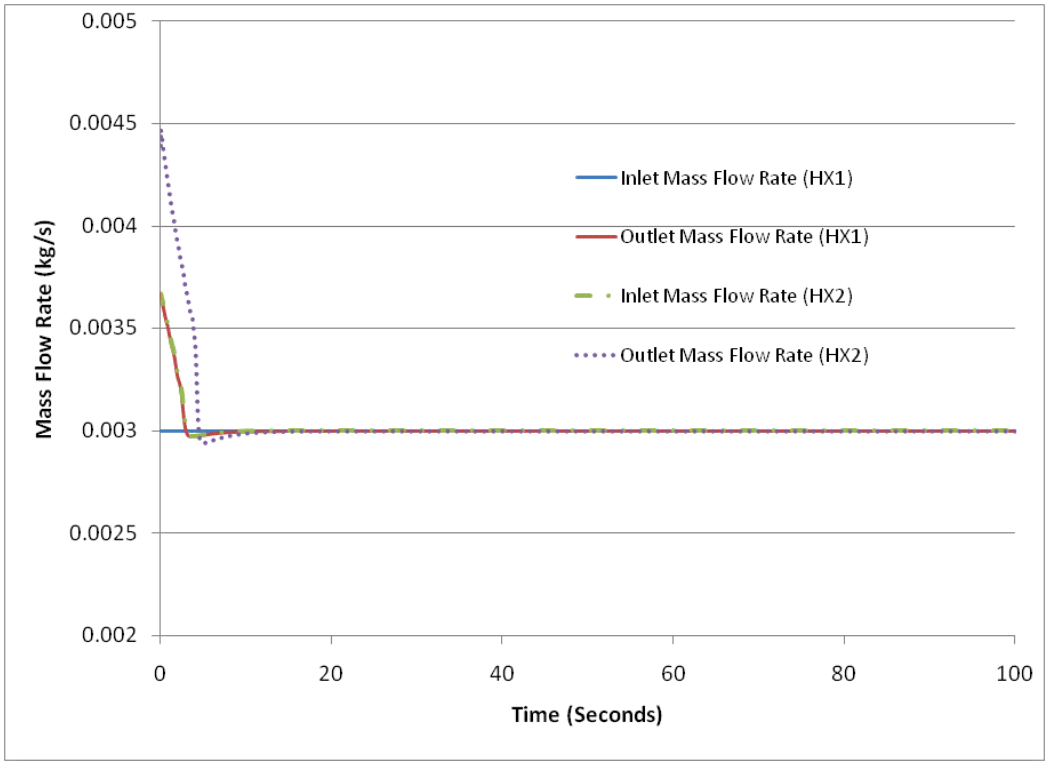

Figure 3.24 Inlet and outlet mass flow rate profile with time

The inlet and outlet mass flow rates of both heat exchangers are plotted in figure 3.24. Since the heat exchangers are connected in series, obviously, the outlet mass flow rate of the first heat exchanger is same as the inlet mass flow rate of the second heat exchanger. In both heat exchangers, the initial refrigerant quality is the same as the inlet quality of the first heat exchanger. When the refrigerant is warmed by the hot wall and air, refrigerant will be pushed out from the heat exchangers until a

stable flow rate is established and a steady state is approached.

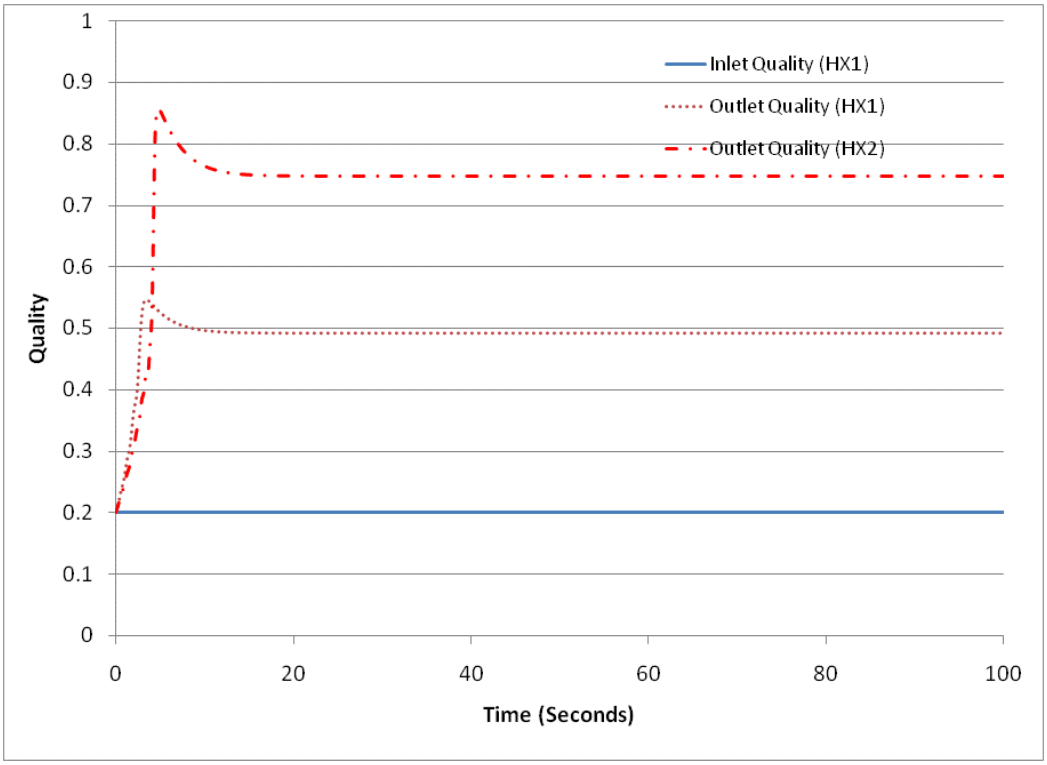

Figure 3.25 Refrigerant inlet and outlet quality profile with time

The heat exchanger inlet and outlet quality are plotted in Figure 3.25. The inlet quality of the second heat exchanger is not plotted due to its overlap with the first one's outlet quality. From the plot, it can be found that both outlet qualities increase with time. However, at the beginning, the outlet quality of the second heat exchanger is even smaller than the first heat exchanger, even though both heat exchangers are the evaporator type. This is because the refrigerant quality is not only impacted by heat transfer but also the initial condition and internal energy change caused by pressure drop. At the beginning, the increased internal energy in the second heat exchanger might be more than the transferred heat between the wall and refrigerant.

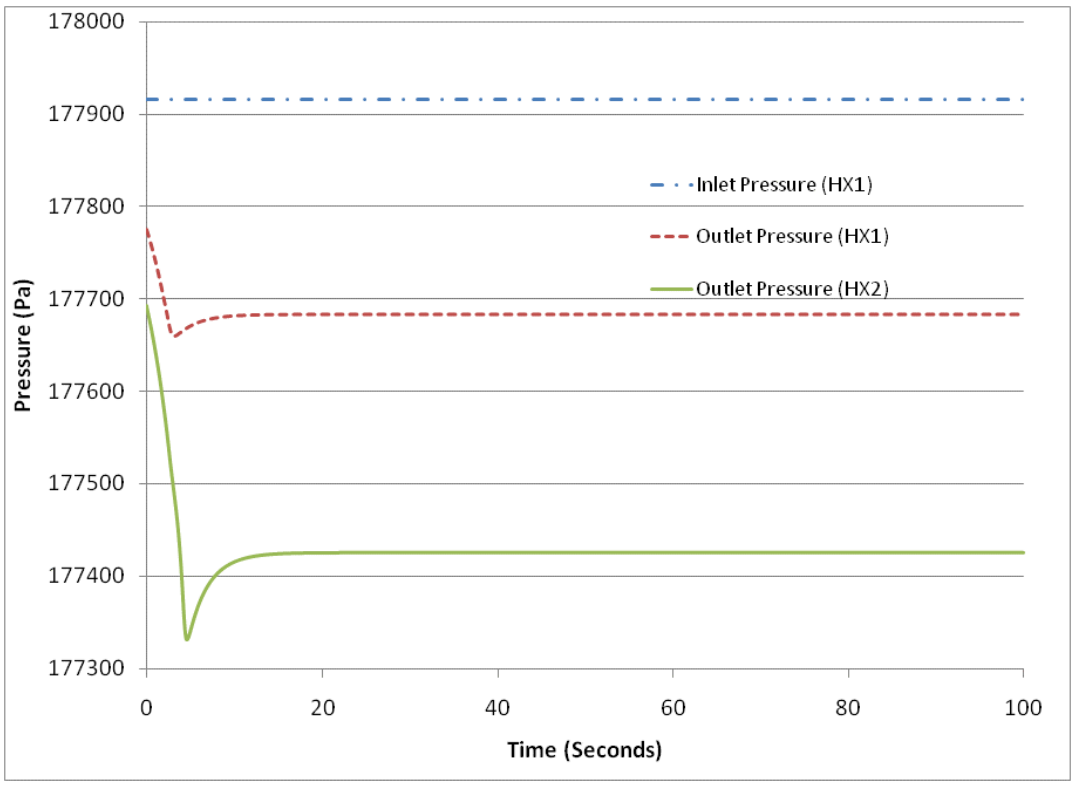

Figure 3.26 Inlet and outlet pressure profile with time

The inlet and outlet pressure profiles are shown in Figure 3.26. The second heat exchanger inlet pressure profile is also ignored in the plot due to the overlap with the outlet pressure of the first heat exchanger. Since the vapor phase weight is increased in both heat exchangers, the pressure drops in both heat exchangers increase with time; but the pressure drop in the second heat exchanger is larger due to a higher vapor quality in the heat exchanger.

3.2.7 Validation with a Steady State Simulation Tool

Since experiments have not yet been performed specifically to validate our simulation results, here we will compare our preliminary results with those obtained from another simulation for steady-state conditions. This steady-state simulation tool

(CoilDesigner) (Jiang et al., 2002, 2006) has been validated extensively and has shown very good agreement with measured data. The results from our generic dynamic model and Jiang's modeled result will be compared. The agreement between the two will show the validity of our method.

The heat exchanger used for this comparison is a very simple one: a single-row evaporator with cross-flow air, as shown in Figure 3.27. The tube diameter is 0.5 inches and the total length of tube is 1 meter. These parameters were taken from the simulation settings in Jiang's simulation tool.

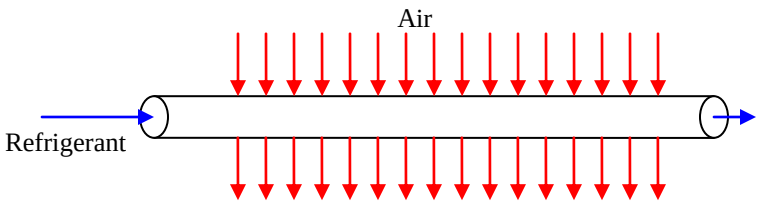

Figure 3.27 Schematic of a simple heat exchanger

In the first application, the refrigerant inlet temperature was set at 280.15 K, the inlet quality at 0.2, and the air inlet temperature at 290 K. The same tube geometries were used in both the steady-state software (Jiang's model) and our generic heat exchanger model. At steady-state conditions, the following results were obtained:

	Steady-State Simulation Tool (Jiang's model)	**Generic HX**
Heat Load	121.83 W	122.74 W
Pressure Drop	95.96 Pa	95.01 Pa
Outlet Quality	0.36	0.3583

Table 3.1: Results comparison for an evaporator simulation

The second application employed the same tube geometry but different inlet and boundary condition settings: the refrigerant inlet temperature was 325 Kelvin, the inlet quality was set as 1.0 and the air inlet temperature was 300 Kelvin. At steady state conditions, the obtained results were:

	Steady State Simulation Tool	**Generic HX**
Heat Load	247.96 W	249.398 W
Pressure Drop	1666.74 Pa	1697.7 Pa
Outlet Quality	0.45	0.436

Table 3.2: Results comparison for a condenser simulation

Both models yield agreed results of 248 Watt on heat load, pressure drop and outlet quality for the two applications with very different refrigerant condensing and evaporating conditions. The agreement between the two models is excellent: less than 2% difference is observed. This validates our model at steady-state condition. The comparison of our model with the sophisticated heat exchanger simulation tool legitimizes our model's mathematics and algorithm implementation.

3.2.8 The Effect of Changing Segment Size

The segment size will affect the accuracy of the results and the execution speed. A large segment size will reduce the computing time but increase inaccuracy because the thermal properties in this segment come from the average value of inlet and outlet conditions in this model. A small segment size improves the model accuracy due to better estimating on segment average thermal properties, but if

sufficient accuracy can be reached with a larger size, choosing a smaller segment size becomes unnecessary and computationally expensive.

Figure 3.28 compares the results for different segment sizes. It shows the effects of segment size implemented on the same air-to-air heat exchanger used with the simulation tool discussed above. In the simulation the heat exchanger had a length of 0.4 meter and was divided into 5, 10, 20, and 40 segments. Different simulations were performed until a steady-state condition was met. The result with 5 segments differs greatly from those with more segments (10-40). By increasing the number of segments to 10, the curve lies lower. However, the temperature curve saturates with further increase in segments. The difference on the curves with 20 segments and 40 segments is very small and can be ignored, which means that further increasing the number of segments (i.e., >20) will not increase accuracy to a noticeable extent. A segment number of 20 may be adequate in this case. In other words, a segment length of 0.01~ 0.02 meters is probably appropriate for heat exchanger simulation using combined finite volume and moving boundary algorithm. Therefore, this segment length was used most often for the rest of the simulations in this thesis.

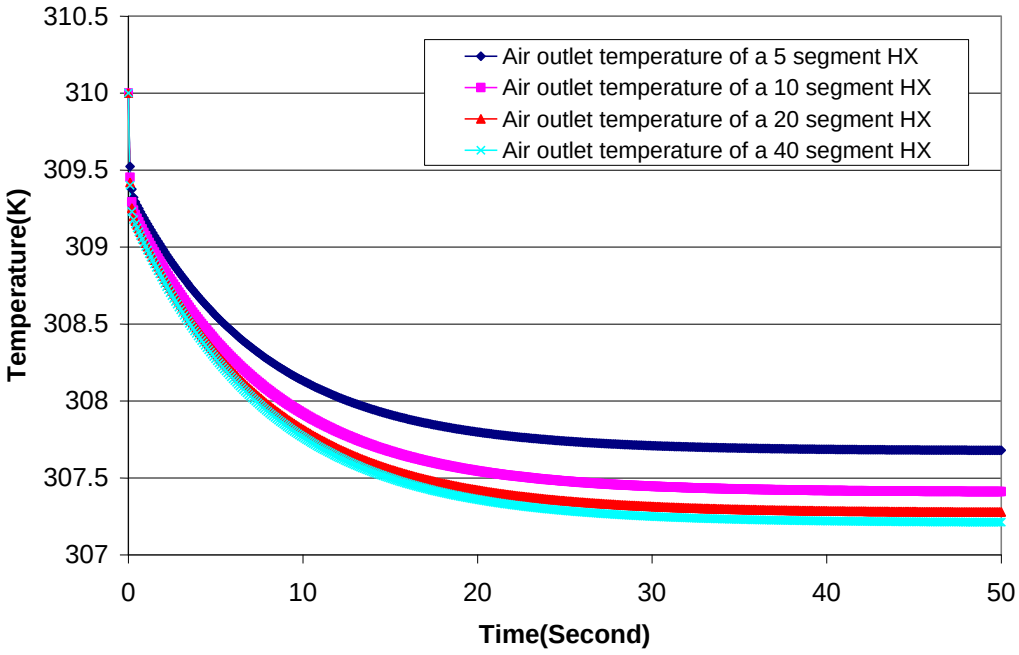

Figure 3.28 Temperature comparison for different segment sizes

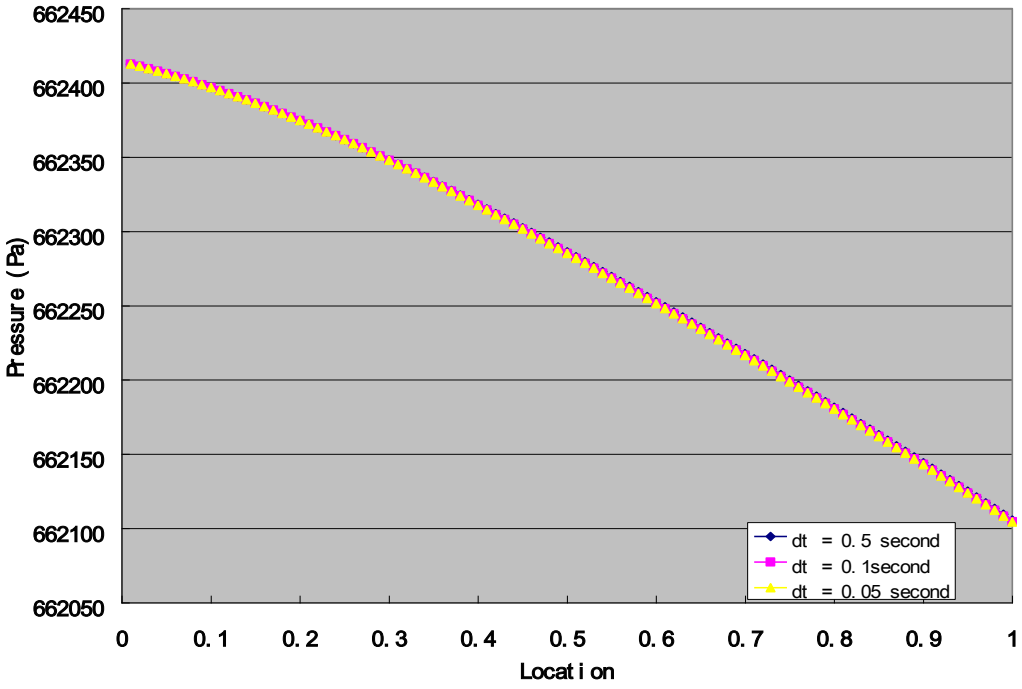

Figure 3.29 Pressure comparison for different time steps

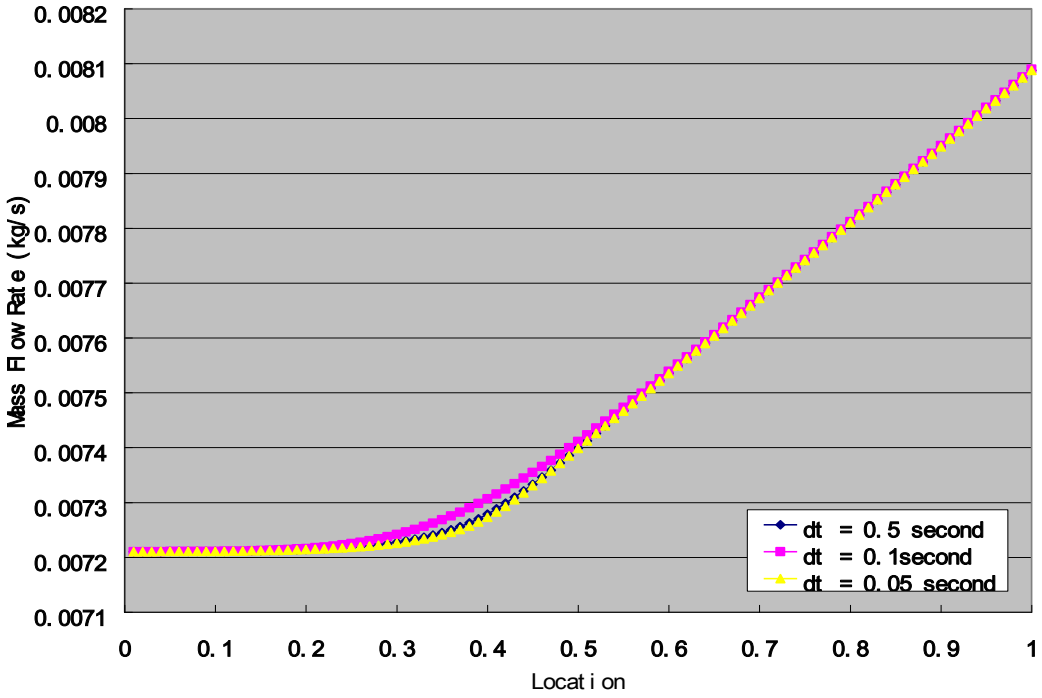

Figure 3.30 Mass flow rate comparisons with different time steps

3.2.9 Time Step Dependency Study

Time step significantly affects the computation speed and time-dependent characteristics. The time step can be either a fixed value or a variable determined by time and derivatives. Because there is a trade-off between computing time and accuracy, it is important to find the optimal time step to balance the two.

Figure 3.29 and Figure 3.30 show the results of pressure drop and mass flow rate to demonstrate the impact of different time steps. The time steps in the test vary from 0.05-0.5s. The time step in this range does not affect the result significantly, as seen from the good overlap between the three curves. However, the computation time decreases roughly 10 times when the time step increases from 0.05s to 0.5s.

Therefore, we will use 0.5 seconds as the time step size throughout this model. It is worth noting that if the heat exchanger is integrated in a vapor compression system, a smaller time step might be desired at the starting period of the compressor. This is because during the starting period, some parameters (e.g., mass flow rate) of the compressor are very sensitive to time step size and may be dramatically affected.

3.2.10 Adaptive Time Step Algorithm Testing

The proposed adaptive time step algorithm is already discussed in Chapter 2. In order to test this algorithm, this method is implemented into the generic heat exchanger model to compare with the results using fixed time step values. In this simulation, a total 300-second simulation time is run, which is long enough to ensure steady state is approached. In the simulation, the most dramatic changes of the heat exchanger performance happened in the first 10 seconds. From the heat exchanger wall temperature profile of the first 10 seconds (Figure 3.31), it can be found that the result accuracy is not impacted much if the time step size is less than 0.1 second or the adaptive time step algorithm is used. Once a 300-second simulation is finished, it can be observed that the total computational time of the test case that uses variable time step algorithm is only 59.8%, 10.1 and1.97% compared to the other three test cases (Figure 3.32).

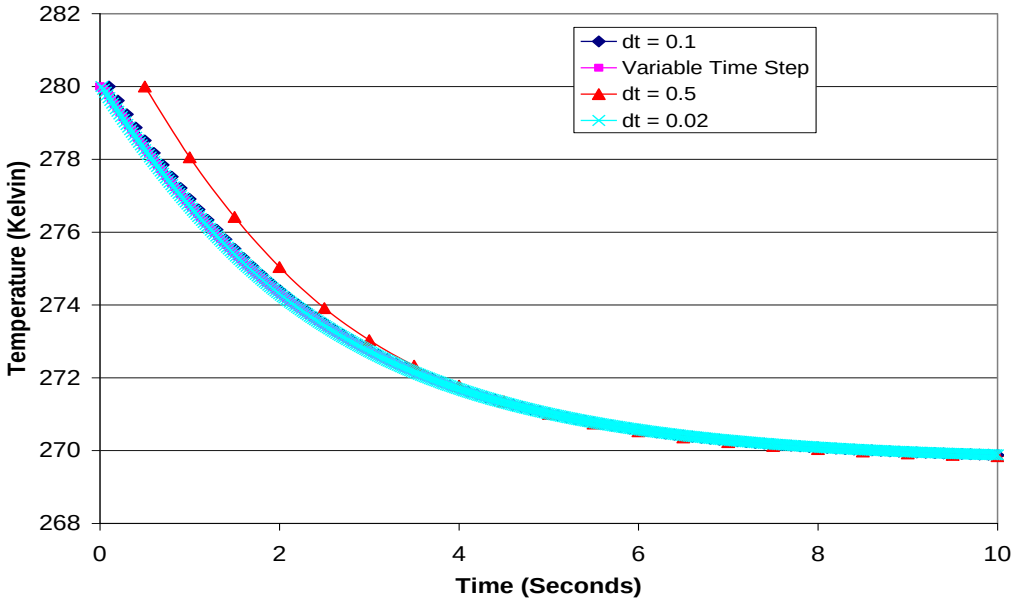

Figure 3.31: HX wall temperature profile with different time step sizes

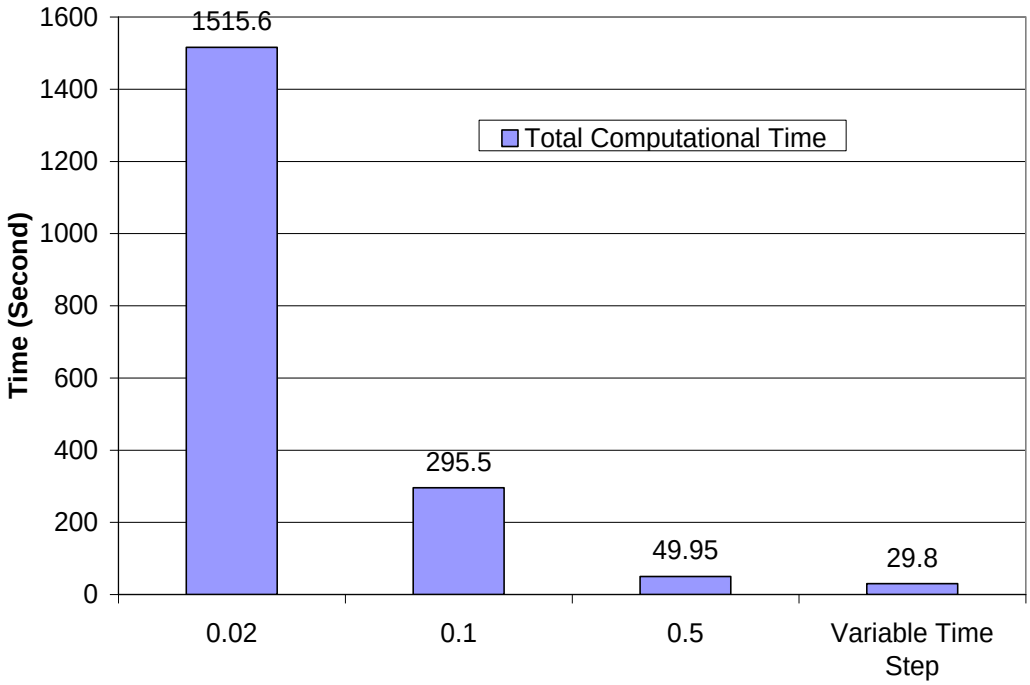

Figure 3.32: Total simulation time comparison

Compared to the existing adaptive time step methods, the proposed method simplifies the calculation procedure and reduces the calculation time which is needed to determine the new time step size. This method also maintains the accuracy level of the results, compared to the methods using a small fixed time step. The only disadvantage of this method is that when a large time step size is being used but the system performance has a sudden and dramatic change, the reduced time step size may not be small enough to ensure the accuracy in a few time steps. However, this disadvantage can be compensated if a reasonable maximum time step is predefined in the algorithm or a new algorithm to address such cases in introduced.

3.3 Simulation of a Generic Compressor

An accurate compressor model must take into account many processes and interactions within a real compressor. Many models of different complexity levels have been developed in previous studies. Simple ones use simple curve fitting models, whereas complex ones must resolve many sets of multi-dimensional energy, momentum and mass balance equations.

One of the earlier compressor models that did not implement the ideal gas assumption was developed by Ng (Ng et al., 1976). This model has three control volumes for which continuity, momentum and energy equations are solved. The compression process is assumed to be adiabatic. The refrigerant flow is assumed to be one-dimensional. However, it was developed for a steady-state simulation only.

One of the most simple and frequently used models is the curve fit approach. It models the compressor by curve fitting the experimental data or compressor map. Murphy and Goldschmidt (1985) defined the compressor mass flow rate, discharge state and power as a function of suction states and pressure ratios using this method. This type of model is accurate for a steady state simulation, but is not generic for other applications. In addition, the transient effects were neglected.

MacArthur (1984) developed a complex distributed parameter compressor model. This model divides the compressor into different states, and the compression process is assumed to be polytropic and isentropic. Heat transfer between different compressor sections is considered, and thermal storage is accounted for. However, the compressor was assumed to rotate at a constant angular velocity, and valve dynamics are neglected.

Welsby et al. (1988) developed a general lumped-parameter compressor model for an air conditioning and heat pump simulation. In this model the compressor rotates at a constant speed and does not account for volumetric efficiency. This means that the volume flow rate though the compressor is constant. The compressor power and discharge state were determined by assuming a polytropic compression process with a constant polytropic index. This model neglects transient effects of thermal storage and variable RPM.

Compared with other models, Lio's model (Lio et al., 1994) solved one-dimensional conservation equations by dividing the compressor into several control volumes. In addition, a finite element method was used to model the motion of valves. This model gives a more accurate representation of the dynamics of a

compressor.

Wang et al. (2000) developed a centrifugal chiller dynamic model, which includes a two-stage compressor. The centrifugal compressor is modeled in extensive detail using the conservation equations of mass, energy and angular momentum and the appropriate velocity triangles across the inlet guide vanes and the impeller. The process is assumed to be polytropic and isentropic. They also assume that both stages have the same compression ratio and that the compression ratio equals the expansion ratio.

These modeling techniques and others not discussed here can be classified into simple lumped methods and complex distributed methods. In the first approach, the compressor is considered as a lumped system, and the compression is a polytropic and isentropic process. The power is determined by suction pressure and discharge pressure. Usually the valve dynamics are neglected. In the second (distributed models), the compressor is divided into several control volumes. Usually the valve dynamics are considered.

3.3.1 Generic Compressor Model

Even the geometry of a compressor is very complex in different compression methods. From the modeling point of view, the entire compressor can be divided into three parts: the suction section, compression section, and discharge section. The suction section and discharge section can be treated as a simple heat exchanger, and the previously discussed heat exchanger model in Chapter 3.1 can be implemented for both sections. The compression section is the key component of the entire

compressor, where two working properties, given below, are used to evaluate the compressor performance:

Volumetric efficiency, $$\eta_v = \frac{\dot{m}_{actual}}{\dot{m}_{\max}} = \frac{\dot{m}_{actual}}{\rho VRPM} \tag{3.18}$$

Isentropic efficiency, $$\eta_s = \frac{\dot{W}_{isen}}{\dot{W}_{actual}} \tag{3.19}$$

where the RPM is the compressor speed (compressor speed in revolutions per minute) and V is the displacement volume.

In the compression section, in order to simplify the model, it is assumed there is no mass storage in the compression section; hence, the mass balance equation can be simplified as:

$$\dot{m}_{in} = \dot{m}_{out} \tag{3.20}$$

The inlet mass flow rate is calculated by

$$\dot{m}_{in} = \rho V_{dispalcement} RPM \eta_v \tag{3.21}$$

In this equation, the volumetric equation is calculated (Arora, 1981) using the relation

$$\eta_v = 1 + c - c\left[\frac{P_{out}}{P_{in}}\right]^{\gamma} \tag{3.22}$$

$$c = \frac{V_{clearance}}{V_{displacement}} \tag{3.23}$$

where $V_{clearance}$ is the clearance volume; $V_{displacement}$ is the displacement volume of the compressor, and γ is the polytropic expansion coefficient.

Once we know the volumetric efficiency, isentropic efficiency and mechanical efficiency (the latter two coefficients vary with compressor model and are rated by the manufacturer), the outlet conditions of the compressor can be determined as:

$$h_{out} = h_{in} + \frac{(h_s - h_{in})}{\eta_s \eta_m} \tag{3.24}$$

The work done by the compressor is

$$\dot{W} = \frac{\dot{m}(hs - hin)}{\eta_s \eta_m} \tag{3.25}$$

where h_s is the enthalpy for isentropic compression and η_m is the mechanical efficiency of the motor.

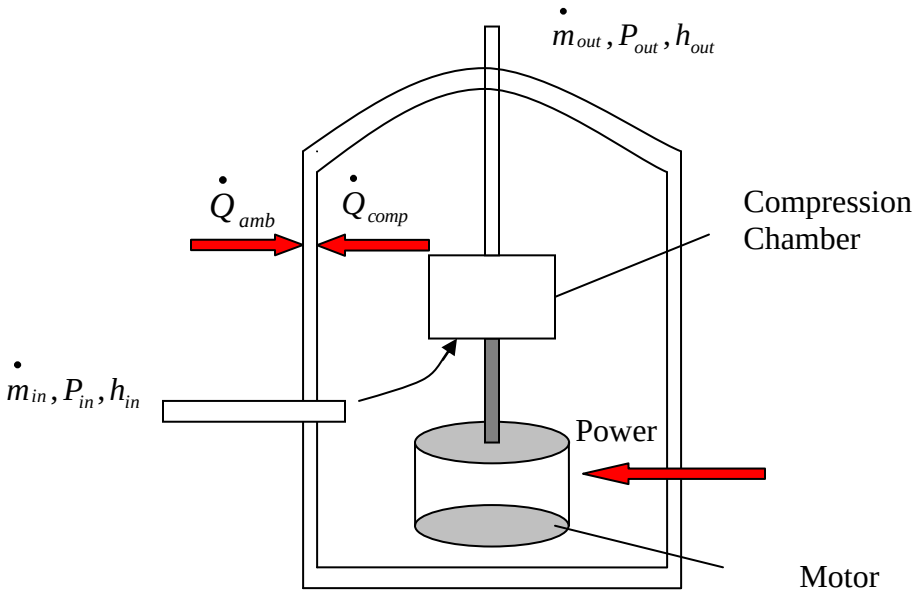

Figure 3.33 Schematic of a reciprocating compressor

In a dynamic vapor compression system, the compressor inlet condition changes very quickly once it starts to run. However, the refrigerant state in the compressor will be influenced by the heat rejection from the motor to refrigerant and by heat transfer between refrigerant and the compressor shell. Due to the thermal characteristics of the metal shell that houses the compression chamber and motor, the transient response of the shell temperature is relatively slow. Once the shell is treated as a lumped element, the shell temperature can be calculated from

$$\begin{aligned} C_{shell}\frac{dT_{shell}}{dt} &= \dot{Q}_{amb} - \dot{Q}_{comp} \\ \dot{Q}_{amb} &= (UA)_o (T_{shell} - T_{amb}) \\ \dot{Q}_{comp} &= (UA)_i (T_{ref} - T_{shell}) \end{aligned} \qquad (3.26)$$

where T_{shell} and C_{shell} are the shell temperature and effective capacitance, and $\dot{Q}_{amb}$ and $\dot{Q}_{comp}$ are the rate for heat transfer from the ambient and refrigerant to the compressor shell.

This model is capable of a generic simulation for different types of compressors. It requires only the input of the operating characteristics and geometry information of the compressor. Once the thermodynamic boundary conditions (inlet and outlet pressure, inlet enthalpy) and initial conditions are provided, the model can calculate the mass flow rate of the compressor and its outlet parameters.

3.3.2 Simulation Results of the Generic Compressor Model

Since the boundary condition of the compressor model includes the compressor suction and discharge pressure, an idealized condenser and evaporator is assumed to exist which provides mimic condensing and evaporating pressure as a function of time. The compressor inlet mass flow rate is calculated by equation 3.20, and will be fed into the generic component framework with other inlet conditions. Compare to the generic heat exchanger model , the outlet pressure in the compressor model will not require any calculation or correlations but be directly assigned based on either the pre-defined boundary condition or a given value from system simulation.

Figure 3.34 shows how a compressor inlet and outlet pressure ratio changes with time. Before the compressor starts up, the condenser side and evaporator side have equal pressures at room temperature as the expansion device is opened. Once the compressor starts up, the suction pressure and discharge pressure change dramatically, and the pressure ratio increases greatly in a short time period.

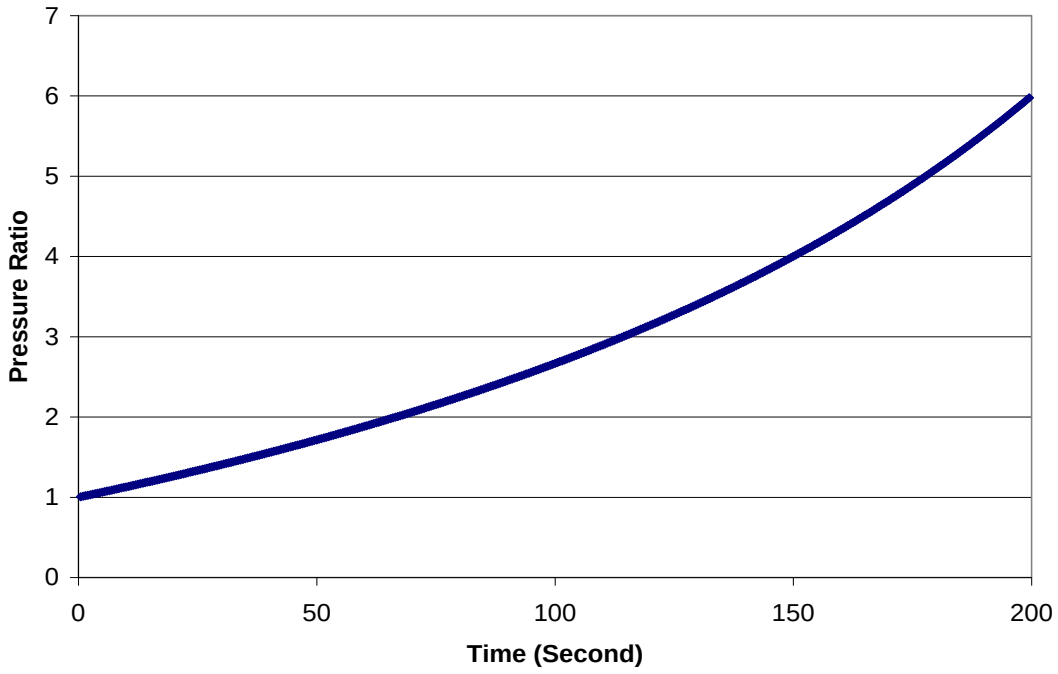

Figure 3.34 Compressor inlet and outlet pressure ratio

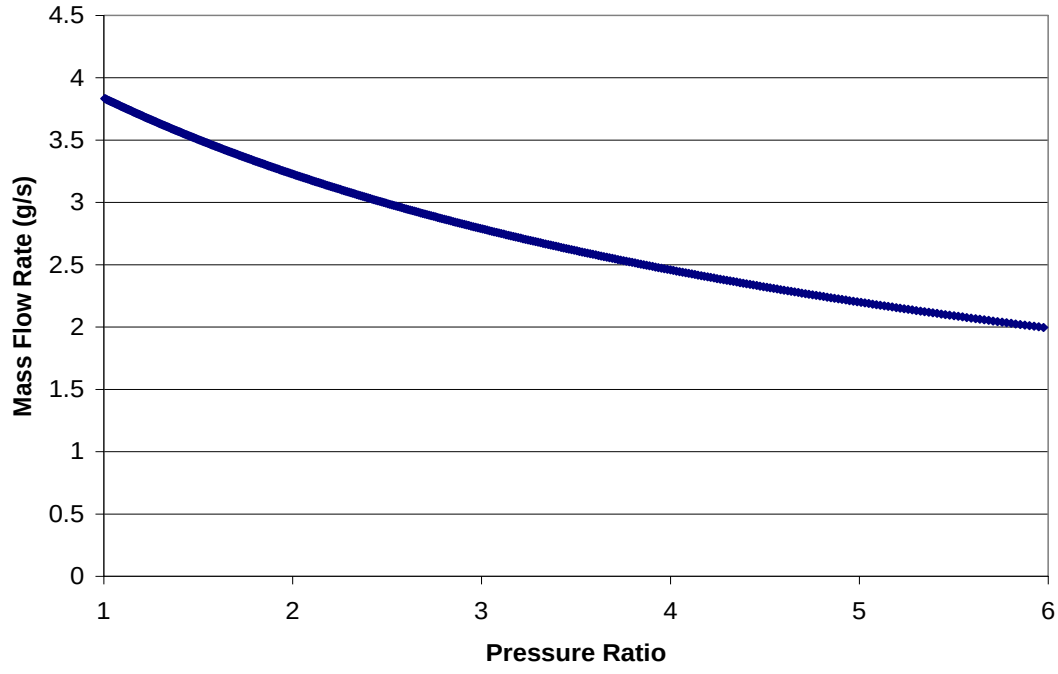

Figure 3.35 Compressor mass flow rate at different Pressure ratios

Figure 3.35 demonstrates how the compressor mass flow rate changes after its start-up. In this simulation, a 4°C degree superheat is provided at the exit of the mock evaporator. Meanwhile, the change of pressure ratio is shown in Figure 3.26, which shows that at the beginning, a maximum mass flow rate occurs due to the high evaporating pressure. Once the evaporating pressure decreases with time, the mass flow rate of the compressor decreases as well.

In practice, the inlet of the compressor must be vapor because liquid could damage the compressor. However, in the numerical simulation, it is possible to have a two-phase flow entering the compressor. This is because when the compressor starts up, the evaporator does not have a large load. Hence, in the numerical simulation, the exit of the evaporator (it is also considered as the inlet of the compressor) could be a two-phase flow. However the large refrigerant inventory loss in the evaporator will cause its pressure and temperature to drop quickly. The result is superheated vapor generated at its exit; hence, the period of two-phase flow in the compressor is very short and will not affect the entire simulation.

Figure 3.36 shows the power consumption of a compressor (y-axis) with time (x-axis). From the equations in section 3.3, it is known that compressor power consumption is a function of compression ratio and compressor mass flow rate with fixed mechanical and volumetric efficiency. At the beginning of the running period after the compressor starts up, the compressor power consumption is very small due to the small compression ratio. This is because the compressor power consumption is the product of mass flow rate and enthalpy difference (equation 3.24). There is almost no compression at the compressor starting moment, and the enthalpy difference is a

very small number. Once the compression ratio increases with time, the power consumption rises very quickly because the increase of the enthalpy difference is larger than the decrease of the mass flow rate. During this period, the compression ratio is the dominant factor in the power consumption. Afterwards, the power consumption slowly decreases with time because the compression ratio increases slowly, and the decreased mass flow rate becomes the dominant factor in the total power consumption.

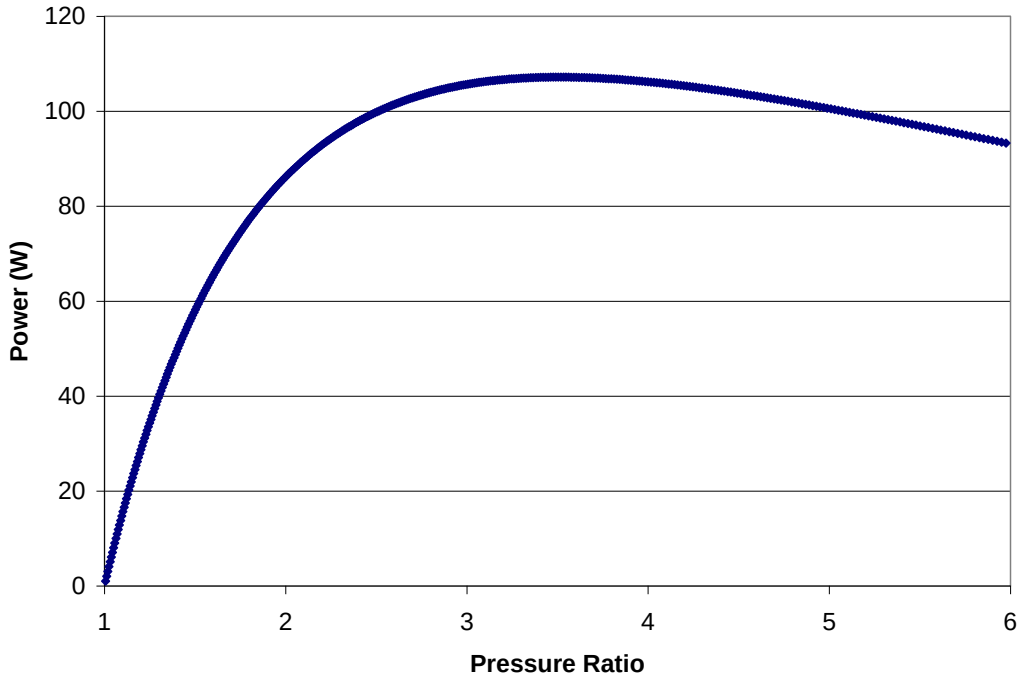

Figure 3.36 Compressor power consumption at different pressure ratios

Figure 3.37 shows how the compressor inlet (suction), outlet (discharge), and shell temperature changes with time. Assuming that the condenser and evaporator have the same pressure, the decrease in inlet temperature and the increase in discharge temperature are observed after the compressor starts up. The shell

temperature here is room temperature (298 K) before the compressor starts up. This temperature drops during the first 40 seconds due to a low average refrigerant temperature in the compressor chamber and a small compression work. The rise in compression ratio indicates that more and more work has been demanded to compress the working fluid. This increases the internal energy and temperature of the working fluid and heats the compressor shell.

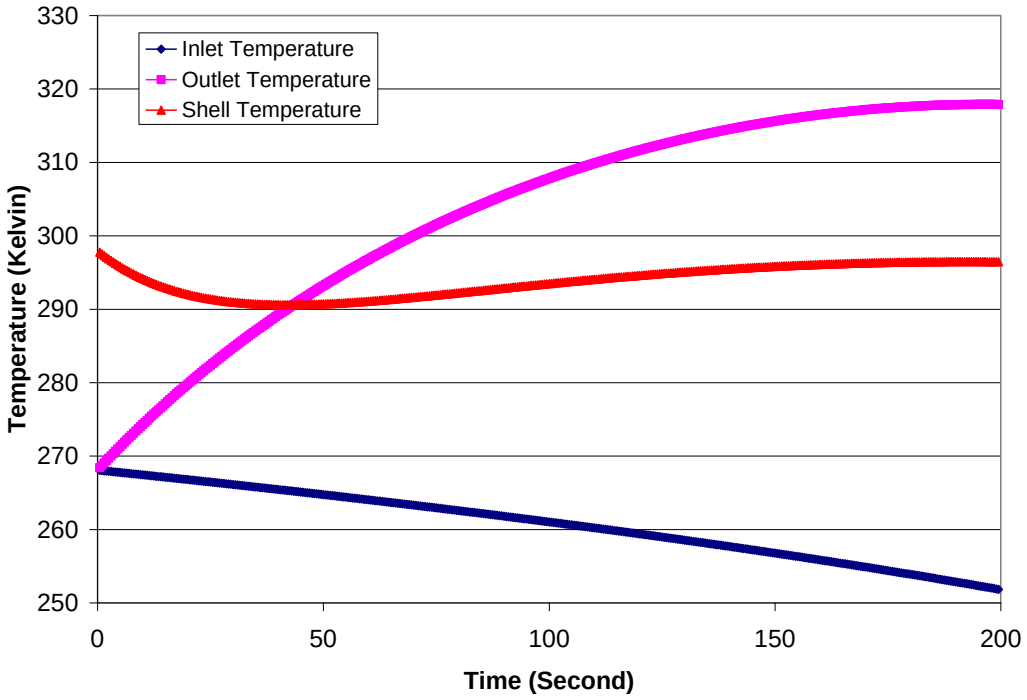

Figure 3.37 Plot of temperature in the compressor

3.4 Generic Expansion Device Model

The purpose of the expansion device is to reduce the pressure of the refrigerant. In the process of doing this, a part of refrigerant is evaporated to reduce its temperature in an isenthalpic process.

Due to the complexity of this process, the model needs to accurately incorporate the difference between refrigerants and boundary conditions.

The most commonly cited model of a short-tube restrictor was developed by Aaron and Dmanski (1990). The model was based on large samples of accurately measured experimental data. The authors make several important observations in the paper. They found that increasing the sub-cooling also increases the mass flow rate through the device and that mass flow rate varies in the "choked" region depending on downstream pressure. The effect of the length on mass flow rate was also investigated. However, the model is basically empirical and limited to the application of R22.

Kuehl and Goldschmidt (1990, 1991) developed an empirical model and another theoretical model for R22 flow in a capillary tube. For a given capillary tube, the theoretical model could determine the pressure at the outlet of the tube based on the inlet conditions. This was achieved by dividing the tube into a sub-cooled liquid region and a two-phase region. The pressure drop in the single-phase region was modeled by calculating friction factor. The two-phase region was modeled as homogenous, adiabatic, and isenthalpic flow. However, this theoretical model still needs to be manipulated to fit the experimental data.

Among the expansion device models, two types of methods are adopted to develop the models. Most simulations assume isenthalpic flow and utilize the orifice equation to determine the outlet state (MacArthur, 1984; Welsby et al., 1988; Vargas and Parise, 1995). Another simulation approach is specially designed for capillary

tubes. It divides the capillary tube into two single-phase regions and a two-phase region. In the single-phase region, the friction factor is used to model the pressure drop. In the two-phase region, Fanno flow is assumed to model the outlet state.

3.4.1 Generic Orifice Model

Since different expansion devices have different working principles, it is difficult to use a generic model to simulate all of the expansion devices. This generic component model, once it is applied to the expansion device, also provides different applications to the orifice and the capillary tube.

For application to the orifice, this model adopts a correlation developed by Stoecker (1983),

$$\dot{m} = KD^2\sqrt{\Delta P \rho} \tag{3.27}$$

Figure 3.38 shows how the mass flow rate changes with change of pressure difference once the correlation is implemented in the orifice model.

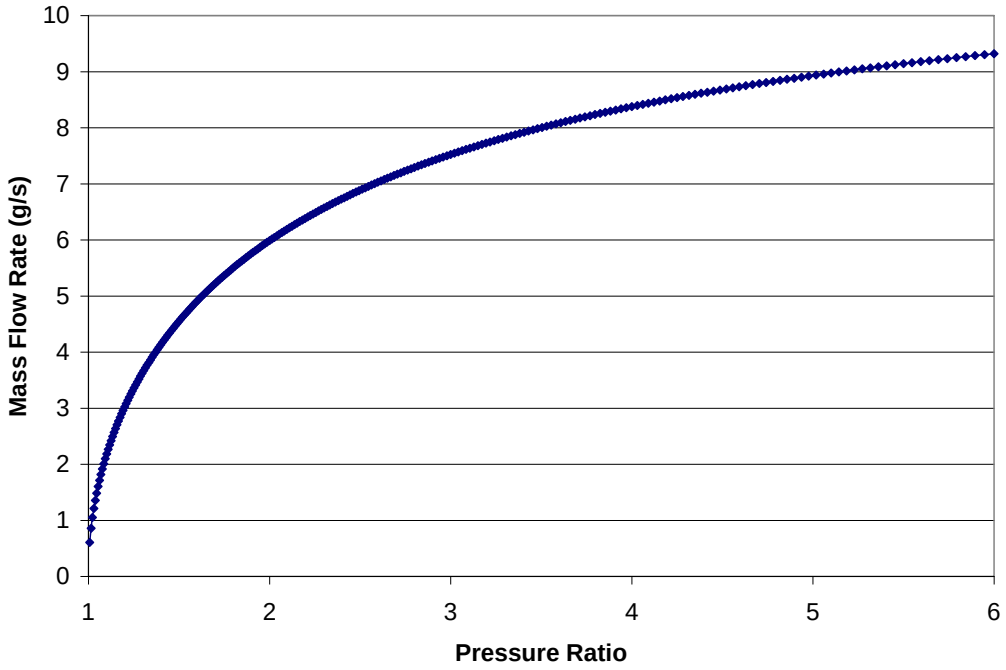

Figure 3.38 Plot of orifice mass flow rate with change of pressure ratio

3.5 Generic Tube Model

A tube or connecting pipe can be considered as a simple heat exchanger. The simulation of a tube is same as that of a heat exchanger. The only difference between the two is that the outside does not have fins and it is not a forced convective heat transfer but rather a natural convective heat transfer.

The tube is simply treated as a horizontal cylinder in order to calculate the air-side heat transfer coefficient. The natural heat transfer coefficient in this model is developed by Churchill and Chu (1975), who used a single correlation for a wide Rayleigh number range described in following equation:

$$\overline{Nu}_D = \{0.60 + \frac{0.38Ra_D^{1/6}}{[1+(0.599/\Pr)^{9/16}]^{8/27}}\}^2 \qquad Ra_D \le 10^{12} \tag{3.28}$$

This correlation provides the average Nusselt number over the entire circumference of an isothermal cylinder.

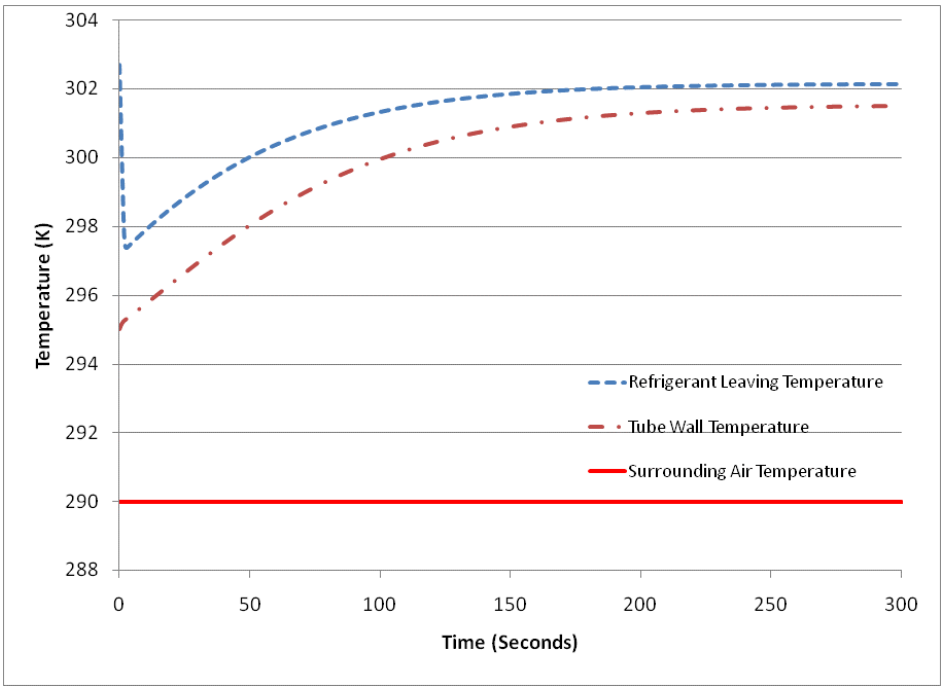

Figure 3.39 Tube temperature profile with time

Because the simulation phenomena is very like a simple heat exchanger, only the refrigerant leaving temperature and tube wall temperature change with time are plotted in figure 3.39 as an example of the simulation results.. Since the tube's internal surface area is fairly close to its external surface area, but the refrigerant side heat transfer coefficient is much larger than the natural heat transfer coefficient, the temperature difference between tube and refrigerant is much smaller than the temperature difference between tube and air.

3.6 Summary

In this chapter, we discussed the methodologies and algorithms for the existing models in the literature. The generic component framework proposed in Chapter 2 was established and implemented to simulate different components in a vapor compression system. Individual component features were represented in the simulation results as well.

In the heat exchanger model, a combined finite volume and moving boundary method was used to simulate heat exchangers. The model allows users to select a segment size to balance model accuracy and execution time. When a large number of control volumes are used, relatively high accuracy can be achieved by implementing the moving boundary approach in the control volume.

Different correlations were used to calculate heat transfer coefficient, pressure drop and mass flow rate for different components. This gives the user a wide range of applications of the model.

We also presented the numerical results of the dynamic component or subsystem models as a function of time or component location within the cycle. The results demonstrate that the general trends associated with time and component location agreed well with physical principles. This validates our component models in a general way. Additional quantitative validations were conducted for a specific heat exchanger (steady-state condition) and good agreement between our modeled results and literature data was reached.

3.7 References

Bendapudi, S., Braun, J.E., Groll, E.A., Dynamic Modeling of Shell and Tube Heat Exchangers Moving Boundary vs. Finite Volume, International Refrigeration and Air Conditioning Conference at Purdue, July 12-15, 2004

Chang, Y., Wang, C., 1997, "A Generalized Heat Transfer Correlation for Louver Fin Geometry", International Journal of Heat and Mass Transfer, Vol.40, pp. 533 - 544.

Chang, Y., Hsu, K., Lin, Y., Wang, C., 2000, "A Generalized Friction Correlation for Louver Fin Geometry", International Journal of Heat and Mass Transfer, Vol.43, pp. 2237-2243.

Churchill, S.W., and H.H.S. Chu, "Correlating Equations for Laminar and Turbulent Free Convection from a Horizontal Cylinder,' Int. J. Heat Mass Transfer, 18, 1049, 1975

Dhar, M. & Soedel, W., 1979, "Transient Analysis of a Vapor Compression Refrigeration System" XV International Congress of Refrigeration, Venice

Gunger, K.E., Winterton, R.H., 1986, "A General Correlation for Flow Boiling in Tubes and Annuli", International Journal of Heat and Mass Transfer, Vol., 29, No. 3, pp. 351-358

Jakobsen A., Antonius J. & Hogaard-Knudsen H.J., 1999, "Experimental evaluation of the use of homogenous and slip-flow two-phase dynamic models in evaporator modeling", Proc. 20th International Congress of Refrigeration, Sydney, Paper No. 135

Jung, D.S., Radermacher, R., 1989a, "Prediction of pressure drop during horizontal annular flow boiling of pure and mixed refrigerants", Int. J. of Heat and Mass Transfer, vol.32, pp.2435-2446

Jung, D.S., McLinden, M.O., Radermacher, R., Didion, D., 1989b, "A Study of Flow Boiling Heat Transfer with Refrigerant Mixtures", International Journal of Heat and Mass Transfer, Vol. 32 No 9, pp.1751-1764

Jung, D.S., Radermacher, R., 1991, "Prediction of Heat Transfer Coefficient During Evaporation of Various Refrigerants", ASHRAE Transactions, Vol. 97, Part 2, Paper #3492.

Jung, D.S., Radermacher, R., 1993, "Prediction of Evaporation Heat Transfer Coefficient and Pressure Drop of Refrigerant Mixtures", International Journal of Refrigeration, Vol. 16, No. 5, pp. 330-338.

Jiang, H.B, 2006, "Development of a Simulation and Optimization Tool for Heat Exchanger Design", Ph.D. Thesis, University of Maryland

Kandlikar, S.G., 1990, “A General Correlation for Saturated for Two phase Flow Boiling Heat Transfer in Horizontal and Vertical tubes”, Journal of Heat Transfer, Transactions of ASME, Vol.112, pp.219-228.

Kandlikar, S.G., 1991, “A model for correlating flow boiling heat transfer in augmented tubes and compact evaporators”, Journal of Heat Transfer, Transactions of ASME, Vol.113, pp.966-972.

Kim, M-H, Bullard, C., 2002, “Air-side Hydraulic Performance of Multi-louvered Fin Aluminum Heat Exchangers”, International Journal of Refrigeration, Vol. 25, pp. 390-400

Kim, N.H., Youn, B., Webb, R.L., 1999, “Air-Side Heat Transfer and Friction Correlations for Plain Fin-and-Tube Heat Exchangers with Staggered Tube Arrangements”, Journal of Heat Transfer, Transactions of ASME, Vol.121, pp.662-667.

Kim, N.H., Yun, J.H., Webb, R.L., 1997, “Heat Transfer and Friction Correlations for Wavy Plate Fin-and-Tube Heat Exchangers”, Journal of Heat Transfer, Transactions of ASME, Vol.119, pp.560-567

Kandlikar, S.G., 1997, “Boiling Heat Transfer with Binary Mixtures, Part II-Flow Boiling in Plain Tubes”, ASME National Heat Transfer Conference, Vol.4, pp.27- 34.

MacArthur, J.W., 1984a, “Analytical Representation of the Transient Energy Interactions in Vapor Compression Heat Pumps.” ASHRAE Paper, HT-84-19, Vol. 90, Part 1

MacArthur, J.W. & Grald, E.W., 1987, “Prediction of cyclic heat pump performance with a fully distributed model and a comparison with experimental data”, ASHRAE Transactions Vol. 93, Part 2

Murphy, W. & Goldschmidt, V., 1984, “Transient response of air-conditioners – a qualitative interpretation through a sample case”, ASHRAE Transactions, Vol. 90, Part 1

Murphy, W. & Goldschmidt, V., 1985, “Cyclic characteristics of a typical residential air-conditioner – modeling of start-up transients”, ASHRAE Transactions, Vol. 91, Part 2

Nyers, J., Stoyan, G., 1994, "A dynamical model adequate for controlling the evaporator of a heat pump", International Journal of Refrigeration, Vol. 17, pp.101-108

Rossi, T.M and Braun, J.E., 1999, “A real-time transient model for air conditioners”, Proc. 20th International Congress of Refrigeration, Sydney, Paper No. 743

Wedekind, G.L., Bhatt, B.L. Beck B.T., 1978, “A system mean void fraction model for predicting various transient phenomena associated with two phase evaporating and condensing flows.”, International Journal of Multiphase Flow, Vol. 4, pp. 97-114

Williatzen, M., Petit, N.B.O.L. & Ploug-Sorensen, L., 1998, “A general dynamic simulation model for evaporators and condenser in refrigeration: Part 1 – moving boundary formulation of two phase flows with heat exchange”, International Journal of Refrigeration, Vol. 21, No. 5, pp. 398-403.

Rossi, T.M and Braun, J.E., 1999, “A real-time transient model for air conditioners”, Proc. 20th International Congress of Refrigeration, Sydney, Paper No. 743

Shah, M.M., 1989, “A General Correlation for Heat Transfer during Film Condensation inside Pipes”, International Journal of Heat and Mass Transfer, Vol.22, pp.547-556

Soliman, et al, 1968, “A General Heat Transfer Correlation for Annular Flow Condensation”, ASME Journal of Heat Transfer, May 1968, pp.269-276

Sahnoun, A., Webb, R., 1992, “Prediction of Heat Transfer and Friction for the Louver Fin Geometry”, ASME Journal of Heat Transfer, vol.114, pp.893-900

Stoecker, W. F. Refrigeration and Air Conditioning. 2nd ed. McGraw-Hill, 1983

Traviss, D.P., Rohsenow, W.M., and Baron, A Condensation in Tubes: A Heat Transfer Correlation ASHRAE Transactions, Vol.79, pt1, pp.157-165

Chapter 4: System Solving Algorithm

4.1Introduction

Once all the component models are created, they can be integrated to form a system model. Then a system solver (mathematically, a set of simultaneous equations relating the operating variables) needs to be provided to solve this system model.

The most popular method of solving a set of equations involves setting up the equations in a matrix/vector form and solving the inverse of the matrix to obtain the solution. For complete system simulation, this method has been used by various investigators, including Yuan and O'Neal (1994), Sami and Zhou (1995), Xu and Clodic (1996), and Ploug-Sorensen et al. (1997).

This technique is also used in most of the commercial computational fluid dynamics codes that solve for the generalized Navier-Stokes equation in three directions (CFX, 1995). Mathematically, the equations are written in the format

$$A\vec{x} = B \tag{4.1}$$

where x is a vector that denotes the variable set of pressures, temperatures/enthalpies and velocities. A is a matrix that denotes the coefficients of the variables in vector x, which comprises the list of variables of the system, and B is the vector of constants combining each equation. The solution basically comprises the inverse of matrix A and can be given by

$$\vec{x} = A^{-1}B \tag{4.2}$$

This method has a strong mathematical foundation (Hirsh, 1990; Patankar, 1980) for discretization of the equations and convergence of the system. This method is mostly used for solving specific two- or three-dimensional flows, which are very computation intensive, as they involve a very fine grid structure (CFX, 1995). However, these solver routines do not include equations for component walls and external fluids, which are required for the current system modeling and hence cannot be used.

The other commonly used method involves setting up all the equations as functions and solving them (Mullen et al., 1998) using various techniques for equation solving like the Newton-Raphson techniques (Conte and Boor, 1980) to obtain convergence. This method of system solving also has a systematic convergence algorithm of the second order.

The main problems with these methods are the initialization of the variables and ensuring that the system variables are always within a specified range of the property routines (Mullen et al., 1998).

The third approach to solving all the components is using a successive substitution technique. The state of the system is calculated once, using the initially assumed properties. The new properties that are evaluated then replace the old properties, and the state of the system is calculated again. This successive substitution is self-convergent (Xu and Clodic, 1996). The main disadvantage of this system is that it may be slower than the other methods.

In this thesis, a Broyden non-linear solver is used to replace the Newton-Raphson technique to obtain convergence due to its better computational efficiency (Broyden, 1965; Selim, 1994).

4.2 Components

Systems consist of components, and the component model has already been discussed in the last chapter. The component model is represented by equations and can be solved by providing initial conditions and boundary conditions, including both external boundaries and internal boundaries.

In this context, external boundary conditions are boundary conditions imposed on the component from outside the thermo-fluid energy system, which surrounds the component. External boundary conditions could be, but are not limited to, heat exchanger secondary fluid flow rates and temperature, an environmental temperature, or a compressor's speed.

In this context, internal boundary conditions refer to the boundary conditions imposed on a component by the coordinating thermo-fluid energy system of which the component is a part. Internal boundary conditions are limited to the fluid properties from fluid flow interactions with other components. Internal boundary conditions include, but are not limited to, pressure, temperature, enthalpy and/or a fluid mass flow.

As mentioned in chapter 2, a thermal element needs to communicate with other elements; similarly, a component needs to communicate with other components to pass the necessary fluid properties. The location where components communicate is called a junction. The junctions contain necessary fluid properties and should be

given by the system or the other components in order to properly obtain component properties.

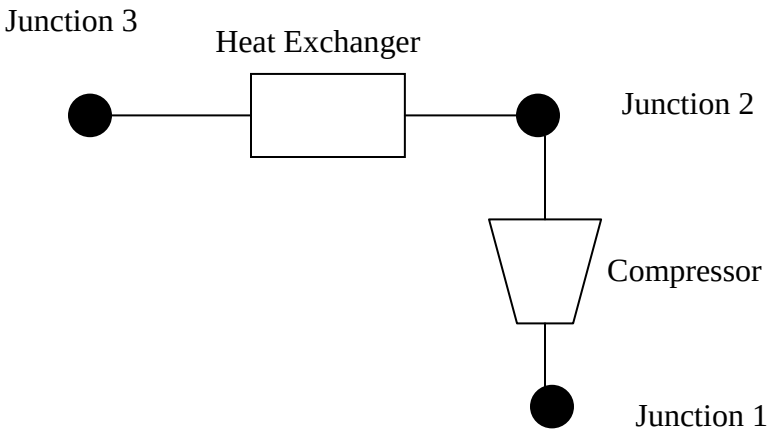

Figure 4.1 Schematic of an energy system component

4.3 Junctions

Junctions are points which allow for communication between components. Within the scope of this thesis, a junction is considered to be adiabatic and does not allow any heat or work interaction with its environment. Unlike components, junctions do not possess geometry, and therefore are only characterized by their unique mass flow rate and thermal properties. Therefore, the fluid states that flow into and out of a junction are the same. The energy and mass balance equations have to be satisfied at each junction.

4.4 Constructing a Thermal Fluid System

Figure 4.2 shows two general energy systems: an open system and a closed system. Each system contains several components that are connected via junctions. Assuming we have a system in operation, then at each junction, we will have a unique pressure, mass flow rate, and enthalpy. In other words, any component's inlet state is the outlet state of the preceding component.

In a component, if there is no extra work added to the component, the pressure difference of different junctions and temperature gradients between the two streams are the driving forces for the flow; thus necessary pressures must be assigned to junctions to determine the inlet and outlet mass flow rates of each component.

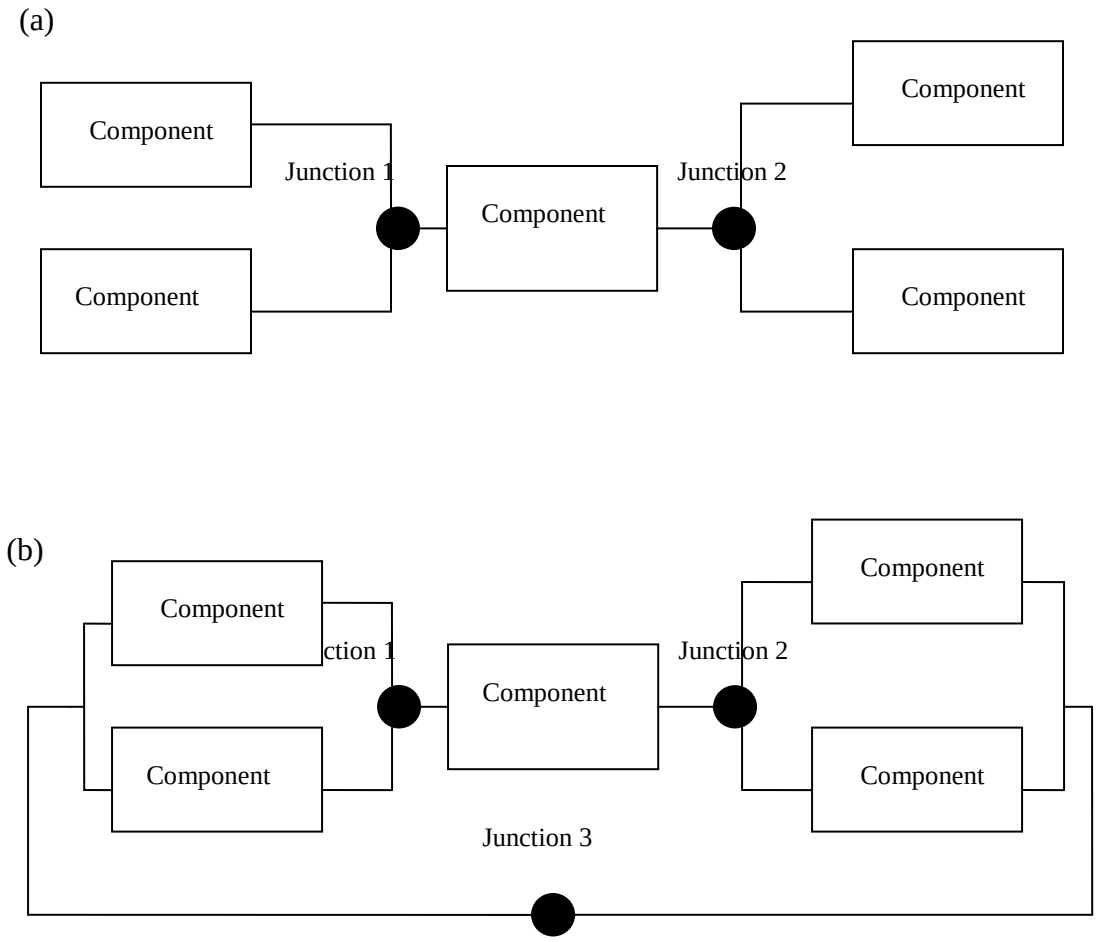

Figure 4.2 Open energy system (a) and closed energy system (b)

4.5 Enthalpy Marching Solver

The Broyden method provides the techniques to obtain convergences. However, in order to solve the system model, some formulations are still needed to assign necessary guessed values to the math solver.

Richardson (2005) described a junction solver to simulate a vapor compression system. In this solver, all the inlet enthalpies and pressures are assigned at junctions. These properties at the junctions are used as the boundary conditions to

run the component. All of the component models will output the mass flow rate, or outlet enthalpy. This method makes the solver independent of the component types, easily extends the cycle with additional components, and extends the original cycle to different types.

Winkler (2009) compared several system solvers which can be used to do vapor compression system steady state simulation. All solvers were run through a text matrix either by specific system charge or specific system subcooling. After running thousands of cases, the enthalpy marching solver showed the best potential. The advantage of enthalpy marching solver is that it needs to solve fewer unknowns in a system cycle. Since numerical equation solvers require the computation of the Jacobian, fewer variables will result in fewer component model executions per equation solver iteration. In addition, the enthalpy marching solver also utilizes mass flow rate based heat exchanger models which execute faster compared with pressure boundary condition models. This will have a large impact on computational time.

Although this method is used for steady-state system simulation, it is also good to use as the dynamic system solver due to its advantages. Considering the characteristics of the dynamic component model mentioned above, a new general-purpose thermo-fluid solver can be developed.

In the system model, this general purpose thermo-fluid simulation solver is created to coordinate the system and components. In this thesis, this solver is also referred to as an enthalpy marching solver. The features of this solver are listed below:

1. Single solver for many thermo-flow energy systems

2. Capable of handling additional components in a basic 4-componet vapor compression system
3. Capable of handling mass flow rate stream merging and splitting
4. Robust and high-speed

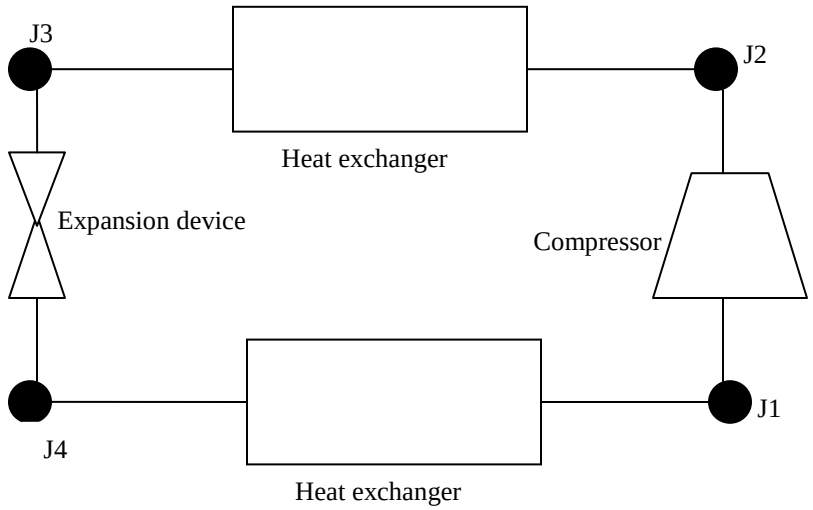

Figure 4.3 A basic vapor compression system with junctions

Figure 4.3 illustrates how a basic vapor compression system is simulated. In this system, necessary pressure and suction enthalpy will be guessed and assigned to the junctions, which are suction enthalpy h1, suction pressure P1, and condenser and evaporator inlet pressure P2 and P4. Those four guessed unknowns ensure that all the components in the system to obtain enough inputs in order to run those components. The detailed procedure is represented in the flow chart below (Figure 4.4).

1. Guess the necessary pressure and suction enthalpy – P1, P2, P4 and h1.
2. Run the compressor model to get the compressor mass flow rate, and then use its inlet conditions to calculate its outlet condition.

3. Run the condenser model to calculate its outlet conditions based on its inlet condition which comes from compressor's outlet
4. Run the expansion device model and obtain the mass flow rate and outlet enthalpy by using its inlet condition and given P4.
5. Run the evaporator model to obtain its outlet condition by using its inlet condition.
6. Check the residuals of this system solver. Since there are four unknowns in this solver, four residuals need to be checked, which are

$$P_{evap,out} - P1 = 0 \tag{4.3}$$

$$h_{evap,out} - h1 = 0 \tag{4.4}$$

$$\dot{m}_{evap,out} - \dot{m}_{comp} = 0 \tag{4.5}$$

$$\dot{m}_{cond,out} - \dot{m}_{\exp} = 0 \tag{4.6}$$

7. If the system is not solved, adjust the guessed values and re-run the entire system until the system is solved, then go to next time step. This process is approached by using either the Broyden solver or Newton-Raphson solver.

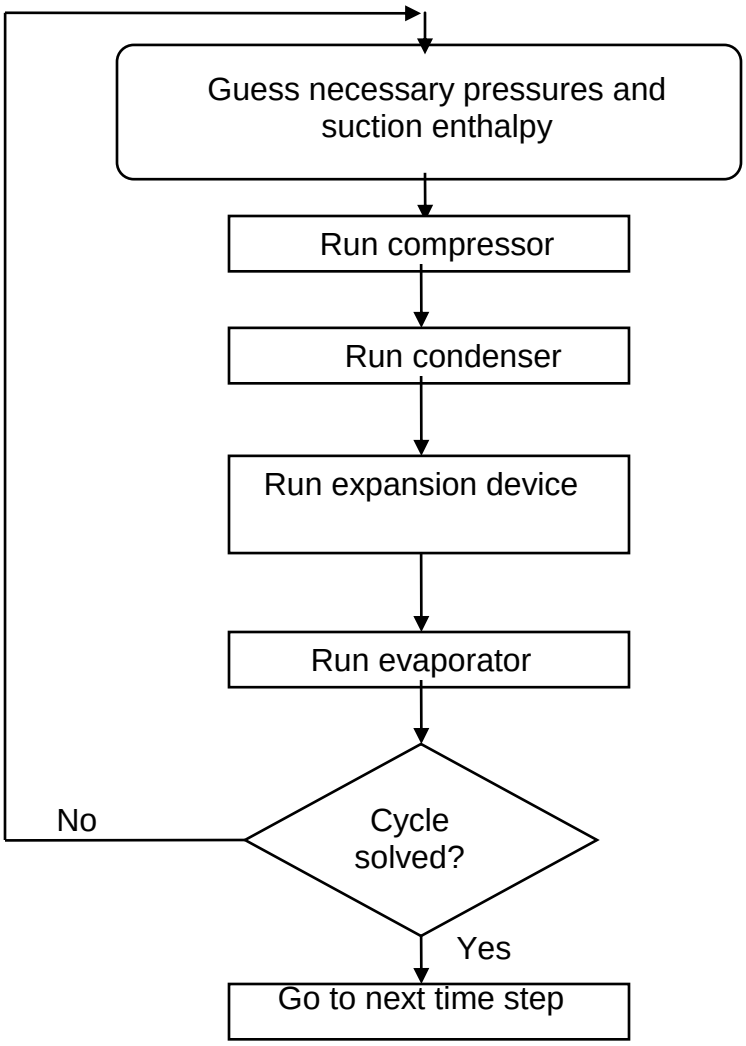

Figure 4.4 Flow chart of system solution methodology

From the above flow chart and knowledge of the Broyden solver, it is clear that solving the system is based on solving this set of residual equations. Obviously, this set of residual equations is nonlinear in nature due to the thermo-fluid physical properties and the various heat transfer and pressure drop correlations.

The system solver developed in this thesis incorporates an iterative solution technique, which requires the solution of auxiliary linear systems. Rather than preconditioning the system variables, this enthalpy marching solver incorporates scaling techniques to accelerate the iterative process. The scaling technique scales all system variables between a minimum and a maximum value. Hence, all of the variables have the same order and become dimensionless values between 0 and 1.

The system variables in this specific system are pressures and enthalpy. These dimensionless values can be defined as

$$P_i^* = \frac{P_i - P_{low}}{P_{high} - P_{low}} \tag{4.7}$$

$$h_i^* = \frac{h_i - h_{low}}{h_{high} - h_{low}} \tag{4.8}$$

The enthalpy marching solver will provide the highest and lowest values for scaling, which ideally come from the highest and lowest pressure and enthalpy encountered in the system.

4.6 Integrated System Solver for Steady State and Transient Simulation

In this chapter, a system solver is developed to accommodate the generic components, to construct vapor compression systems and to do the system transient simulation. If the system solver is also good for the vapor compression system simulation, a unique set of tool can be developed used for component/system steady state/transient simulation.

Since there are no time step related items in the system solver, in order to check solver's suitability, the guessed unknowns and residual equations used in transient simulation should be checked to judge if they are also good for the steady state system simulation. From chapter 2, it is already known that all component simulations are self solved in the generic component framework, no matter it is transient simulation or steady state simulation, which means the guessed unknowns should suffice to run the generic component steady state simulation.

The residual equations used to solve those unknowns in the transient simulation can also be inherited in the steady state simulation because the energy and mass balance always should be satisfied at the junctions. However, the last two residual equations become redundant because the mass flow rate will be the same in the entire system. It's not difficult to find an additional residual equation to restrain the system. The default new residual equation indicates that the total charge is conserved:

$$m_{charge\_calculated} - m_{change\_design} = 0 \tag{4.9}$$

However, the other type constrains, such as designed subcooling, designed superheat etc, also can be used as the additional residual equation to define the system instead of using the system charge.

Figure 4.5 shows the solution methodology of the integrated system solver. This solution methodology is exactly the same as the one which is used to solve the dynamic system, except a simple logic judgment will happen at the last step. Rather than moving to the next step time, if the logic signal shows it is a steady state

simulation, it will escape the time loop, directly stop the simulation, and return the system performance.

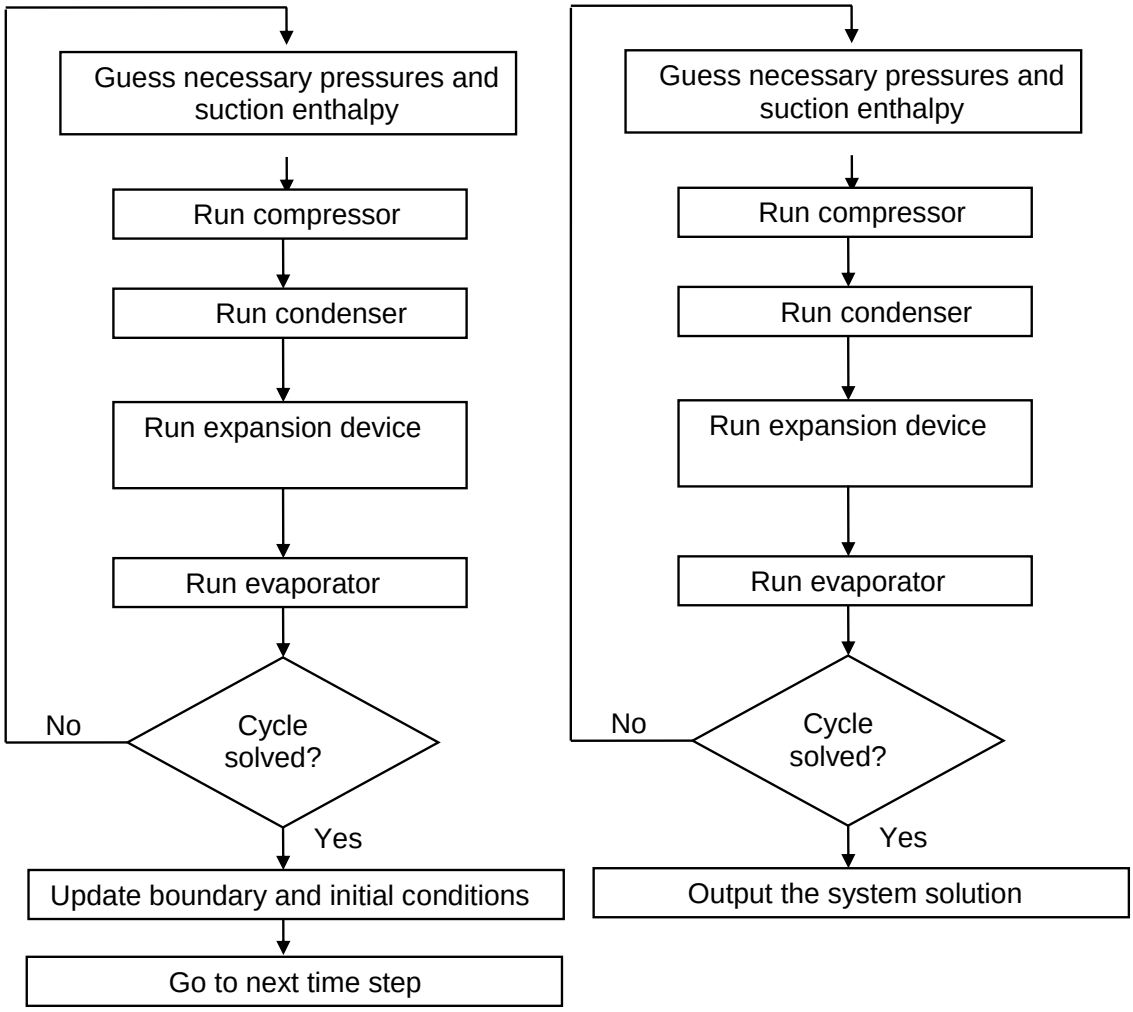

Figure 4.5 (a) Solution methodology comparison for transient simulation and steady state simulation

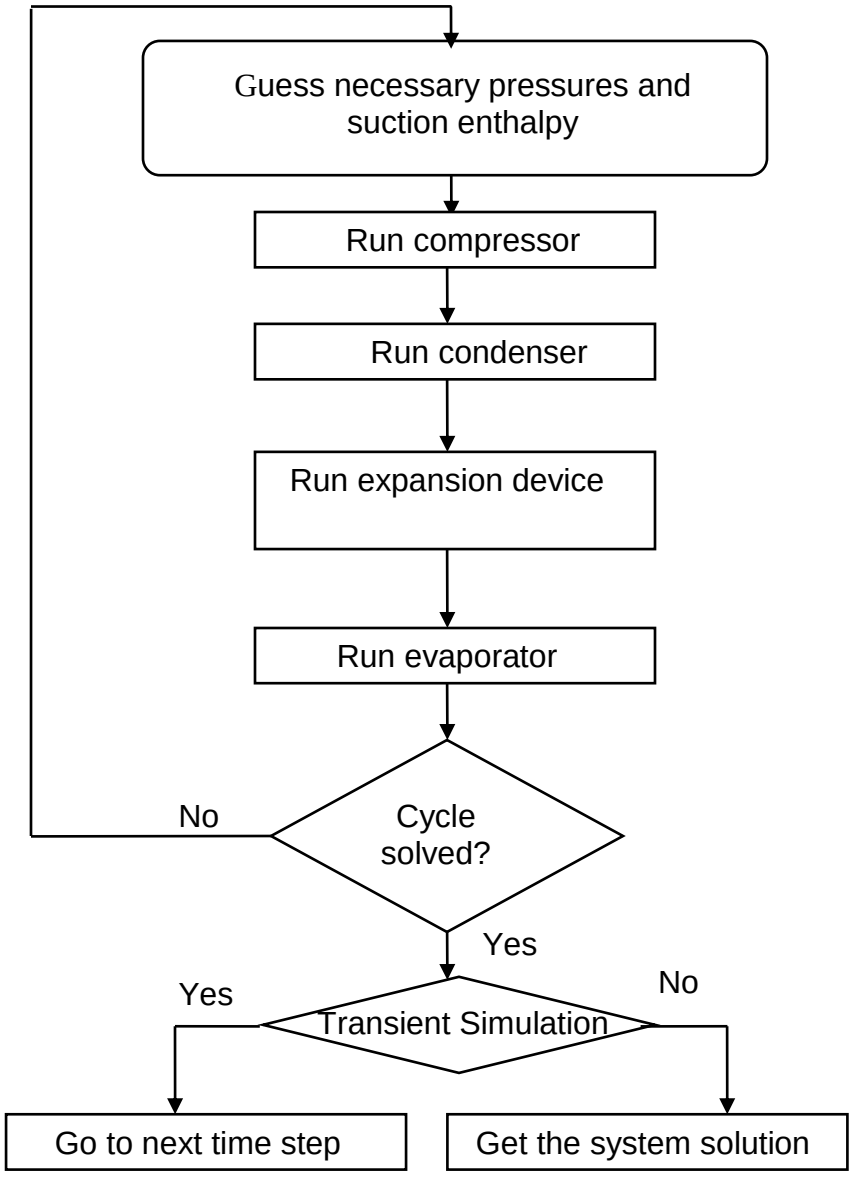

Figure 4.5 (b) Flow chart of integrated system solver solution methodology

4.6.1 Integrated System Solver Testing

In order to test the integrated system solver, a simple refrigeration system is constructed by using the generic component framework and the integrated system

solver. This system will run a transient simulation with enough time to approach steady state. At the same time, it also directly runs a steady state simulation and compares its system performance with the results generated by transient simulation.

	Steady State Solver	Transient Solver	Difference
m_dot (g/s)	2.4765	2.48155	0.20%
Pc (Pa)	1561848	1568164.9	0.40%
Pe (Pa)	222570.7	223129.9	0.25%
Tc_sat (K)	313.9	314.07	0.05%
Te_sat (K)	250.642	250.72	0.03%
Hevap_out	402134	402120	0.00%
Superheat (K)	9.358	9.28	-0.84%
Subcooling (K	5.75	5.92	2.87%

Table 4.1 Simulation results comparison

Seven key parameters are listed and compared in table 4.1. All differences of compared parameters are less than 1% except for the subcooling. However, the absolute difference of system subcooling is still less than 0.2K and is thus judged acceptable.

4.7 Transient Simulation Technique Comparison

Recently, at the Center for Environment Energy Engineering (CEEE) of University of Maryland, another transient simulation technique is also developed and studied (Winkler, 2009). This transient simulation technique employs the popular "tube tank" concept to simulate the heat exchangers in the system. It will be interesting to compare both simulation techniques to analyze their advantages and disadvantages.

In order to do the comparison, an air conditioning system is constructed by using both simulation techniques. After running both system models, similar system performances are generated (they will be discussed in next chapter) which indicates there are no errors or mistakes caused by inconsistent inputs for the comparison.

By studying both simulation techniques, all of them have advantages and disadvantages due to different research objectives. The details of comparison are summarized next.

1) The component model of both system simulations are written in a standard framework, which will make for easy component replacement and exchange, and is also suitable for component based simulation.
2) The heat exchanger model in Winkler's study is constructed in the "Tube and Tank" model. This heat exchanger model calculates the heat transfer and pressure drop separately in the tube and tank, which improves its computational speed and robustness. However, solving the model requires its inlet and outlet mass flow rate which means it only can be used in system simulations but not in stand-alone heat exchanger simulations. In addition, if the tube number is limited, the tank model may need to be divided into multiple control volumes to minimize the inaccuracy generated at nearby phase change region boundaries.
3) The heat exchanger model in this dissertation is constructed using the generic component model. This model can be used for stand-alone component transient simulation, and also can be accommodated in system simulation. Since all conservation equations should be solved in each thermal element, the

generic component based system simulation will be significantly slower if there are the same numbers of control volumes. However, since the phase change region boundary is always sought in the thermal element, less control volumes are needed.

4) The equation solver used in tube-tank model based system simulation requires only the guessed junction pressure to solve the system mass balance; the required junction enthalpy is updated based on the fourth order Runge-Kutta method. The enthalpy marching solver used in the generic component based simulation requires junction pressure and enthalpy. However, the guessed numbers are the same and guessed parameters are similar (three are guessed pressures at the same location) in both system simulations. Mathematically, if the initial conditions are the same and guessed values are the same while using the same Broyden solver, the equation solver iteration numbers in each time step should be close. Practically, most iteration numbers in both simulations are between 10-15 when the system residual equations are solved

4.8 System Control

4.8.1 Control Functions in the Generic Component Framework

One important purpose of developing the transient system/component simulation is to develop the control algorithm for vapor compression systems. In the current generic component model, two types of control functions are embedded to implement the control algorithm.

The first type of control is the on/off control. The on/off control can be considered as a simplified proportional control, but the output signal only has two status levels: on or off. In each time step, the actual temperature/pressure signal is obtained to compare against the set value. Depending on whether the deviation is larger or smaller than the tolerance, the control function will send an on/off signal to the actuator to reduce the deviation.

The second type of control is the PID control. PID control is a very generic control loop feedback algorithm used in industry. This control includes three terms, which are the proportional term, the integral term, and the derivative term. This control function can be represented by below equation In this equation, u(t) is the output signal, Kp, Ki and Kd are the tuning parameters: the proportional gain, integral gain, and derivative gain. The error between set value and actual values is e; t is the time, and τ is a time integration variable.

$$u(t) = K_p e(t) + K_i \int_0^t e(\tau) d\tau + K_d \frac{d}{dt} e(t) \tag{4.10}$$

4.8.2 Demonstrating Control Functions

Since the generic component can represent any of the basic components in a refrigeration system, several examples will be demonstrated to show how the system maintains a proper temperature/pressure via implementing the control algorithm to those components. The control function used in the examples is the PID control.

Figure 4.6 shows how the condenser pressure is maintained for a given system. In order to test the controller, there are no controls for any components in the refrigeration system at the beginning, and the system will gradually approach a steady state based on its given initial condition and boundary condition. As the steady state is approached, the condenser air temperature suddenly drops 4K at the 200th second; hence, the saturated condensing temperature also drops correspondingly. In this controller, the target condensing temperature is 313K with 1K tolerance. From this figure, it can be seen that once the condensing temperature is lower than its low limit, the PID control function starts to output an active signal. It will continually output a new expected condenser fan speed signal (a percentage of standard fan speed) to condenser fan. In this example, a lower condenser fan speed is produced, which pushes the condensing temperature back to the proper region.

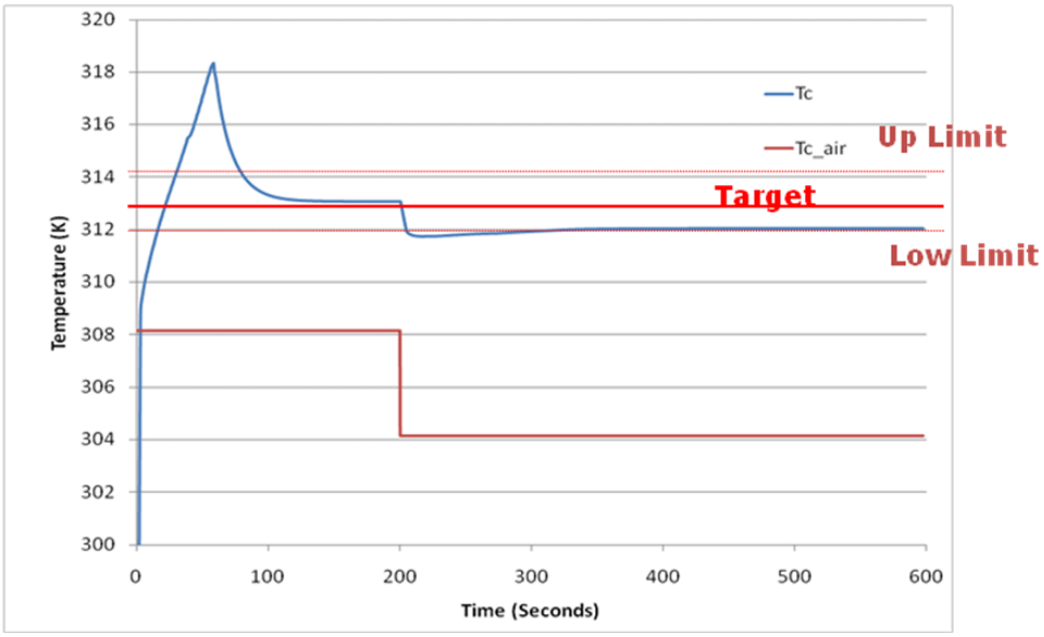

Figure 4.6 Saturated condensing temperature control via adjusting fan speed

Figure 4.7 shows the same control and controller setting to maintain the saturated condensing temperature. However, the condenser fans are not variable speed fans but cycling fans. Same as the first example, the condenser air temperature is reset at the 200th second. Once the condensing temperature leaves its target, the controller starts to work and generate an output signal. This output signal cycles the condenser fans and forces the saturated condensing temperature to change in the proper direction.

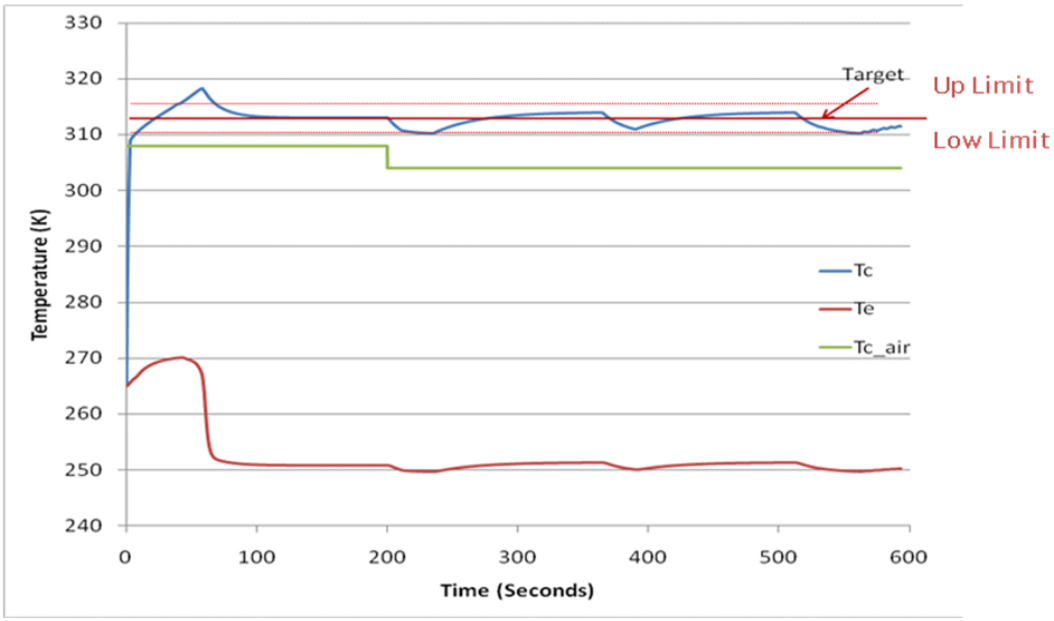

Figure 4.7 Saturated condensing temperature control via cycling fan

The third example is the saturated evaporating temperature control. This temperature can be controlled either by controlling evaporator fan or compressor speed if the compressor type is the variable speed compressor. In this demonstration, the evaporating temperature is controlled by adjusting compressor speed, which is shown in figure 4.8. The target temperature is 251K with 1K tolerance. After the evaporator air temperature drops, the saturated evaporating temperature also starts to

decrease. From that time, the controller starts to work to maintain the evaporating temperature. After a certain time, the evaporating temperature starts to rise and finally stays in a proper region.

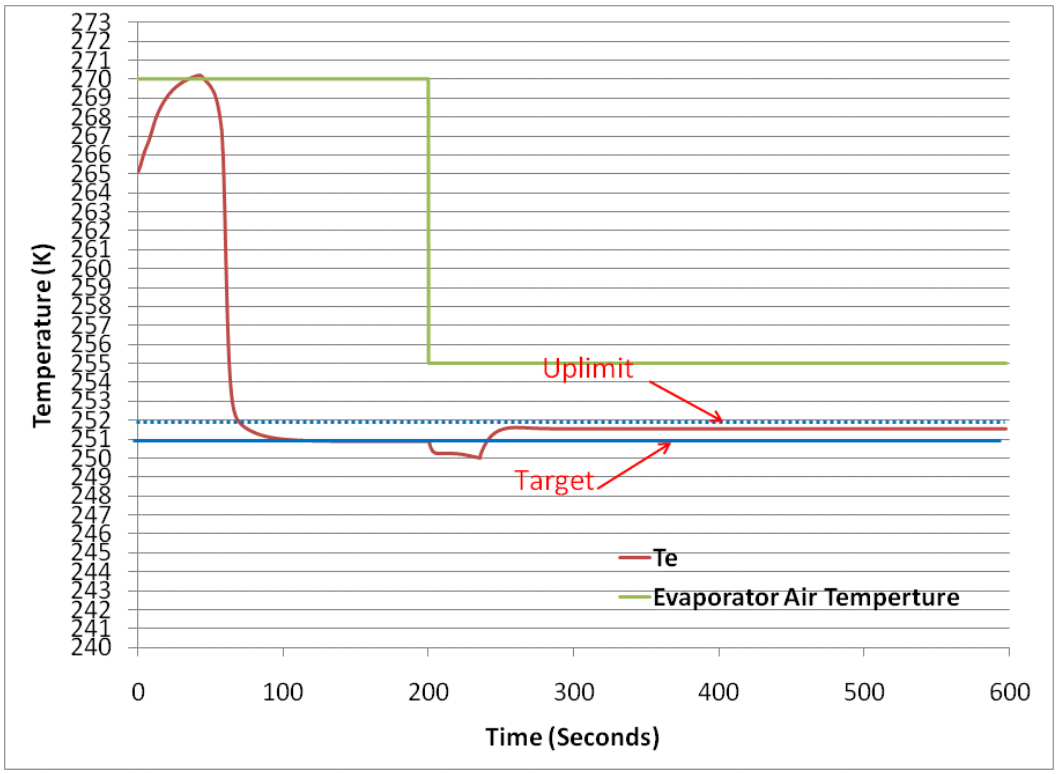

Figure 4.8 Saturated evaporator temperature control

Another important control among vapor compression system control is the evaporator superheat control. Figure 4.9 shows how it's controlled in the system. At the beginning, the expansion value diameter is set at a small, value which causes a larger superheat in the evaporator. After 200 seconds, the system approaches a steady state; then the controller starts to work to reduce the superheat. The set value is 10K with 1K tolerance. From figure 4.9, it can be seen that the superheat drops to the target region after the expansion valve diameters is adjusted. Figure 4.10 shows the exact same control except the tolerance in the control function is narrowed into 0.5K. Based on the results displayed in figure 4.10, it is proven that the superheat is still

well controlled by implementing this control algorithm, even though a narrowed target region is set.

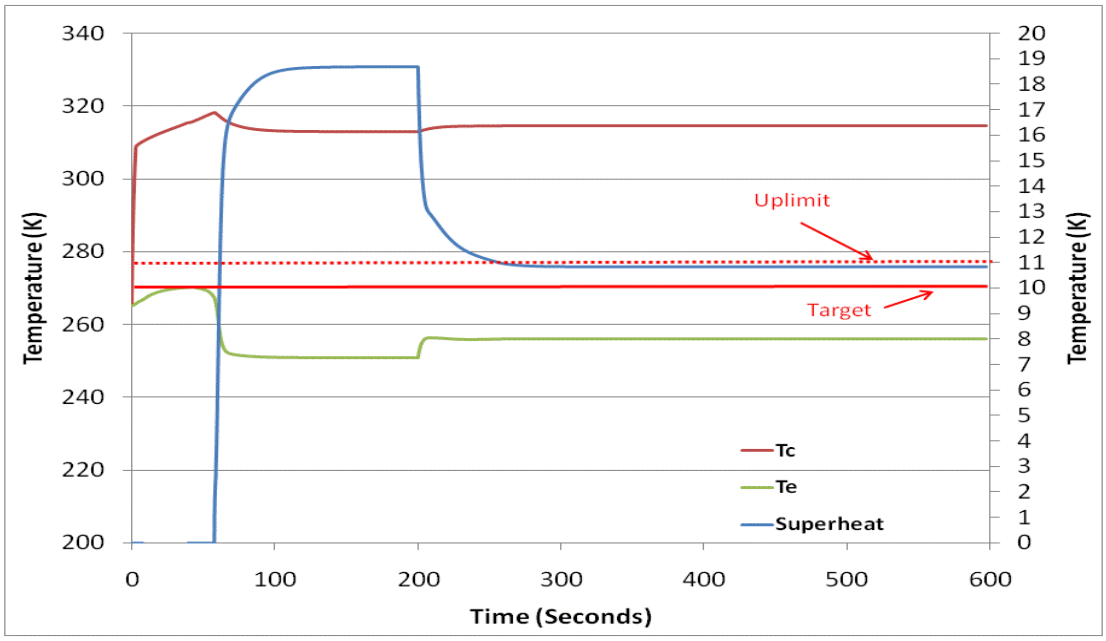

Figure 4.9 evaporator superheat control with 1K tolerance

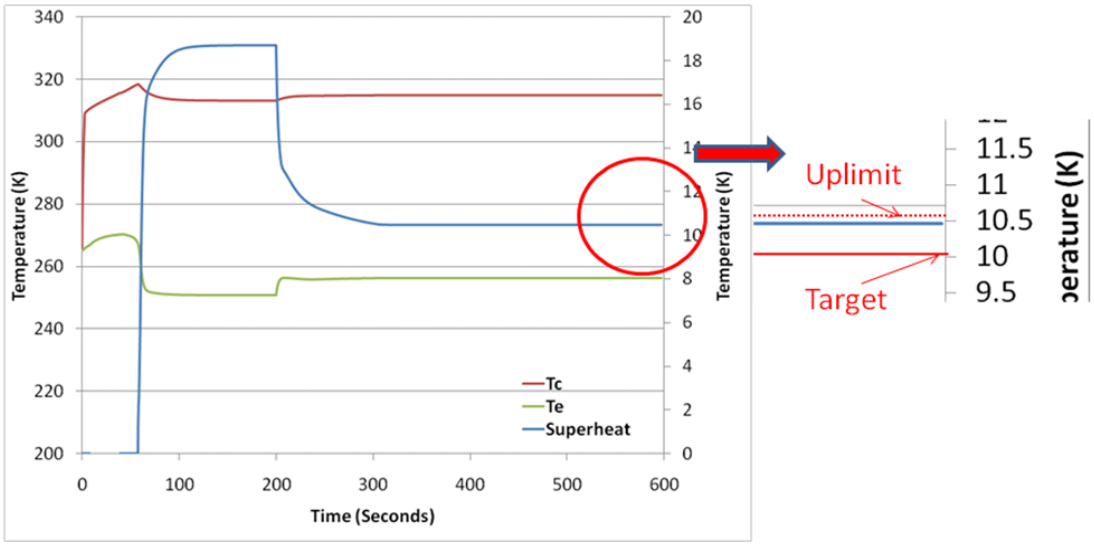

Figure 4.10 Evaporator superheat control with 0.5 K tolerance

4.9 Summary

In this chapter, based on the features and characteristics of the component models, a general-purpose thermo-fluid system solver was developed and described to solve a thermal system model consisting of component models. This method, compared with other solvers, reduces the number of variables in the system and increases the robustness of the simulation. During the system solving, a scaling technique was used to scale the system variables, which improves the numerical stability of the system solver by proving the maximum and minimum values in the thermo-fluid system.

Besides solving a transient system, the developed system solver also can be used to solve a steady state system with very minor changes. Eventually, this solver becomes an integrated system solver for both steady state and transient simulation. This integration makes using one set of tool to do transient and steady state simulation possible.

4.10 References

Winkler, J., 2009, Development of a Component Based Simulation Tool for the Steady State and Transient Analysis of Vapor Compression Systems, Ph.D. dissertation, University of Maryland.

Ploug-Sorensen, L., Fredsted, J. P. and Willatzen, M., 1997, HVAC&R Research, vol 3, no. 4, p 387-403

Richardson, D., 2006, "An Object Oriented Simulation Framework for Steady-State Analysis of Vapor Compression Refrigeration System and Components", Ph.D. dissertation, University of Maryland

Sami, S. M. and Zhou, Y., 1995, "Numerical prediction of heat pump dynamic behavior using ternary non-azeotropic refrigerant mixtures", International Journal of Energy Research, vol 19, p 19-35

Xu, Xiaoqiang and Clodic, D., 1996, Dynamic Simulation model of a vapor compression domestic refrigerator running with R134a, Proceedings of International Refrigeration Conference, Purdue

Yuan, Xiuling and O'Neal, D. L., 1994, Development of transient simulation model of a freezer Part I: Model development, Proceedings of International Refrigeration Conference, Purdue

Yuan, Xiuling and O'Neal, D. L., 1994, Development of transient simulation model of a freezer part II: Comparison of experimental data with model, Proceedings of International Refrigeration Conference, Purdue

Chapter 5: System Validation

This generic component and system dynamic model described so far can be extended and potentially simulates many types of different thermo-fluid systems, including open systems and closed systems. In this dissertation, it is used to simulate only a vapor compression system.

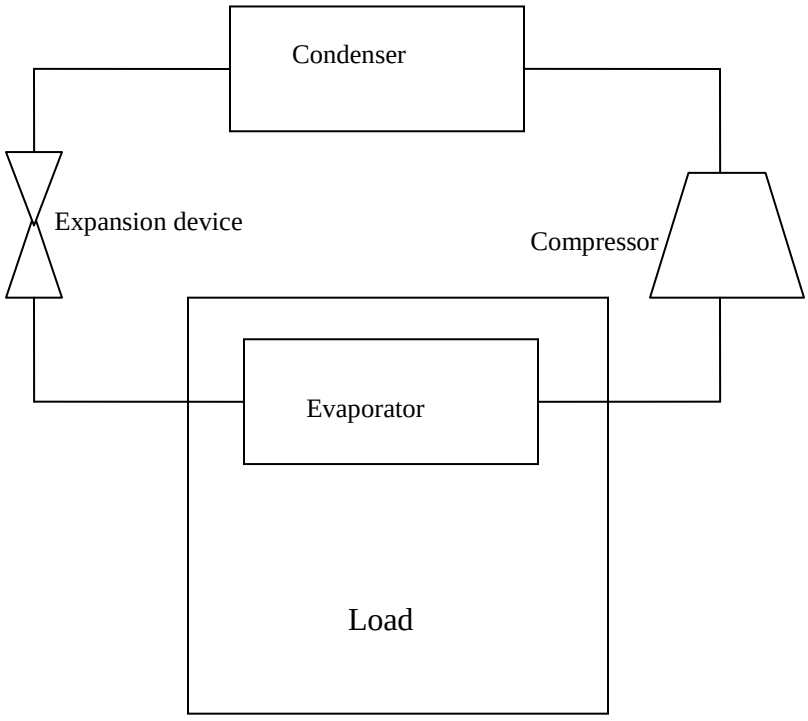

Figure 5.1 A Basic vapor compression system

A vapor compression system is a closed system. A basic vapor compression system contains four basic components: a compressor, a condenser, an expansion device, and an evaporator. Based on different load types, this system can represent residential air conditioning systems, refrigeration systems or vehicle air conditioning

systems. In this chapter, by setting different initial conditions, boundary conditions, and load types, it will be shown how this model also can represent different applications of a vapor compression system. In order to do a compressive study, different applications of this model will be validated.

5.1 Validation of a Refrigeration System

The first system to be validated is a refrigeration system. In this system, the evaporator has seven banks to cool the air temperature to a relatively low temperature. The condenser only has one bank, but it has enough capacity to ensure condensing the refrigerant flow to the subcooling state at its outlet. The geometry of the evaporator is displayed in Figure 5.2.

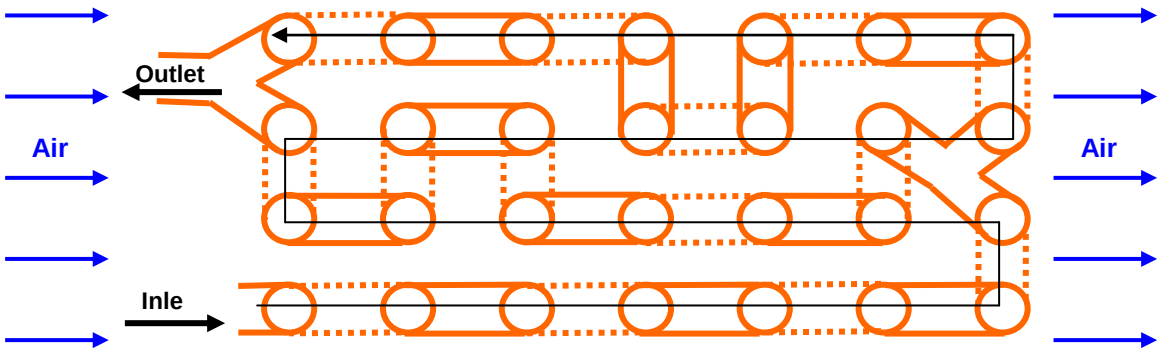

Figure 5.2 Schematic of an evaporator in a refrigeration system

In this schematic, the circuitry is not simple and contains the splitting and merging of streams. In order to simplify the problem, a substitute heat exchanger is simulated individually first. The substitute coil has the same number of tubes and the same banks as the original one, but the flow splitting and merging is ignored in this

coil. The new refrigerant circuitry is displayed in the original schematic and following the arrow direction.

The refrigerant used in this system is R22; the operating conditions tested in the lab are listed in the table below (Table 5.1).

Evaporation Temperature	-10 °F	-23.33 °C
Refrigerant vapor temperature	-2 °F	-18.89 °C
Superheat	8 °F	4.45 °C
Condensing Temperature	110 °F	43.33 °C
Liquid refrigerant temperature	95 °F	35 °C
Subcooling	15 °F	8.33 °C

Table 5.1 Vapor compression system test conditions

The air temperature and mass flow rate in the test are listed in Table 5.2.

Air Inlet Temperature	0 °F	-17.78 °C
Air Flow	240 ft3/min	0.113 m3/s
Air Speed through HX		2.06 m/s

Table 5.2 Air side parameters

The measured pressure and mass flow rate of this system are listed in Table 5.3.

Condenser Pressure	1662 kPa
Evaporator Pressure	215 kPa
Mass Flow Rate	3 g/s

Table 5.3 Refrigerant side parameters

In the experimental setup, in order to obtain and maintain the required environmental temperature, both heat exchangers are placed in different chambers. The mass flow rate is controlled by a manually controlled expansion valve, and the expansion valve open rate is pre-adjusted to obtain the desired mass flow rate. Since the evaporator and condenser remain at different environmental temperatures, the initial pressure and temperature are determined by the system charge and environmental temperature.

Figure 5.3 shows the variation of pressure from start-up to steady-state over a time span of 8 minutes. At the start up period, too much refrigerant is pushed into the condenser since the compressor mass flow rate is not restricted in the compressor model. This causes an over-prediction of condensing pressure and under-prediction of evaporating pressure. However, the pressures are predicted with about a 5% error in condenser pressure and a 3% error in the evaporator during the most transient operations.

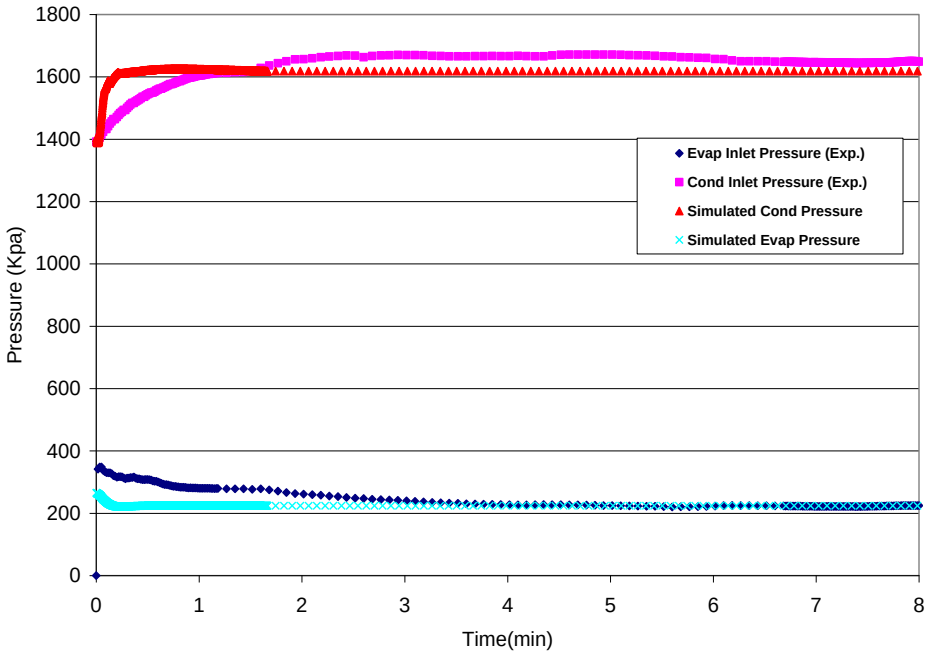

Figure 5.3 Comparison of system pressures

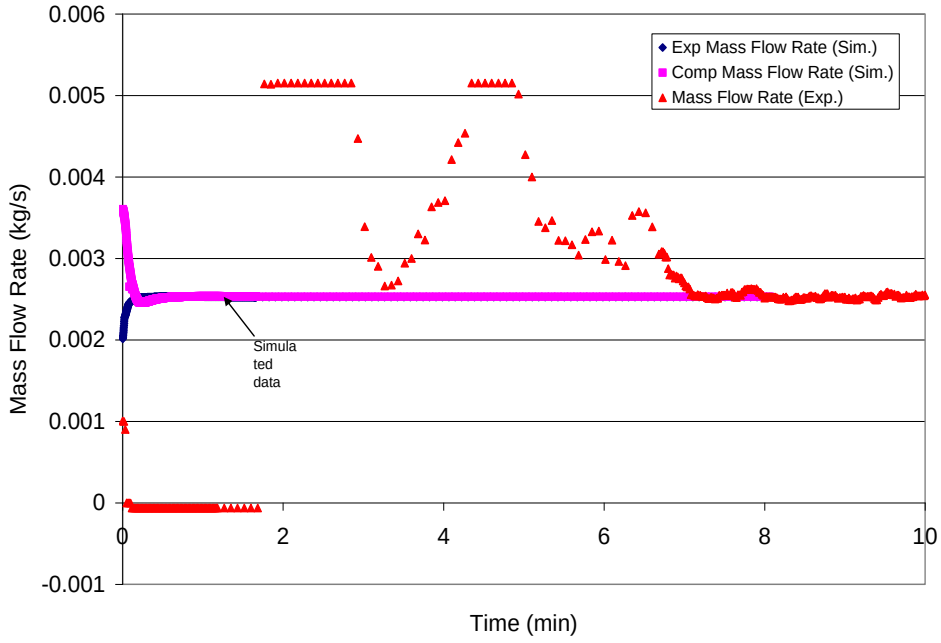

Figure 5.4 System mass flow rate during transients

The mass flow rate of the system is shown in Figure 5.4. In the experimental setup, the mass flow rate meter is placed after the condenser and before the expansion valve. During the start-up period, the flow through the mass flow rate meter is two-phase flow, and hence the meter doesn't properly read the flow rate. After about 7 minutes in the condenser, the refrigerant is completely cooled and the refrigerant becomes single-phase flow at the outlet of the condenser. At this point, the measured mass flow rate matches well the predicted mass flow rate in the simulation. Also in this figure, we can see that the initial mass flow rate in the expansion device is small (about 2g/s) and that the initial mass flow rate in the compressor is large (about 3.6g/s) due to the pressure difference and inlet refrigerant density of both devices. As time passes, the mass flow rate through the compressor becomes smaller, and the mass flow rate through the expansion valve becomes larger, until the same mass flow rate (about 2.7g/s) is reached for both.

Figure 5.5 shows the system cooling capacity during the transients. Both cooling capacities are calculated based on the refrigerant mass flow rate and the refrigerant state at the inlet and outlet of the evaporator. Due to difficulties in measuring mass flow rate, the measured cooling capacity only can be properly calculated after obtaining the accurate mass flow rate. However, once the right mass flow rate is obtained, we can see that the cooling capacity is well predicted by the model.

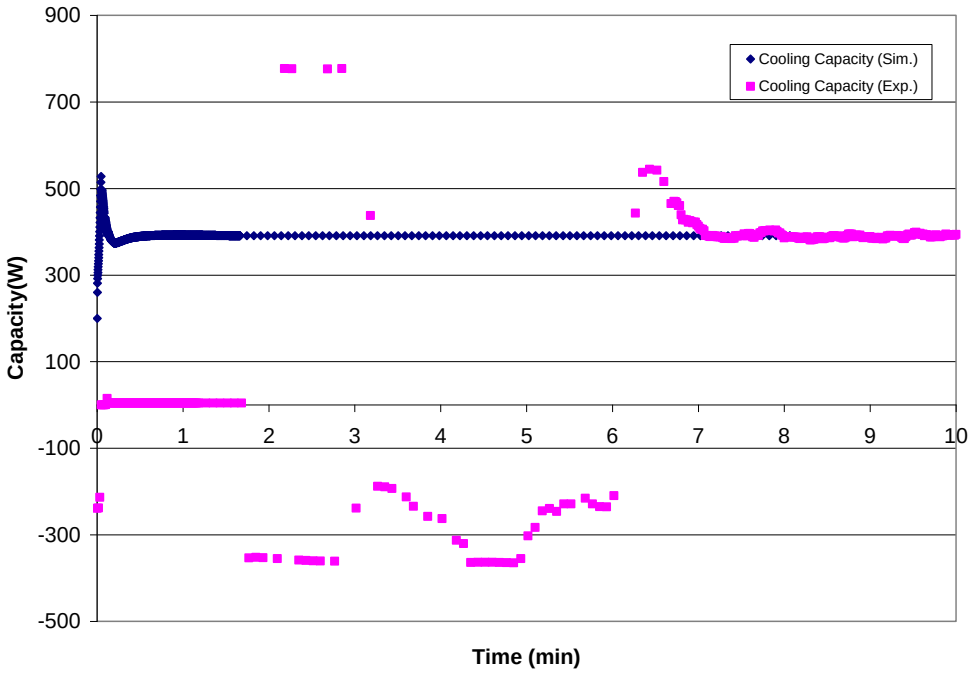

Figure 5.5 System cooling capacity during transient operation

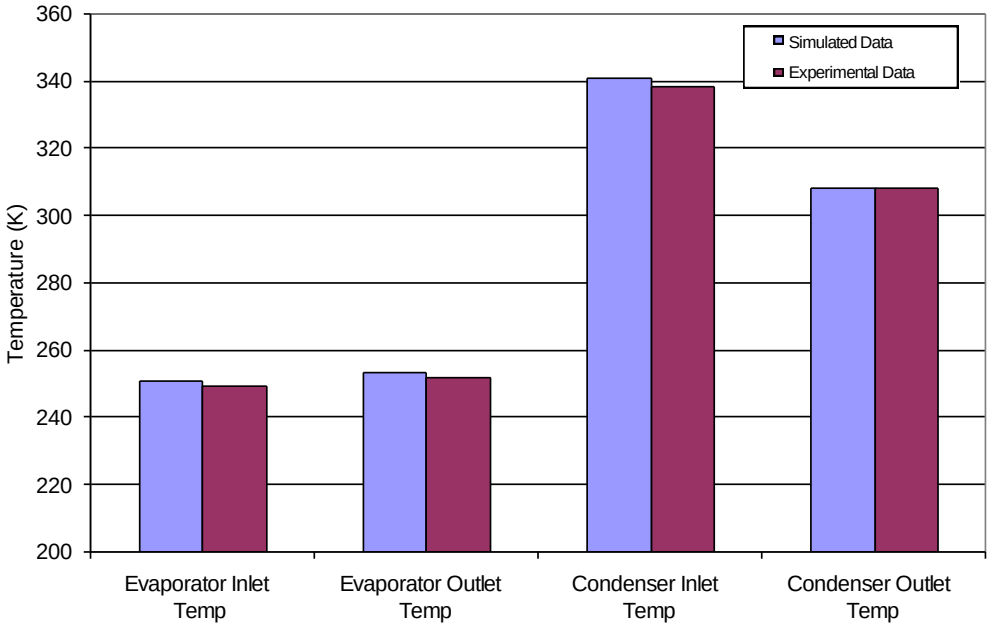

Figure 5.6 Condenser and evaporator inlet and outlet temperature

Figure 5.6 compares the temperature at both the inlet and outlet of the condenser and evaporator at steady state. The maximum temperature difference is around 2.5 K at both the condenser and evaporator's inlet and outlet.

5.2 Validation of an Automotive Air Condition System

The second example validated here is an automotive air conditioning system. Unlike a basic vapor compression system, a real automotive air conditioning system cools the mixture of the environmental air and cabin air. The temperature and humidity ratio is controlled by the environmental air ratio. Hence, to simulate an automotive air conditioning system, a cabin model has to be developed.

5.2.1 Automotive Cabin Model

After reviewing several cabin models, Gado (2006) proposed a new cabin model in his Ph.D. thesis. In this model, the cabin and cabin air are considered as a lump system. Cabin temperature, cabin air temperature and humidity ratio in the cabin are changed homogeneously. The equations used are listed below.

$$T_m = \frac{[m_{iv} Cp_{amb} T_{amb}] + [(m_e - m_{iv}) Cp_r T_r}{m_e Cp_m} \tag{5.1}$$

$$Q_{sen} = m_e Cp_e (T_m - T_s) \tag{5.2}$$

$$\frac{dT_r}{dt} = \frac{h_c A_c (T_c - T_r) - Q_{sen} + Q_{ps} + [U_o A_o (T_{amb} - T_r] + [m_{iv} Cp_{amb} (T_{amb} - T_r]}{M_r Cp_r} \tag{5.3}$$

$$\frac{dT_r}{dt} = \frac{-h_c A_c (T_c - T_r)}{M_c Cp_c} \tag{5.4}$$

$$W_m = \frac{(m_e - m_{iv})W_r + m_{iv}W_{amb}}{m_e} \tag{5.5}$$

After each time step, the three important dynamic variables can be updated by using following equations:

$$T_r = T_r + \frac{dT_r}{dt} * TimeStep \tag{5.6}$$

$$T_c = T_c + \frac{dT_c}{dt} * TimeStep \tag{5.7}$$

$$W_r = W_r + \frac{dW_r}{dt} * TimeStep \tag{5.8}$$

5.2.2 Comparison of the Experimental Data and the Simulation Data

Gado (2006) developed an automotive air conditioning system model by modifying an existing simulation tool: *TransRef*. The simulated results were compared with the measured experimental data in a dynamic test facility. Using the same parameters in Gado's model, the same automotive air conditioning system was modeled using the generic component model developed here, along with its system solver. The predicted results are compared with both the experimental data and the results predicted by Gado's model.

TransRef (Anand, 1999) was originally developed to simulate a dynamic refrigerator and has undergone successive improvements; this tool also can be used to simulate an automotive air conditioning system by integrating it with the corresponding cabin model. Unlike the generic model developed here, TransRef

considers all the heat exchangers as a lump system. In addition, the pressure drop in the heat exchangers is also ignored. Hence, the execution speed is improved.

All of the parameters used in the TransRef model are listed in Tables 5.4 through 5.6 (Gado, 2006). These parameters are also used in the generic model.

Parameters	**Value**	**Unit**
Internal Volume	0.006	m^3
External Area	3	m^2
Internal Area	4.6	m^2
Heat Capacity	1749	J/K
Air Side Heat Transfer Coefficient	80	$W/m^2.k$
Refrigerant Side Heat Transfer Coefficient	850	$W/m^2.k$
Initial Charge	0.2	Kg
Air Flow Rate	0.13	m^3/s
Initial Wall Temperature	41	°C
Void Fraction Constant	0.8	--

Table 5.4 Parameters of evaporator

Parameters	**Value**	**Unit**
Internal Volume	0.006	m^3

External Area	8.41	m^2
Internal Area	0.46	m^2
Heat Capacity	1952	J/K
Air Side Heat Transfer Coefficient	95	$W/m^2.k$
Refrigerant Side Heat Transfer Coefficient	1200	$W/m^2.k$
Initial Charge	0.24	Kg
Air Flow Rate	0.645	m^3/s
Initial Wall Temperature	41	°C
Void Fraction Constant	0.7	--

Table 5.5 Parameters of condenser

Parameters	**Value**	**Unit**
Displacement Volume	0.000155	m^3
Speed	2500	RPM
Clearance Volume	4%	--
Polytropic Index	1.09	--
Isentropic Efficiency	0.6	--
Mechanical Efficiency	0.95	--

Table 5.6 Parameters of compressor

Figure 5.7 compares the mass flow rate of the compressor and orifice from the experimental data and the simulation results conducted by TransRef and the generic model. Since two-phase flow is allowed in the generic compressor model, at the start-up of the compressor, the compressor suctions much more refrigerant than in reality due to the high density of two-phase flows. This scenario boosts the condenser's pressure and temperature quickly and causes the system pressure to balance faster than in reality. As time passed, when the system approaches the steady state, both simulation software tools predicted good results compared with the experimental data.

Figure 5.8 compares the system pressures predicted by the two simulation tools with the experimental data. Both predicted evaporating pressure (at the inlet of evaporator) a little bit lower than the experimental data. The predicted pressures at the twentieth minute in the generic model and the TransRef model were 2.6 bar and 2.4 bar respectively, and the measured pressure was 3.1 bar. At the twentieth minute, the measured condensing pressure was 20 bar, and the predicted condenser pressures in the generic model and the TransRef model were 20.02 bar and 24.2 bar, respectively. The generic model had better agreement with the measured experimental data compared with the TransRef model.

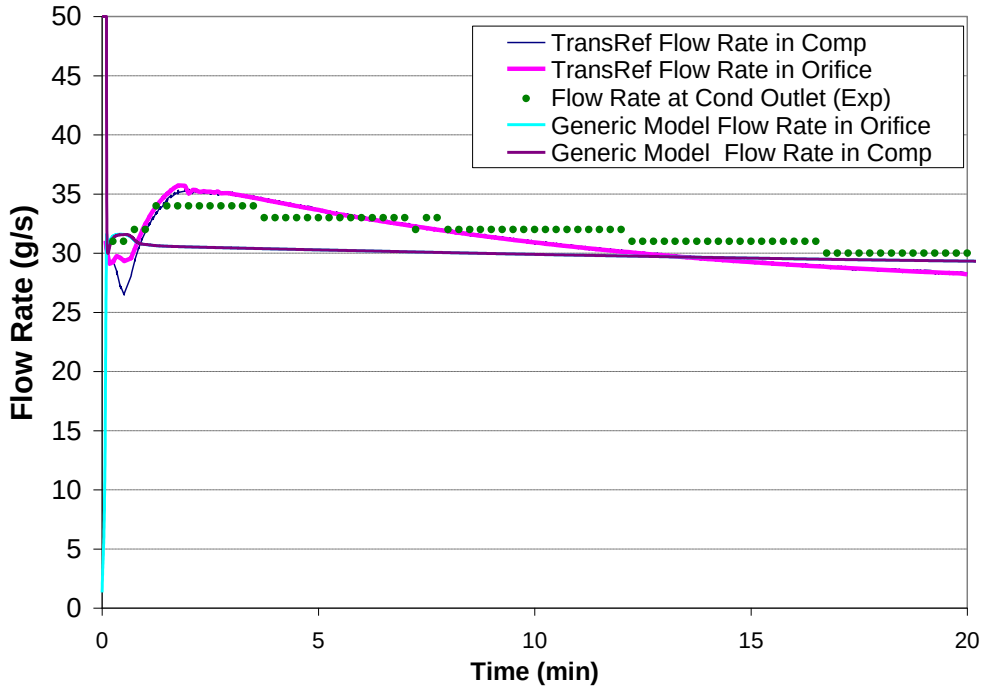

Figure 5.7 Comparison of system mass flow rates

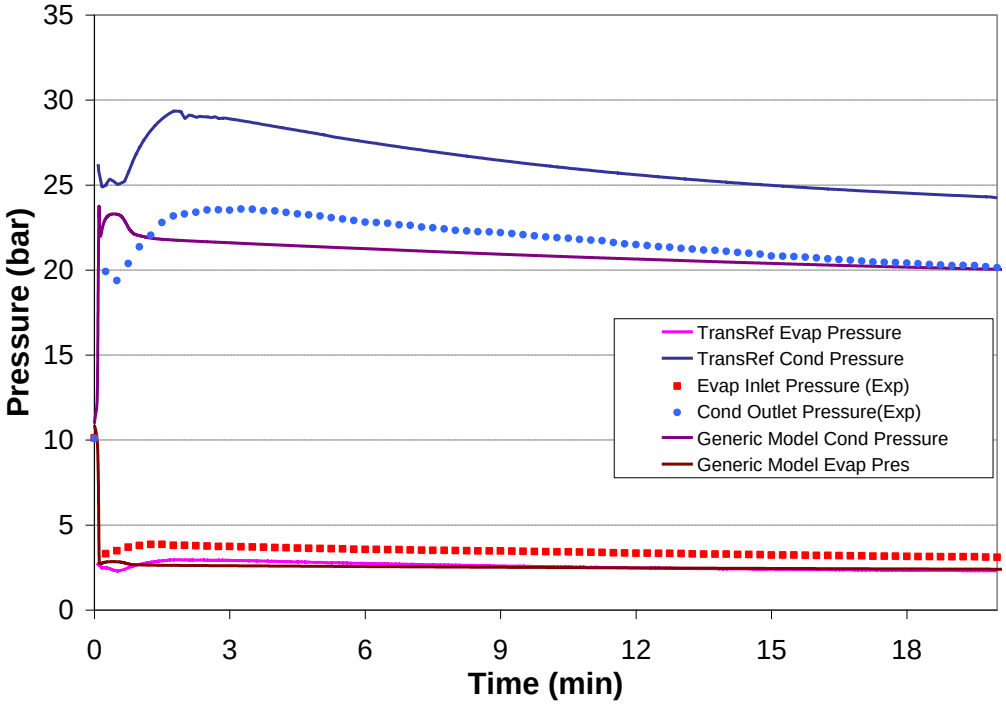

Fig

Figure 5.8 Comparison of system pressures

5.3 Validation of an Air Conditioning System

5.3.1 Description of the Validated System

The modeled system was a 9.5 kW residential air conditioner. This system was validated by Winkler (2009); hence all of the boundary initial conditions required for the modeling are inherited from Winkler's work. The experimental work was conducted and presented by Wang (2008). During the test, the heat exchanger air inlet temperatures were held constant.

Since all required boundary and initial conditions are coming from Winkler's work, besides comparing with the experimental data, additional comparison with the results generated by Winkler's model is also made. The additional comparison can help us to better understand the differences between the numerical simulation and real systems.

5.3.2 Validation Results

A comparison of simulated and experimental suction and discharge pressure is shown in Figure 5.9. At the steady state, both simulation results show good agreement with the experimental data. Even though the simulated discharge pressure of the generic component based model is a little bit higher, the maximum gap is still only around 3% compared to the experimental data. The error between both condensing pressure predictions is partly caused by the difference between the compressor

models. In the generic component based system simulation, a discharge pipe and pressure drop in the discharge pipe were ignored which make the predicted discharge pressure slightly higher than it should be.

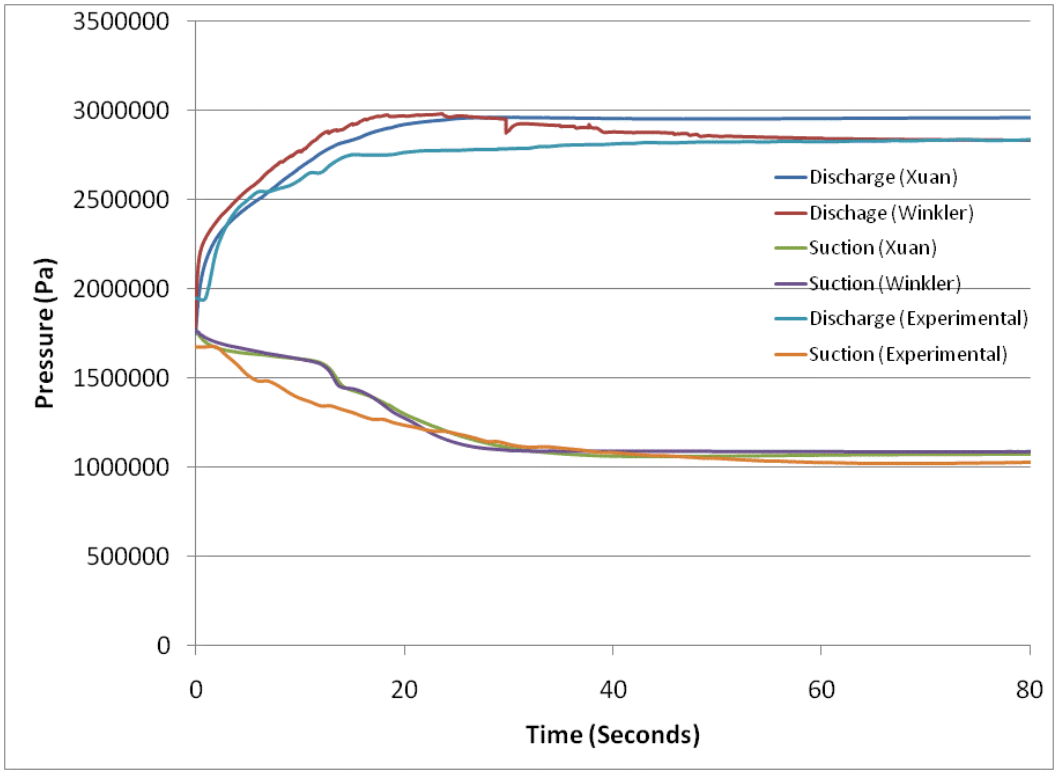

Figure 5.9 Transient validation results – system pressure

The simulated and measured mass flow rates are compared in figure 5.10. In the experiment, the flow rate meter was installed at the condenser outlet (Wang, 2008). The experimental data should compare with the simulated expansion device flow rate. Since the flow meter only can measure the single phase flow and the condenser outlet flow was two phase at the start up period, the measured data is not very accurate at the beginning. However, once the system approaches stability, the mass flow rate gap becomes smaller and smaller, eventually becoming very close at the steady state. If the measured mass flow rate is excluded and only both simulated

results are compared, it can be found that both simulation results show the same trend and very close values during the simulation period. At the steady state, the maximum error between both simulations is less than 5%.

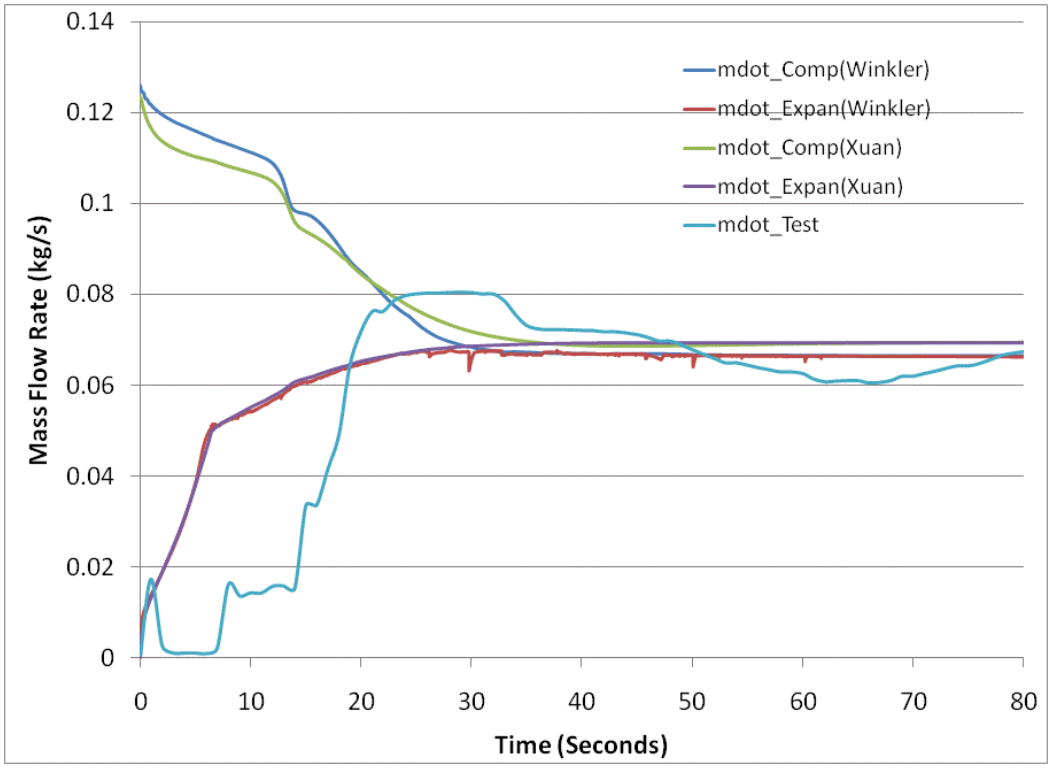

Figure 5.10 Transient validation results – refrigerant mass flow rate

The evaporator air and refrigerant side load comparison is shown in Figure 5.11. In Winkler's work (2009), a good agreement was reached when comparing the simulated load and measured load on the air side. Since the measured refrigerant side capacity during transient period is not accurate due to the inaccurate flow rate measurement, only both simulated results are compared in this dissertation.

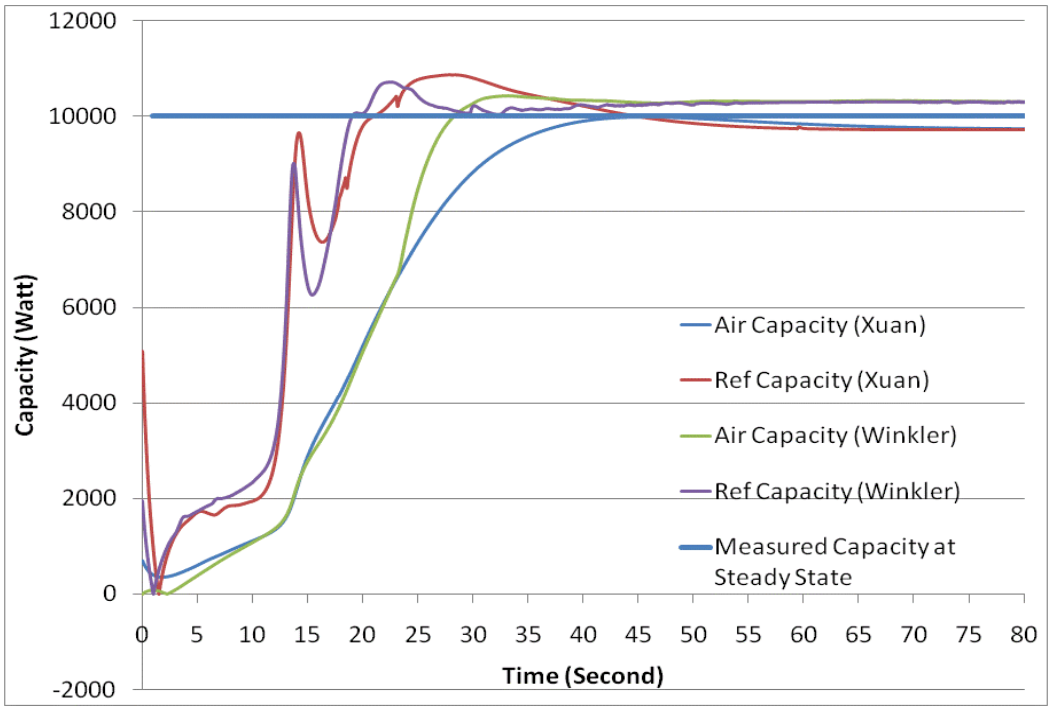

Figure 5.11 Transient simulation comparison – evaporator capacity

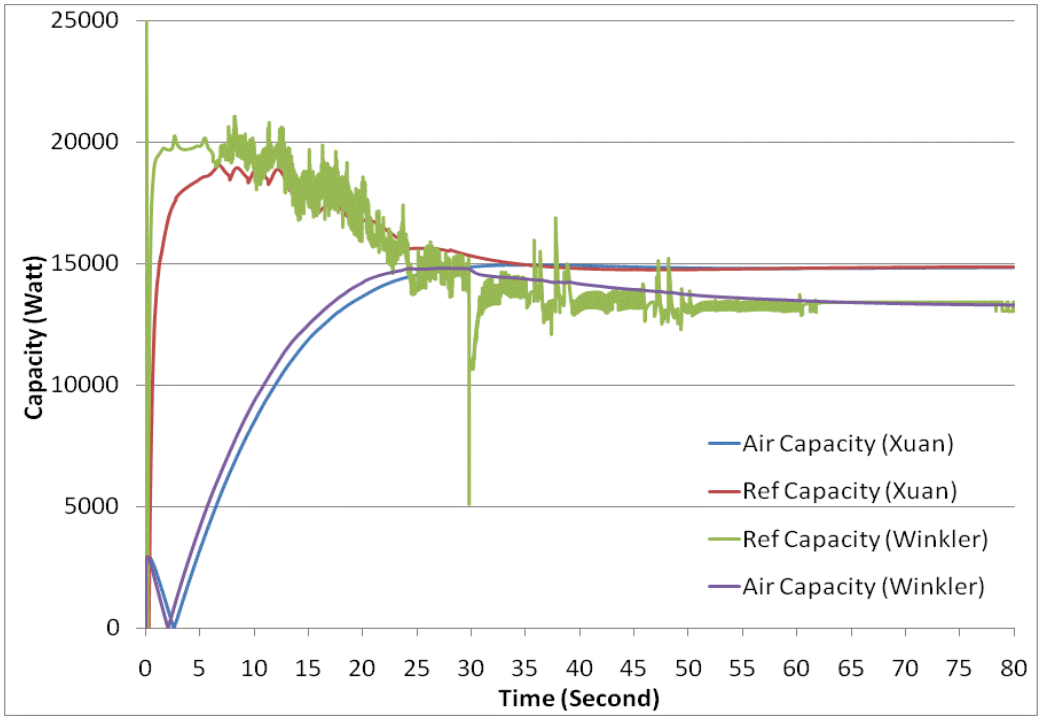

Figure 5.12 Transient simulation comparison – condenser load

Overall, the evaporator/condenser air side and refrigerant capacities in both simulations have good agreements. Both simulations prove the energy balance on the refrigerant side and air side when its steady state is approached. The capacity gap of both simulations is around 5%.

5.4 Summary

In this chapter, several vapor compression systems were simulated using the generic component model with its system solver. The dynamic values of system pressures, mass flow rates, temperatures, and capacities were compared with the experimental data or results predicted by another simulation tool. Good agreement was reached.

One inadequacy of the generic model was observed, which is the generic model's application to compressor simulation. Since a two-phase flow is fed by the evaporator at the start-up of the compressor, a much larger mass flow rate is suctioned, which quickly boosts the condenser pressure and temperature and affects the transient performance.

5.5 References

Anand, G., A Household Refrigerator Simulation Tool – TransRef, CEEE, University of Maryland

Gado, A., Development of a Dynamic Test Facility for Environmental Control Systems, Ph.D. thesis, University of Maryland, 2006

Winkler, J., 2009, Development of a Component Based Simulation Tool for the Steady State and Transient Analysis of Vapor Compression Systems, Ph.D. thesis, University of Maryland.

Wang, X. 2008, Performance Investigation of Two-Stage Heat Pump System with Vapor-Injected Scroll Compressor, Ph.D. Thesis, University of Maryland.

Chapter 6: Conclusion

The research presented here develops a dynamic system model that incorporates generic component models with their related system solvers, and demonstrates how to use this model to dynamically simulate energy conversion systems. The major work performed for this dissertation is summarized in the following sections.

6.1 Generic Component Framework

In this thesis, a generic component model was developed as part of a specific framework for use in both component and system dynamic simulation. This generic component model was developed to simulate the dynamic behavior of the component itself; it also can be adopted in a robust system solver as part of a system model.

By developing a streamlined, internally consistent model architecture, the dynamic behavior of thermal system components can be simulated to achieve increased speed, accuracy, and ease in code maintenance and code development. This allows the user to quickly develop new component models as needed.

6.2 Component Model Development

In this framework, the component model can handle a primary working fluid, secondary working fluid and the boundary between both working fluids. It adopts many correlations to quickly and accurately calculate the local heat transfer coefficient, pressure drop and other necessary information, which makes the model

comprehensive, realistic and accurate. Model implementation on different applications has been discussed and component simulation results showed accurate trends. Along with time and steady-state results, the results were validated by recognized software.

6.3 A Combined Finite Volume and Moving Boundary Method

The moving boundary approach divides the component into different sections based on the phase regime, which makes the execution speed of modeling much faster than the finite volume method. However, large control volumes cause the model to lose detailed spatial information and accuracy. In this generic dynamic component model, a combination of both approaches is applied to track the phase-change boundary in segment and subdivided segments. This approach results in an accurate simulation even if the user chooses a large control volume. The combined approach also provides flexibility for users to choose between accuracy and execution speed, since in the control volume the moving boundary approach is still implemented.

6.4 Integrated Transient and Steady State Simulation Solver Investigation

In this thesis, an integrated transient and steady state simulation solver is developed and its performance investigated. By slightly modifying the existing generic dynamic component framework, it can be used to do both transient and steady state simulation for components. The existing transient system solver also can be directly used for system steady state simulation by only changing one residual

equation. This investigation supports building a unique tool used for vapor compression system transient and steady state analysis.

6.5 Robust System Solver Development

This thesis developed a marching enthalpy system solver, which partly inherits the concept of a junction solver. The vapor compression system was simulated by using the solver to solve the component model sequentially. The prior-solved component model provides the boundary conditions for the next solved component, which reduces the number of unknown variables in the system and improves the robustness and efficiency of the system solver.

6.6 Model Validation with Experimental Data

In this research work, several different vapor compression systems have been constructed and modeled. The performance predicted by the system model has been compared to experimental data at steady-state and transient data. All validation results show the maximum error between predicted value and experimental data is less than 10%

6.7 Limitations in Current Generic Component Model

This research work targets to make users creating vapor compression system component model easier by constructing a generic component framework. Major

component models in a vapor compression system have been created as a demonstration. However, there are still some limitations in current model, which are:

1. Current model cannot handle the situation when a component has several physical boundaries and more than two working fluids.
2. The mass transfer phenomenon is not considered in this model. Therefore current model lacks capability to model a heat and mass exchanger.
3. If an evaporator operates at a very low evaporating temperature, not only condensation occurs, but also frost builds up on its surface. When current model is used to simulate this complicated condition, the accuracy level will decrease because the frost build-up significantly changes the thickness and surface geometry of the physical boundary.

6.8 Summary of Accomplishments

In this dissertation, the major accomplishments and distinguishing contributions of this research are as follows:

1. A generic thermal component concept has been developed in an object-oriented manner. The application of this model to simulate different vapor compression system components has been demonstrated. This is the first time a single generic model has been used to simulate various vapor compression system components. In addition, we have proved that this generic model can be used for the transient simulation, as well as the steady state simulation. The novelty of the model concept and the robustness of its application are the most important contributions of this research work.

2. An adaptive time step algorithm is investigated and integrated in the generic component framework. The adaptive time step algorithm will speed up the simulation time by employing a larger time step size when a steady state is being approached.
3. Two sets of control functions are integrated in the generic component framework. The capability of these control functions is demonstrated through several examples.
4. A related system solver has been developed to solve systems composed of different components, communicating through their ports. Several vapor compression system models, which employ the generic component, have been created using this system solver.
5. A combined finite volume and moving boundary method has been developed and applied as part of a generic dynamic model. This method was previously used for heat exchanger steady-state simulation. Here, it is modified and expanded for a generic component dynamic simulation under dynamic conditions.
6. The vapor compression system models developed by using this generic model have been validated with experiments. The validation results show all of the error between predicted value and experimental data are less than 10%.

6.9 Recommended Future Work

Although this research work successfully developed a generic dynamic model and demonstrated its application capability to vapor compression systems, there is still much room for additional work. The following are suggestions for future research as a continuation of this thesis:

1. Improving the model's application to compressor simulations, to avoid two-phase flow entering the compressor.
2. Simulating frost accumulation for heat exchangers operating in low temperature environments.
3. Improving the robustness of the model. Since thermal properties have physical meaning, their numerical range is limited to a certain range. During the system solution process, the math solver sometimes was not "smart" enough, and occasionally, the guessed thermal property value was out of the property's range, which caused the model to crash.
4. Implementing mass transfer equations into the framework to extend its capability to heat and mass exchanger applications.
5. Implementing more correlations into the generic component framework.